UNIVERSITY OF OKLAHOMA

GRADUATE COLLEGE

THE ROLE OF MEMBRANE FUSION PROTEINS IN TRANSPORT OF DIVERSE SUBSTRATES IN BACTERIA

A DISSERTATION

SUBMITTED TO THE GRADUATE FACULTY

in partial fulfillment of the requirements for the

degree of

Doctor of Philosophy

By

SZE YI LAU
Norman, Oklahoma
2007

UMI Number: 3291239

UMI Microform 3291239

ProQuest Information and Learning Company
300 North Zeeb Road
P.O. Box 1346
Ann Arbor, MI 48106-1346

THE ROLE OF MEMBRANE FUSION PROTEINS IN TRANSPORT OF DIVERSE SUBSTRATES IN BACTERIA

A DISSERTATION APPROVED FOR THE
DEPARTMENT OF CHEMISTRY AND BIOCHEMISTRY

BY

_____
Dr. Helen I. Zgurskaya, Chair

_____
Dr. Valentin V. Rybenkov

_____
Dr. Ann H. West

_____
Dr. George B. Richter-Addo

_____
Dr. Tyrrell Conway

Acknowledgements

My experience here at the University of Oklahoma had been a life-changing one, both as an individual and a scientist. I am largely indebted to so many individuals, without whom I would not have accomplished this milestone.

I want to express my sincere gratitude to my major professor, Dr. Helen I. Zgurskaya for her support, advice and instruction through the years. I want to also thank Dr. Valentin V. Rybenkov for his thoughtful advice and encouragement. Both Dr. Zgurskaya and Dr. Rybenkov's passion, dedication and professionalism have helped instill in me a positive attitude in science and motivated me in maintaining my excellence. I wish to thank my advisory committee members, Dr. Ann H. West, Dr. George B. Richter-Addo and Dr. Tyrrell Conway as well as Dr. Phillip E. Klebba who had served as chair during my general exam. Their insights, comments and suggestions have helped me develop critical thinking.

I am extremely grateful to members of Dr. Zgurskaya's and Dr. Rybenkov's lab with whom I have enjoyed working and who have made my learning experience a pleasant and memorable one. I want to thank Dr. Elena Tikhonova who has been a great teacher to me. Dr. Lucine Demirkhanyan, Dr. Zoya Petrushenko and Dr. Yuanbo Cui for their help and support. Kelly Stratton, for getting me started when I first joined the lab as an undergraduate. Special thanks to Vishakha Dastidar, Girija Dhamdhere, Ganesh Krishnamoorthy and Yun Liu, not only for their help and support but most importantly for their friendship. I also thank Qiang Ge, Weifeng She, Jonathan Lai, Kostyantyn Bobyk and Nick Huffmaster for their comments, support and encouragement.

I want to express my utmost gratitude to my family for their love and support. Their unconditional love and constant encouragement have been the source of my strength. I am thankful for my mom and dad for the values that they instill in me and for believing in me always.

Above all, I want to give all praise, honor and glory to my Lord and Savior Jesus Christ, with whom nothing is impossible.

Table of Contents

Appendices

List of Tables

List of Figures

Introduction

Chapter 1

Chapter 2

Chapter 3

Abbreviations

ABC	ATP binding cassette
ATP	Adenosine triphosphate
BSA	Bovine serum albumin
CBB	Coomassie brilliant blue
CFU	Colony forming units
CHAPS	3-[(3-cholamidopropyl)dimethylammonio]-1-propanesulfonate
DDM	Alkyl-β-D-maltoside
DNA	Deoxyribonucleic acid
DTT	Dithiothreitol
EDTA	Ethylenediaminetetraacetate
IG	Igepal
IM	Inner membrane
IPTG	Isopropyl-β-D-thiogalactopyranoside
kDa	Kilodalton
KDO	2-keto-3-deoxyoctonate
LB	Luria-Bertani
LPG	Lysophosphatidylglycerol
LPS	Lipopolysaccharide
MATE	Multidrug and toxic compound extrusion
MFP	Membrane fusion protein
MFS	Major Facilitator Superfamily
MIC	Minimal inhibitory concentration

MW	Molecular weight
NBD	Nucleotide binding domain
OD	Optical density
OG	Octyl glucoside
OM	Outer membrane
PBP	Penicillin binding protein
PEG	Polyethylene glycol
PG	Peptidoglycan
PMSF	Phenylmethylsulfonyl fluoride
RNA	Ribonucleic acid
RND	Resistant-Nodulation-Cell division
RPM	Rotation per minute
RT	Room temperature
RT-PCR	Reverse transcriptase-polymerase chain reaction
SDO	Sodium deoxycholate
SDS-PAGE	Sodium dodecyl sulfate-polyacrylamide gel electrophoresis
TEM	Transmission electron microscopy
TMD	Transmembrane domain
TMS	Transmembrane segment
TSDS-PAGE	Tricine SDS-PAGE
TX	Triton X-100

PREFACE

Multidrug resistance (MDR) pumps are responsible for the highly resistant phenotype of many pathogenic Gram-negative bacteria to antimicrobial agents. An inner membrane (IM) transporter, comprising a proton antiporter or an ATPase, functions with an outer membrane (OM) channel and a periplasmic membrane fusion protein (MFP) in the extrusion of a broad range of substrates that are structurally unrelated. The promiscuous nature of these pumps makes the design of novel therapeutic drugs extremely difficult. Drugs that were developed in the past decades are analogues of existing drugs, many of which are no longer effective against this defense. MDR poses serious threat to public health, reflected in increased morbidity and mortality. Clearly, new strategies are warranted in combating this threat. The MDR pumps serve as attractive drug targets. Efforts aimed at developing efflux inhibitors are currently underway. Understanding the mechanism of MDR pumps will significantly aid in the design of efflux inhibitors. My graduate work is focused on understanding the role of MFPs in the efflux process. In the introduction chapter, I presented a brief overview of the current findings on MDR transporters, with emphasis on the role of MFP in the tripartite complex. I also briefly discussed the physiological role of MDR pumps, which is a topic of much debate.

My initial work was focused on studying the role of the MFP AcrA in the MDR pump AcrAB-TolC of *Escherichia coli*, which led to a surprise finding that the overexpression of AcrA induced cell filamentation in AcrEF deficient strain, where AcrEF is a close homologue of AcrAB. In Chapter One of my thesis, I described the characterization of the nature of the AcrA-induced filamentation. We showed that the loss of AcrEF function was responsible for the aberrant phenotype. The filamentous cells

did not exhibit any abnormal localization of overproduced AcrA, changes in membrane protein composition or aberrations in membrane structure but are defective in chromosome condensation and segregation. Our results revealed that AcrEF is expressed under standard laboratory conditions and plays an important role in maintaining the normal cell division. The Transmission Electron Microscopy (TEM) done in this project is made possible with the help of Gregory Strout from Samuel Noble Electron Microscopy Laboratory at the University of Oklahoma.

In Chapter two, I presented our work on the role of MFP in the macrolide transporter MacAB-TolC from *E. coli*. This project is a collective work together with Elena Tikhonova and Vishakha Dastidar. We showed that the MFP MacA stimulates the activity of the ABC transporter MacB in a reconstituted system. C-terminal deletion of MacA abolished both the in vitro stimulation and in vivo macrolide function. Consistent with previous studies, we found that the C-terminus is required for the interaction of MacA with MacB. We also found that MacA exhibit strong binding to lipopolysaccharide (LPS)-like molecules. The characterization of the LPS-like molecules and the possible function of MacAB-TolC are discussed in this chapter.

Membrane fusion proteins were previously thought to be unique to Gram-negative bacteria. However structural homologues of MFPs are also found in Gram-positive bacteria as essential component of ABC transporters. It is unclear whether MFPs function through similar mechanism in both Gram-negative and Gram-positive bacteria. In Chapter three, I described the reconstitution of YknWXYZ, the MacAB homologue from *Bacillus subtilis*. YknX is a putative MFP and YknY and YknZ are putative ATP-binding protein and permease respectively. A fourth protein YknW, encoded in the same operon,

is a putative membrane protein with unknown function. In Chapter three, I described the expression and purification of YknW, YknX and the fusion protein YknYLZ. Our preliminary results showed that the MFP YknX stimulated the YknYLZ protein in lipid vesicles. The stimulation was specific as YknX was not able to stimulate the ATPase activity of MacB, suggesting the MFPs of both Gram-negative and Gram-positive bacteria function through similar mechanism. The results presented in this chapter are still preliminary and more work still needs to be done but I hope that the information provided here might be useful reference for future work on this subject.

In Chapters one through three, a short introduction precedes the result and discussion section. Project specific material and methods are described at the end of each chapter, whereas standard laboratory methods are described in the appendices. Lists of strains, plasmids and primers are also included in the appendices.

I. INTRODUCTION

I.1 Antibiotic Resistance in Gram-negative Bacteria

Antibiotic resistance is a major problem in the treatment of bacterial infections. Treatment of Gram-negative bacterial infections tend to be more challenging as Gram-negative bacteria are generally more resistant to antibiotics than are Gram-positive bacteria. Most currently available antibiotics that are used to treat Gram-positive bacterial infections are ineffective against Gram-negative bacteria (Lomovskaya *et al.*, 2007). The highly resistant phenotype of Gram-negative bacteria was attributed to its unique two-membrane cell envelope. The additional outer membrane layer serves as a permeability barrier to various solutes, including drugs. The narrow porin channels and the low fluidity of the lipopolysaccharide leaflet help slow down the diffusion of hydrophilic and lipophilic solutes across the OM (Nikaido and Vaara, 1985; Plesiat and Nikaido, 1992). However, it was later recognized that the low permeability of the OM alone is not sufficient to provide significant resistance (Nikaido, 1998b) as molecules equilibrate rapidly across the membrane layers (Nikaido, 1989). Active efflux systems are increasingly recognized as major contributors to resistance in clinically resistant isolates (Levy, 1992). Among the most significant efflux systems are those of multidrug resistance efflux pumps (Poole, 2002), characterized by its ability to recognize and expel from the cells structurally unrelated antimicrobials. MDR pumps are normal constituents of bacterial cells (Zgurskaya, 2002), and are responsible for both intrinsic and acquired multidrug resistance in several Gram-negative bacteria. Exposure to antibiotics often leads to the overexpression of active MDR pumps or the production of otherwise silent

MDR transporters (Nikaido, 1998a). MDR poses serious threat to public health as seen in increased morbidity and mortality (Carmeli *et al.*, 1999). The promiscuous nature of MDR pumps makes the design of novel therapeutic drugs extremely difficult. The search for novel antimicrobial agents for the treatment of Gram-negative bacterial infection is seemingly exhausted. Efforts to find new drug targets are imperative in the fight against bacterial infection. MDR pumps are attractive targets in the design of therapeutics.

I.2 Multidrug Resistance Efflux Pumps

Currently identified MDR pumps fall into five classes: the ATP-Binding Cassette (ABC) superfamily, the Small Multidrug Resistance (SMR) family, the Major Facilitator superfamily (MFS), the Resistance-Nodulation-Division (RND) family and the Multidrug and Toxic Compound Extrusion (MATE) family. MDR pumps identified in Gram-negative bacteria belong to SMR, MATE, MFS and RND family of transporters, all of which are driven by the transmembrane electrochemical gradient of protons or sodium ions (Putman *et al.*, 2000). The major MDR pumps in Gram-negative bacteria belong to members of the RND family (Poole, 2001).

I.3 RND Multidrug Efflux Pumps

RND pumps function as tripartite complexes, together with a periplasmic membrane fusion protein (MFP) and an outer membrane (OM) channel. In the opportunistic human pathogen *Pseudomonas aeruginosa*, intrinsic resistance is conferred by MexAB-OprM, where the RND transporter MexB functions with the MFP MexA and the OM channel OprM in providing resistance against various antimicrobials including β-lactams,

tetracyclines, chloramphenicol and fluoroquinolones (Li *et al.*, 1995; Poole *et al.*, 1993). Four other RND-type MDR pumps are known in *P. aeruginosa*, including MexCD-OprJ, MexEF-OprN, MexXY-OprM and MexJK-OprM (Poole, 2002). Even though MexAB-OprM is the only constitutively expressed Mex efflux pump in *P. aeruginosa* and solely responsible for its intrinsic resistance, elevated expression of several Mex efflux pumps including MexCD-OprJ and MexEF-OprN were found in clinically resistant isolates (Piddock, 2006; Poole, 2002). In *Escherichia coli*, AcrAB-TolC contributes to the intrinsic resistance of *E. coli* to antimicrobial as well as dyes, detergents and bile salts (Ma *et al.*, 1995). The *E. coli* genome encodes seven RND pumps, six of which are shown to confer drug resistance: AcrB, AcrD, AcrF, YhiV , CusA and YegO (Nishino and Yamaguchi, 2001). Only AcrAB-TolC, have been found in clinical isolates associated with significant levels of MDR (Piddock, 2006). AcrEF, a close homolog of AcrAB, was shown to restore multidrug resistance phenotype in AcrAB deficient strain when overproduced from plasmids (Nishino and Yamaguchi, 2001). Similar to AcrAB, TolC is also required for the function of AcrEF. However, chromosomal deletion of *acrEF* does not affect the intrinsic levels of multidrug resistance.

All three genes encoding the components of RND efflux pumps are often organized in the same transcriptional unit, such as the MexAB-OprM complex from *P. aeruginosa* (Li *et al.*, 1995) and MtrCDE from *Neisseria gonorrhoeae* (Hagman *et al.*, 1995). Some, however, such as the AcrAB genes from *E. coli* (Ma *et al.*, 1993) and MexXY from *P. aeruginosa* (Aires *et al.*, 1999) are not linked with a corresponding gene of the outer membrane (OM) component. In *E. coli*, the OM channel TolC is shared among several RND transporters such as AcrEF and AcrD as well as other transporter

systems, including the haemolysin and colicin V secretion apparatus (Gilson *et al.*, 1990; Wandersman and Delepelaire, 1990) and a recently described novel ABC-type macrolide efflux transporter MacB (Kobayashi *et al.*, 2001b) . Similarly, the OM channel, OprM from *P. aeruginosa* is shared among MexAB, MexXY and MexJK efflux systems (Mine *et al.*, 1999). All three components are essential for the function of these pumps. Deletion of any one of these components abolishes the function of the pumps.

I.4 Tripartite Assembly in Efflux across Two Membranes

The advantage of having a tripartite assembly is that the tripartite complex, such as that of RND pumps, spans the two-membrane cell envelope of Gram-negative bacteria and thus allows the direct efflux of drugs into the external medium bypassing the periplasm. The efflux of drugs directly into the medium can work synergistically with the low permeability of the OM to effectively lower the intracellular accumulation of drugs (Li *et al.*, 1995), due to a slower influx of drugs across the OM barrier compared to drug efflux. Consistent with this, AcrAB-TolC from *E. coli* confer intrinsic resistance only to large, lipophilic agents that have difficulty penetrating the porin channels (Nikaido, 1996). The direct efflux of drugs directly into the external medium is clearly advantageous and can be found in other classes of drug transporters as well. EmrB, a member of the MFS effllux pumps also function as a tripartite complex with the OM channel TolC and the MFP EmrA in providing resistance against hydrophobic uncouplers and antibiotics in *E. coli* (Putman *et al.*, 2000). MacB, a member of ABC superfamily functions with TolC and the MFP MacA in the extrusion of 14 and 15-membered macrolides in *E. coli* (Kobayashi *et al.*, 2001b).

In addition to drug efflux, the tripartite assembly is also seen in transporter systems involved in the secretion of protein toxins in Gram-negative bacteria. These transport systems, which constitute the Type I secretion systems, secrete proteins directly from the cytoplasm to the extracellular medium without a periplasmic intermediate (Lory, 1998). The export of protein toxins is mediated by an IM transporter belonging to the ABC superfamily, an OM channel and a MFP. The IM transporter derives its energy from the hydrolysis of ATP to drive the transport of protein across two membranes in a single energy coupled step. In *E. coli*, the export of haemolysin, HlyA is carried out by the type I system consisting of the ATPase HlyB, the MFP HlyD and the OM channel TolC (Wagner *et al.*, 1983; Wandersman and Delepelaire, 1990). A similar system involve in the secretion of colicin V, comprises the ATPase CvaB, the MFP CvaA and the OM channel TolC (Gilson *et al.*, 1987).

I.5 Membrane Fusion Protein as a Physical Linker

A common feature among all the tripartite systems is the membrane fusion protein (MFP). MFPs constitute a family of homologous proteins (Dinh *et al.*, 1994). The transporters with which MFPs function are diverse in both structure and function. It is unclear what the precise role of MFPs is in the efflux of diverse substrates. One proposed role of MFP is to act as a link between the IM transporter and the OM component. Consistent with this, MFPs are found to form cross-linked complexes to either one or both components in vivo (Husain *et al.*, 2004; Hwang *et al.*, 1997; Thanabalu *et al.*, 1998; Touze *et al.*, 2004; Zgurskaya and Nikaido, 2000a). MFPs are anchored to the cytoplasmic membrane through an N-terminal transmembrane segment or a lipid moiety,

whereas the rest of the protein extends into the periplasmic space. The MFP AcrA was shown to be a highly asymmetric protein capable of spanning the periplasm (Zgurskaya and Nikaido, 1999a). It was previously thought that MFPs interact with the OM component through its C-terminus. However, more recent biochemical evidence showed that the C-terminus is involved in interaction with the IM transporter. Chimeric analysis with AcrA revealed a region in its C-terminus to be important for interaction with the multidrug efflux pump AcrB (Elkins and Nikaido, 2003). The C-terminal domain of AcrA was also shown to form an energetically favorable interaction with AcrB (Touze *et al.*, 2004). Crystal structures of the MFPs MexA and AcrA (Akama *et al.*, 2004; Higgins *et al.*, 2004; Mikolosko *et al.*, 2006) revealed that MexA and AcrA form elongated structures with lengths of 89 Å and 105 Å respectively. Both structures exhibit a central α-helical hairpin, formed when the central α helices folds back to form a coiled-coil, consistent with previous structural prediction (Johnson and Church, 1999) (Fig. I.1). Adjacent to the α-helical hairpin is a globular β-domain, which is structurally similar to lipoyl and biotinyl domains. This domain is formed by the interlocking of the two lipoyl motifs that flank the central α-helices. The coiled-coil domain, held together by the lipoyl/biotinyl domain, is a unique feature of MFPs. A third domain designated as the α + β or β-barrel domain, composed of a seven-strand β-barrel and one short α-helix, is situated adjacent to the β-domain. A fourth disordered domain contains the N- and C-terminal regions. The crystal structure revealed that the N- and C-terminus are located close to one another, consistent with biochemical evidences that implicate the C-terminus in interaction with the IM transporter. The placement of both the N- and C-terminus near the IM means that the α-helical hairpin extends into the periplasm. Based on the lengths

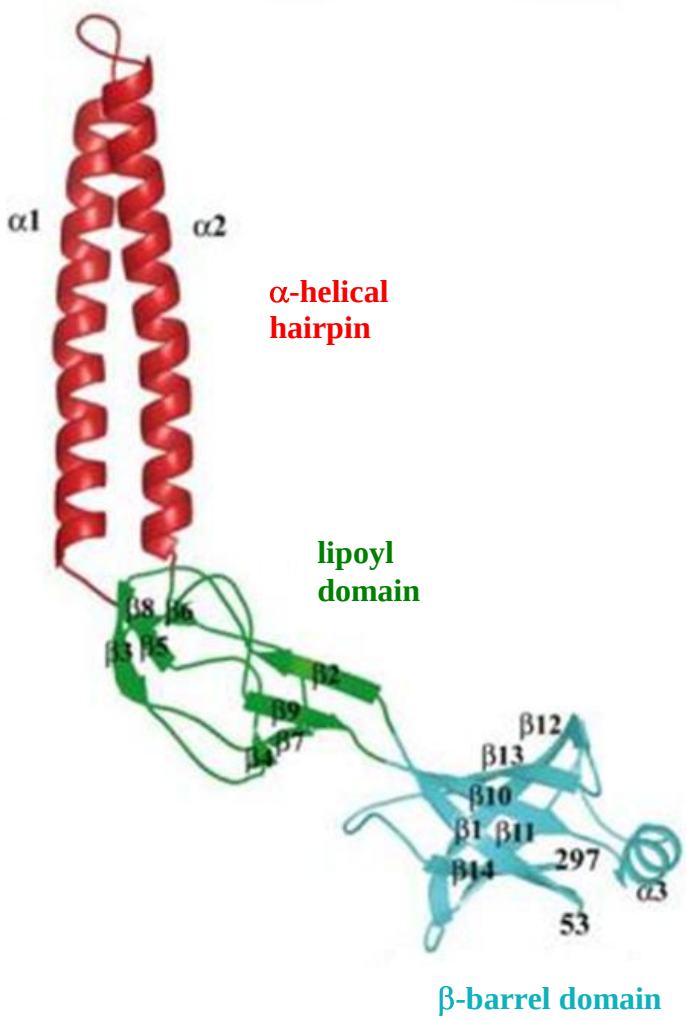

Figure I.1 Crystal structure of AcrA (residues 45-312) (Mikolosko *et al.*, 2006).

of MexA and AcrA, the MFP can extend half the distance into the periplasmic space, which is about 130 Å to 250 Å in depth (Pimenta *et al.*, 1996).

Crystal structures of the OM channel TolC and the RND transporter AcrB are also known. TolC is organized as a homotrimer, forming a continuous, solvent accessible conduit that spans both the OM and the periplasmic space. TolC is embedded in the OM by a 40Å long β-barrel whereas a 100 Å long α-helical barrel projects into the periplasmic space (Koronakis *et al.*, 2000). The β-barrel is wide open and fully accessible to solvent, whereas the α-helical barrel is sealed shut at the periplasmic end by sets of coiled-coils. Opening of the TolC channel requires the untwisting of inner coiled-coils. The coiled-coils of TolC are proposed to interact with coiled-coils of MFPs. Consistent with this, suppressor mutants of mutant TolC mapped within the α-helical region (Gerken and Misra, 2004). In addition, interacting surfaces between TolC and AcrA using site specific cross-linking mapped to the N-terminal α helix of AcrA and the intramolecular groove formed by the lower inner and outer helices of TolC (Lobedanz *et al.*, 2007).

The crystal structure of AcrB also revealed a similar trimeric protein (Murakami *et al.*, 2002). Three AcrB protomers assembled to form a jellyfish-like structure comprising a 50Å thick transmembrane domain and a 70Å thick periplasmic headpiece. The periplasmic head piece is formed by six large periplasmic loops, two from each AcrB protomer. The headpiece is divided into two stacked part. The upper part formed a funnel-like structure, the diameter of which matches that of the bottom of TolC. This part is proposed to be the TolC docking domain (Murakami *et al.*, 2002). The total length of the periplasmic portion of AcrB and TolC is about 170Å, which is sufficient to cross the periplasmic space, suggesting that AcrB and TolC can come into contact with each other.

Site-directed in vivo disulfide cross-linking within this TolC docking domain and tip of TolC demonstrates that AcrB interacts with TolC in a head-to-tail fashion (Tamura *et al.*, 2005). Even though AcrB and TolC can interact with each other, the MFP plays an important role in stabilizing this interaction. AcrB was found to co-migrate with the OM through its association with TolC in the presence of AcrA but in the absence of AcrA, only traces of AcrB was found to co-migrate with the OM, establishing the importance of AcrA in stabilizing the interaction between AcrB and TolC (Tikhonova and Zgurskaya, 2004). Stabilization of the tripartite complex through the interaction of MFP with both the IM and OM components is absolutely vital as the distance between the IM and OM is constantly changing as the volume of the periplasm fluctuates in response to environmental changes (Pimenta *et al.*, 1996). MFP is well suited for this role with the flexibility afforded by its coiled-coil domain.

Docking model of the AcrAB-TolC proposed by (Fernandez-Recio *et al.*, 2004) showed that AcrA interacts with TolC and AcrB by fitting into the grooves of TolC and AcrB through its coiled-coil and lipoyl domain respectively (Fig. I.2). In this model, three AcrA molecules are proposed to interact with TolC and AcrB trimers. To date, the stoichiometry of AcrA involved in the assembly remain controversial as other models involving six (Akama *et al.*, 2004; Stegmeier *et al.*, 2006) and nine (Higgins *et al.*, 2004) molecules of AcrA had been proposed.

I.6 Membrane Fusion Protein as Active Efflux Component

The models based on structures of the OM channel TolC, the MFPs MexA and AcrA and the RND transporter AcrB showed how MFPs interact with the IM and OM component

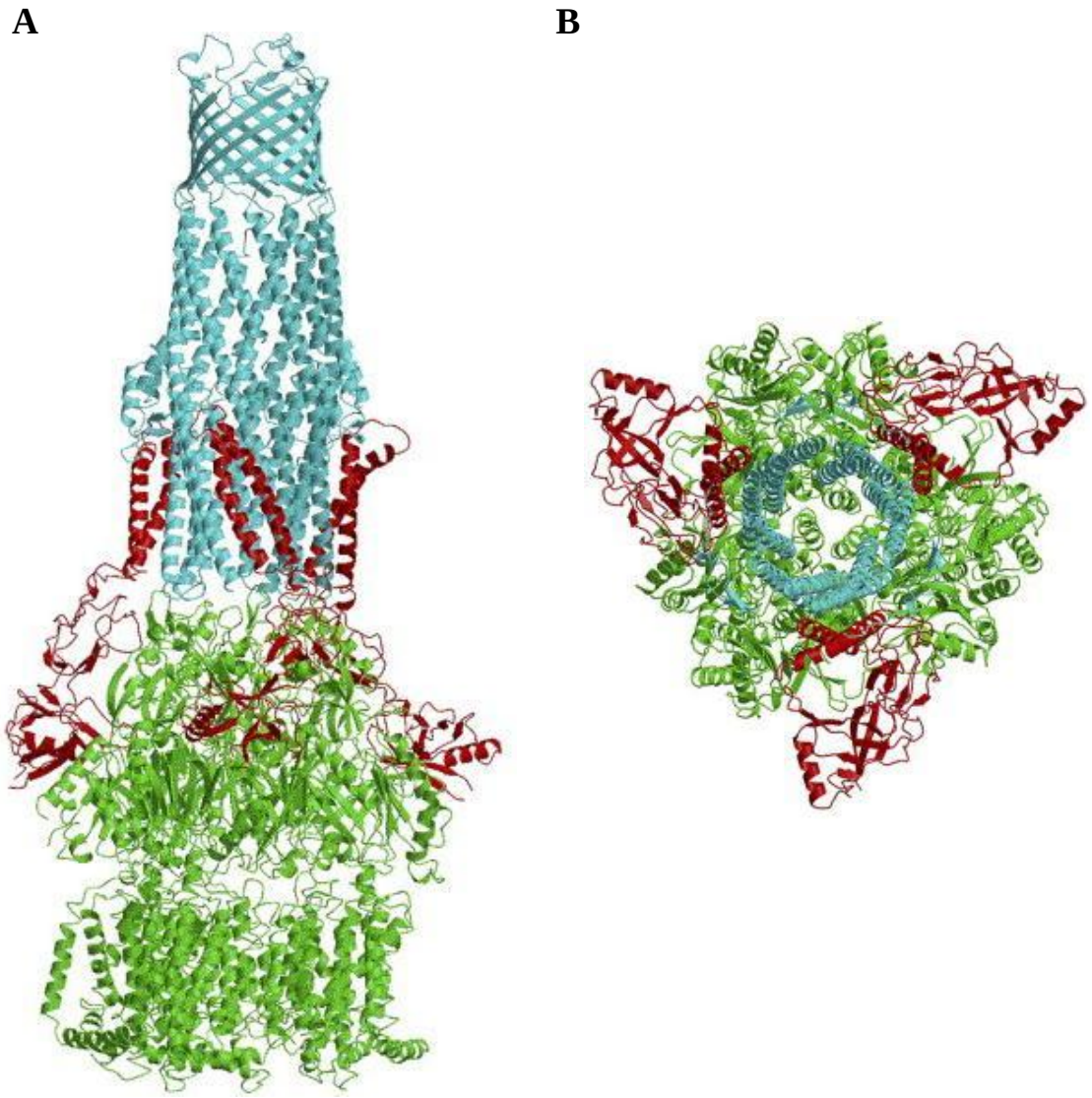

Figure I.2 Docking model of AcrAB-TolC. View of AcrAB-TolC assembly along the (A) vertical threefold molecular axis and along the (B) threefold axis. AcrA is shown to fit in the inter-protomer grooves of TolC and AcrB (Fernandez-Recio *et al.*, 2004).

and provide useful insight into the mechanism of transport in RND efflux pumps. However the models do not explain how MFPs function with other types of efflux system. Unlike RND transporters, which contain a huge periplasmic domain that potentially interacts with MFPs, other types of transporter such as MFS or ABC transporters do not have a huge periplasmic domain (Putman *et al.*, 2000). It is unclear how MFPs coordinate the efflux of substrates in these systems. Adding to the mystery is that MFPs, which are previously thought to be unique to Gram-negative bacteria, are also found in Gram-positive bacteria (Harley *et al.*, 2000). The Gram-positive MFP homologues are found to be essential components of ABC-type transporters in the secretion of endogenously produced bacteriocins. In *Lactobacillus sake*, the putative MFP SapE functions with the ABC transporter SapT in the production of sakacin A (Axelsson and Holck, 1995). SapE and SapT are homologues of HlyD and HlyB respectively. In *Carnobacterium piscicola*, CbnT and CbnD, putative ABC transporter and MFP respectively, are involved in carnobacteriocin production (Quadri *et al.*, 1997). Gram-positive bacteria do not have a two-membrane cell envelope, suggesting that MFPs serve an additional role to that of a structural linker.

The MFP AcrA was previously shown to stimulate the intermembrane transport of fluorescent phospholipid by AcrB (Zgurskaya and Nikaido, 1999b). This was the first study where an MFP is shown to stimulate the activity of it cognate transporter, but the stimulatory effect of AcrA was at that time attributed to the ability of AcrA to promote association of membrane vesicles. More recently, AcrA was shown to stimulate the transport activity of AcrD where no membrane association events occur (Aires and

Nikaido, 2005). These findings suggest that MFPs play an active functional role in addition to its role as a structural linker.

I.7 Physiological Role of MDR Pumps

Even though most MDR pumps expel clinically relevant antibiotics it is unclear whether this is the natural function of these pumps. Recent studies revealed that these MDR pumps may play important physiological roles and antibiotics just happen to resemble the pump's natural substrates. The ability of AcrAB-TolC to pump out such a broad range of substrates may be due to the need of *E. coli* to survive in the presence of high concentrations of bile salts which is known to acquire diverse structures as a result of their metabolism by intestinal flora, including deconjugation and dehydroxylation (Nikaido and Zgurskaya, 2001). The *E. coli* genome encodes 37 drug transporters, out of which 20 have been shown to confer drug resistance (Nishino and Yamaguchi, 2001). Of these 20, 7 belong to the RND family. It is intriguing as to why bacteria need such a large number of seemingly redundant transporters. Interestingly, it was found that nonpathogenic bacteria also contain comparable numbers of chromosomally encoded multidrug efflux systems, suggesting that these systems are inherent properties of bacteria and may play important physiological roles in the extrusion of naturally occurring toxic substances (Saier *et al.*, 1998). Several other lines of evidence also support the notion that the drug substrates of MDR pump is tied to the physiological role of the pump. AcrAB was shown to be regulated by the quorum sensing regulator SdiA, suggesting that AcrAB may normally function to export communication signal molecules (Rahmati *et al.*, 2002). Intriguingly, one of the classes of quorum sensing signals produced in *Pseudomonas* is

quinolones, which is among the most potent, broad-spectrum antimicrobial agents used in the treatment of bacterial infections. In addition, AcrAB is also upregulated by global stress-induced regulators such as MarA and SoxS (Grkovic *et al.*, 2002). It is likely that AcrAB also pumps out endogenous metabolites. The transcription of acrAB in response to stationary phase was shown to differ in different growth medium consistent with the possibility that some metabolite of *E. coli* serves as the signal in the regulation of acrAB (Ma *et al.*, 1996). In another study, resistant *E. coli* strains resulting from mutations that block central biosynthetic pathway are often selected. The mutations were found to activate the AcrAB-TolC pump, suggesting that the pump is required to remove accumulating intermediates that would be otherwise toxic for the cells (Helling *et al.*, 2002).

Chapter 1

Cell Division Defects in *Escherichia coli* Deficient in the Multidrug Efflux Transporter AcrEF-TolC

1.1 Abstract

The AcrAB-TolC complex is responsible for the intrinsic levels of drug resistance in *E. coli*. Inactivation of components of the AcrAB-TolC complex leads to a drug hypersusceptibility phenotype. AcrEF, a close homologue of AcrAB, which also functions in complex with the outer membrane channel TolC, was shown to confer drug resistance when overexpressed in an AcrAB deficient strain. However, inactivation of these AcrEF did not lead to a drug hypersusceptibility phenotype, suggesting that either this pump is silent or expressed at levels insufficient to contribute to multidrug resistance phenotype. We found that the overexpression of the membrane fusion protein AcrA in AcrEF deficient strain leads to cell filamentation. Similar cell filamentation is observed when AcrA is overexpressed in a TolC deficient strain, suggesting that the AcrA induced filamentation is due to the loss of AcrEF function. Fluorescence microscopy revealed that the filamentous cells are defective in chromosome condensation and segregation. Using green fluorescent protein-AcrA fusion protein, we showed that the localization of AcrA is similar in both normal and filamentous cells and is concentrated at defined regions of the cell membrane, independent of AcrEF. In addition, the structure and composition of membranes are similar in both normal and filamentous cells. Our results suggest that the *E. coli* AcrEF transporter is expressed under standard laboratory conditions and plays an important role in the normal maintenance of cell division.

1.2 Introduction

AcrEF is one of the seven resistance-nodulation-cell division (RND) transporters encoded in *E. coli* (Nishino and Yamaguchi, 2001). AcrE and AcrF are close homologues of AcrA and AcrB respectively. AcrA and AcrB function with the outer membrane (OM) channel TolC in providing *E. coli* with high levels of resistance to dyes, detergents and most lipophilic antibiotics (Sulavik *et al.*, 2001). *E. coli* strains deficient in AcrAB are highly susceptible to drugs. AcrEF was shown to complement *acrB* mutation when expressed from plasmids (Kobayashi *et al.*, 2001a; Nishino and Yamaguchi, 2001). Enhanced expression of *acrEF* caused by integration of IS element upstream of *acrEF* suppressed the solvent hypersensitivity of *E. coli* strain lacking acrB (Kobayashi *et al.*, 2001a). Similar to AcrAB, TolC is also required for the function of AcrEF. AcrF, which shares 84% similarity and 77% identity with AcrB was shown to complement a *acrB* mutant (Elkins and Nikaido, 2003; Kobayashi *et al.*, 2001a) in solvent resistance, indicating that AcrA and AcrF form a functional complex. However, chromosomal deletion of *acrEF* does not affect the intrinsic levels of multidrug resistance. Inactivation of *acrEF* also did not reduce the solvent resistance of *E. coli* strains, suggesting that AcrEF is either not expressed or does not contribute to resistance. The role of AcrEF pump seems to be redundant in the presence of AcrAB. However, structural genes of *acrEF* are found to be conserved in *E. coli* (Kobayashi *et al.*, 2001a). The *acrEF* operon is thus suggested to serve as means of survival under conditions where the acrAB genes become inactive (Kobayashi *et al.*, 2001a).

Alternatively, AcrEF may play a physiological role that has not been tested as *acrEF* null mutants are only tested for drug susceptibility phenotype. The gene products

of *acrEF*, previous known as *envCD* was shown to suppress the cell division defects of PM61 *E. coli* strain, which carries a mutation in the *envC* gene (Klein *et al.*, 1991). The defective gene product responsible for the cell division defect of PM61 was later identified as a murein hydrolase (Bernhardt and de Boer, 2004; Hara *et al.*, 2002). It is unclear how AcrEF suppress the cell division defects of PM61. It remains controversial whether AcrEF is expressed under standard laboratory conditions, since no appreciable differences in membrane protein composition can be detected between the mutant strain PM61 and its parent strain P678 (Klein *et al.*, 1991).

In this study, we found that the overexpression of AcrA leads to cell filamentation in AcrEF deficient strains and that the AcrA induced filamentation is due to the loss of AcrF function. The filamentous cells exhibit defects in chromosome segregation, but showed no aberration in membrane morphology or protein composition. Our results argue that AcrEF is expressed under normal growth conditions and plays an important role in cell physiology.

1.3 Results

1.3.1 Increased expression of AcrA leads to filamentation of *E. coli* cells deficient in AcrEF. During our studies with AcrAB transporter, we noticed that the transformation efficiency of the *E. coli* strain AG100AX (Appendix A), deficient of both AcrAB and its close homolog AcrEF, with multicopy plasmid pUC151A expressing AcrA and AcrB under the native P_{acrAB} promoter, was low compared to transformation of the same strain with pUC18 vector. AG100AX/pUC151A also exhibits a slower growth rate compared to AG100AX /pUC18 with growth rates of 0.47 ± 0.04 h^{-1} and 0.72 ± 0.07 h^{-1} respectively

(Fig. 1.1A). When observed under phase contrast microscopy, we found that AG100AX/pUC151A exhibits a filamentous phenotype (Fig. 1.2). To further investigate the nature of the filamentation, plasmid pUC151A was also transformed into wild type (WT) *E. coli* (AG100) or *E. coli* lacking either AcrAB (AG100A) or AcrEF (W4680E). The same filamentous phenotype is observed in *E. coli* lacking AcrEF but not AcrAB, showing that the toxic effect of the overexpression of AcrAB in AG100AX is due to the loss of *acrEF*. Consistent with the filamentous phenotype, the colony forming unit (CFU) of AG100AX/pUC-AcrA was lower by two to three orders of magnitude than those of AG100AX/pUC18 (Fig. 1.1B).

To investigate the effect of overproduction of AcrA or AcrB on the morphology of *E. coli*, multicopy plasmids pUC-AcrA and pBP carrying *acrA* and a*crB* genes were transformed into AG100 (WT), AG100A (ΔacrAB) and AG100AX (ΔacrAB ΔacrEF). The transformants were examined by phase contrast microscopy (Fig. 1.2). Overexpression of AcrA was found to be necessary to induce cell filamentation. Overexpression of AcrB on the other hand did not affect cell morphology, suggesting that the filamentation of the ΔacrEF strain is due to the overproduction of AcrA.

To verify that the filamentous phenotype is induced by the overexpression of AcrA, the amounts of AcrA in isolated inner membrane fractions were determined by immunoblotting with polyclonal anti-AcrA antibodies (Zgurskaya and Nikaido, 1999a). The level of AcrA expressed from plasmid pUC-AcrA is several folds higher than the chromosomal level of AcrA in all the strains tested (Fig. 1.3). The chromosomal expression of AcrA in the AcrEF deficient strain W4680E did not lead to cell filamentation, demonstrating that cell filamentation depends on the amount of AcrA. The

A

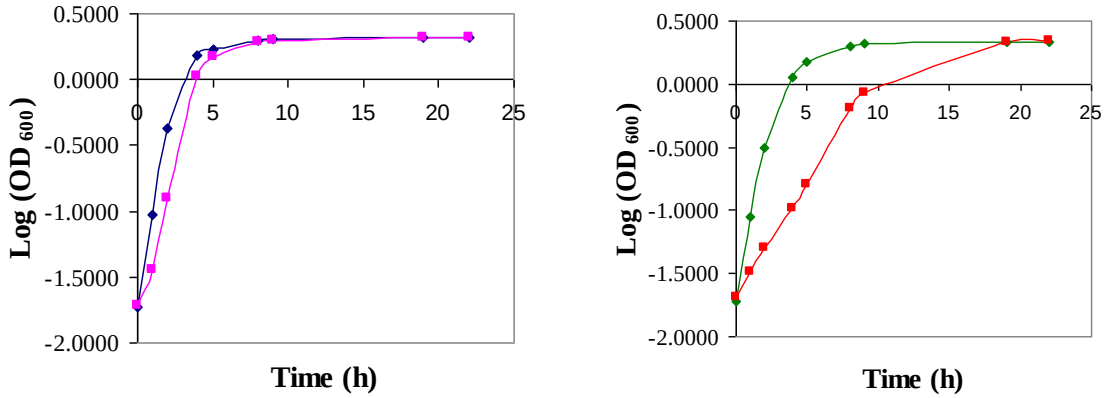

B

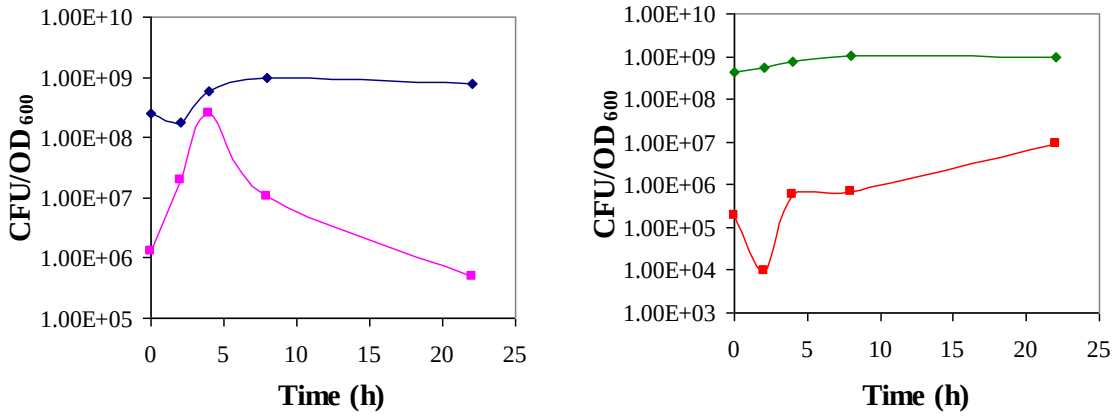

Figure 1.2 Growth curves and CFUs of normal and filamentous cells. (A) Growth curves of AG100AX (left panel) and ECM2112 (right panel) strains carrying either pUC18 (♦) or pUC-AcrA (■). (B) CFUs of AG100AX (left panel) and ECM2112 (right panel) strains carrying either pUC18 (♦) or pUC-AcrA (■).

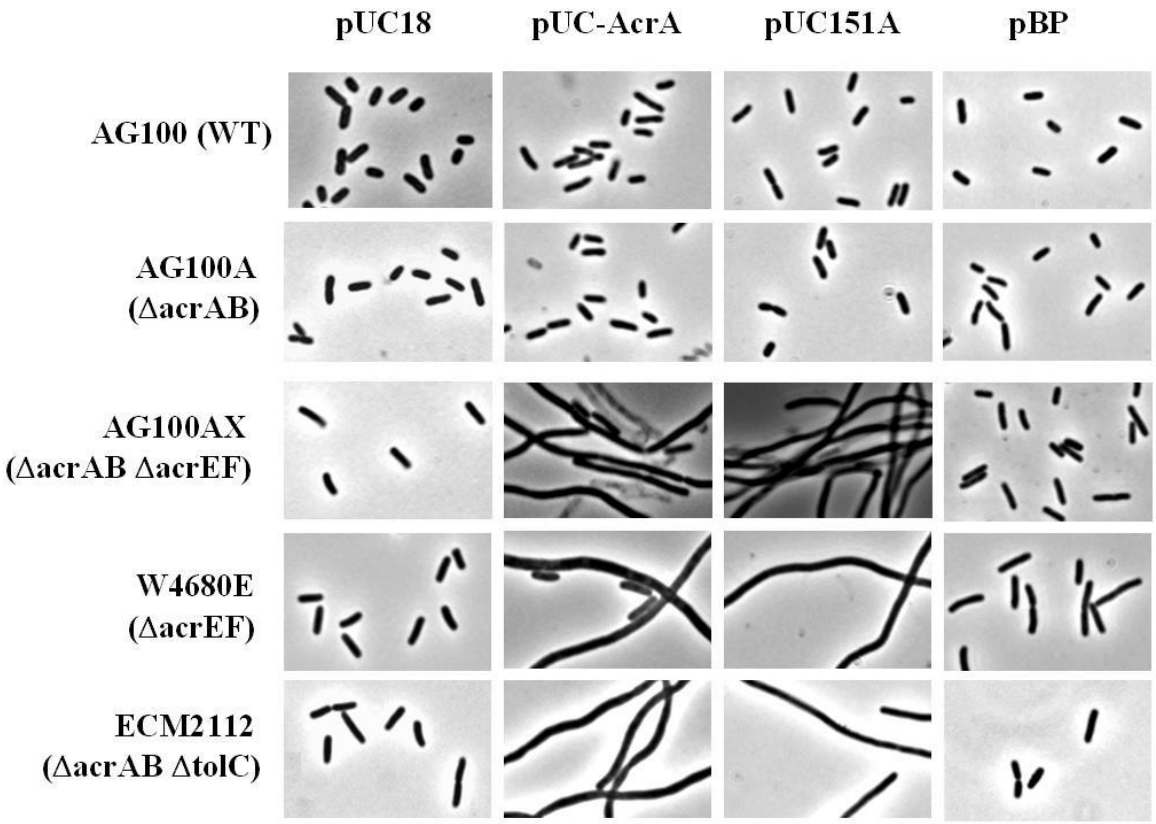

Figure 1.2 Phase contrast microscopy of *E. coli* strains carrying pUC18 vector or pUC18-based plasmids expressing AcrA (pUC-AcrA), AcrB (pBP) or both proteins (pUC151A). Cells were grown at 37^0C to exponential phase in LB medium containing 100μg/mL and examined with phase contrast microscopy as described in Materials and Methods.

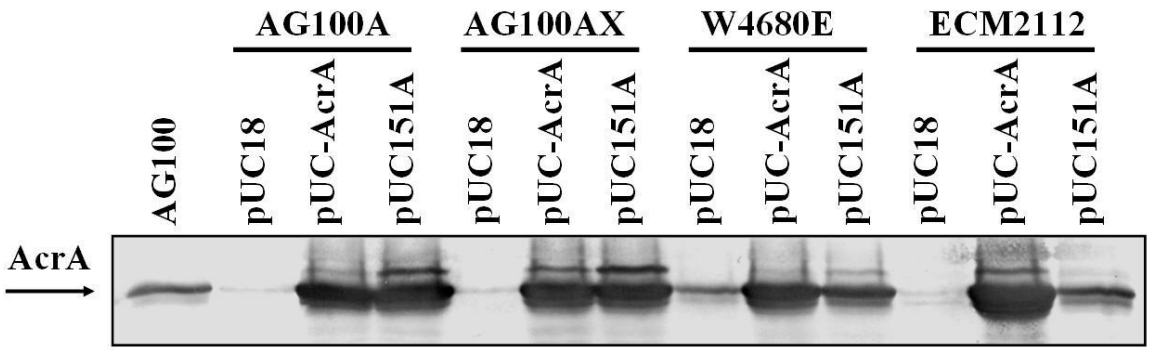

Figure 1.3 Expression of AcrA in normal and filamentous cells. The levels of AcrA expression from pUC-AcrA and pUC151A in normal and filamentous strains were determined by immunoblotting with polyclonal anti-AcrA antibodies (Zgurskaya and Nikaido, 1999a). Inner membrane fractions from *E. coli* strains (Appedix A) were isolated and analyzed as described in Materials and Methods.

expression of AcrA from plasmid pUC151A on the other hand, varies depending on the genetic background of *E. coli*. The amount of AcrA produced in W4680E and ECM2112 is less compared to AG100A and AG100AX. Nevertheless, the level of AcrA expression in these cells is still higher than the chromosomal AcrA level. Thus, the cell filamentation observed is due to the overexpression of AcrA in *E. coli* deficient in AcrEF.

1.3.2 AcrA-induced expression of filamentation is due to the loss of AcrF function. In order to determine whether the AcrA-induced filamentation is due to the loss of AcrEF activity and not due to aberration of acrEF region in the *E. coli* chromosome, we examined the cell morphology of ECM2112 (ΔacrAB ΔtolC) transformed with plasmids producing AcrA (pUC-AcrA), AcrA and AcrB (pUC151A) or AcrB (pBP). ECM2112 is deficient of the OM channel TolC, which is an essential component of the AcrEF transporter (Kobayashi *et al.*, 2001a). We found that similar to the AcrEF null mutants the overexpression of AcrA in the absence of TolC also leads to cell filamentation (Fig. 1.2). However the effect was more severe as the growth rate of the filamentous ECM2112/pUC-AcrA cells was only 0.20 ± 0.022 h^{-1} compared to 0.60 ± 0.009 h^{-1} for the normal ECM2112/pUC18 cells (Fig. 1.1A). Consistent with this observation, the CFU for these two strains differed by 3 to 5 orders of magnitude (Fig. 1.1B). Our result suggested that the function of AcrEF is required to maintain normal cell morphology under conditions of increased production of AcrA.

To examine whether the activity of AcrEF is indeed required for maintenance of normal cell morphology, we cloned *acrF* or *acrEF* into a compatible plasmid, pACYC184. The functionality of AcrF expressed from these plasmids was tested for its

drug resistance phenotype. AcrEF expressed from pACYC-AcrEF was able to restore the drug-susceptible phenotype of AG100AX, with higher resistance to erythromycin, puromycin, ethidium bromide and nalidixic acid compared to AG100AX/pUC18 (Table 1.1). Consistent with previous studies that showed that AcrA, AcrF and TolC formed a functional complex (Kobayashi *et al.*, 2001a), co-expression of AcrF (pACYC-AcrF) with AcrA (pUC-AcrA) in AG100AX conferred drug resistance, albeit only partially (Table 1.1).

To estimate the level of expression of AcrF, total membranes of AG100AX harboring pACYC-AcrEF or pACYC-AcrF were isolated and AcrF was detected using anti-AcrB antibody since AcrF is highly homologous to AcrB (Fig. 1.4A). AcrF is expressed from both plasmids. However, the amount of AcrF produced from pACYC-AcrF is substantially lower. The low level of expression of AcrF from pACYC-AcrF may contribute to the partial drug resistance in AG100AX carrying pUC-AcrA. Therefore, we conclude that the AcrF transporter expressed from these constructs are functional.

The plasmids, pACYC-AcrF or pACYC-AcrEF were then introduced into filamentous AG100AX/pUC-AcrA and AG100AX/pUC151A cells respectively. Unexpectedly, AcrEF expressed from pACYC-AcrEF did not restore normal cell morphology to filamentous AG100AX/pUC-AcrA or AG100AX/pUC151A (Fig. 1.4B). We observed that AG100AX/pUC18 cells carrying pACYC-AcrEF were slightly elongated, suggesting that the overexpression of AcrEF is toxic to the cells. Previous endeavor to overexpress AcrE, which at that time was known as EnvC, from a high copy number plasmid was unsuccessful (Klein *et al.*, 1991). It is likely that the overproduction of AcrE, a close homolog of AcrA contributes to the toxicity to the cells. Since AcrF can

Table 1.1 Antimicrobial susceptibility of AG100AX carrying various constructs

Strains	MIC (μg/mL)						
	SDS	ERY	NOV	CA	PUR	EtB	NAL
AG100A/pUC18	40	4	2	5,000	4	12.5	3.125
AG100AX/pUC18	40	2	2	5,000	2	6.25	0.78
AG100AX/pUC151A	>10,000	64	>128	>10,000	64	200	3.125
AG100AX/pACYC-AcrEF	>10,000	**256**	>128	>10,000	**256**	**>200**	**25**
AG100AX/pACYC-AcrF/pUC-AcrA	39	**8**	**64**	10,000	**8**	**50**	1.56
AG100AX/pUC-Cva-AcrA	>10,000	64	128	>10,000	128	200	3.125
AG100AX/pUC-GFP-AcrA	>10,000	32	128	>10,000	64	100	3.125

Abbreviations: SDS, sodium dodecyl sulfate; ERY, erythromycin; NOV, novobiocin; CA, cholic acid; PUR, puromycin; EtB, ethidium bromide; NAL, nalidixic acid. The MICs of antibiotics for which AcrEF provides greater resistance than AcrAB are in bold.

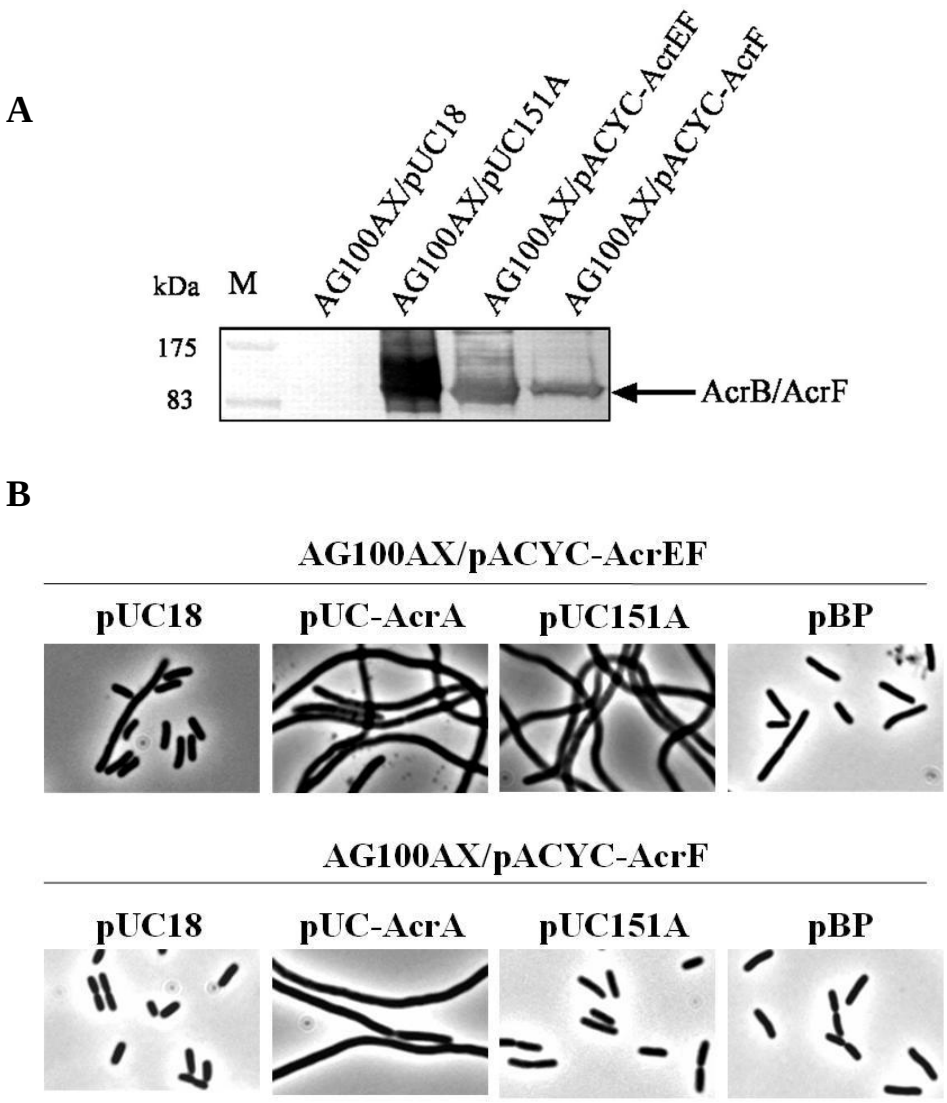

Figure 1.4 Complementation studies of filamentous cells with functional AcrF. (A) Immunoblotting analysis of total membranes isolated from AG100AX carrying pUC18, pUC151A, pACYC-AcrEF or pACYC-AcrF. AcrB/AcrF was detected using polyclonal anti-AcrB antibody (Zgurskaya and Nikaido, 1999b). Ten times less total membranes from AG100AX/pUC151A (2 µg) were loaded onto the gel to avoid overloading. (B) Phase-contrast microscopy of AG100AX/pACYC-AcrEF and AG100AX/pACYC-AcrF carrying as a second plasmid: pUC18, pUC-AcrA, pUC151A, or pBP.

function with AcrA, we can thus examine whether the functional AcrF is sufficient to restore normal cell morphology. Indeed, we found that AcrF alone expressed from pACYC-AcrF restored the cell morphology of AG100AX/pUC151A (Fig. 1.4B), indicating that a functional AcrF is required to maintain normal cell morphology under conditions of increased AcrA production. However, expression of AcrF failed to restore the normal cell morphology to filamentous AG100AX /pUC-AcrA (Fig. 1.4B). It is unclear how AcrB contributes to the complementation of function by AcrF. One possibility is that AcrB form functional complexes with a fraction of AcrA and by this means reduce the toxicity of AcrA overproduction. Taken together, these results suggest that a functional AcrF is required to maintain the normal morphology of *E. coli* under conditions of increased production of AcrA.

1.3.3 AcrEF is expressed under normal physiological conditions. To verify that AcrEF is expressed in *E. coli* strains, RT-PCR was performed. Total RNAs isolated from exponentially growing cells at OD_{600} of 0.8-1.0 or the stationary phase cells were used as template in RT-PCR. AcrEF transcripts were found in both exponential and stationary phase of all strains studied except in AcrEF deficient mutant (AG100AX) (Fig. 1.5). However, small quantities of a longer mutated AcrEF transcript can be detected in the stationary phase. Our results showed that the *acrEF* operon is expressed under normal physiological conditions.

1.3.4 AcrA localizes in a confined manner in the cytoplasmic membrane of normal and filamentous cells. To investigate how the overexpression of AcrA in AcrEF

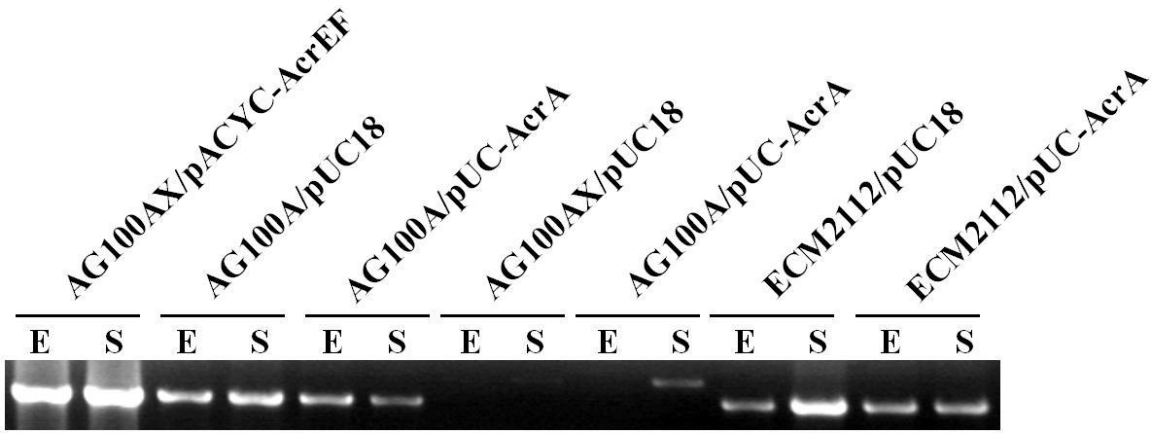

Figure 1.5 RT-PCR analysis of *acrEF* mRNA in *E. coli* with different genetic backgrounds. Total RNA (2 µg) purified from E – exponential or S – stationary phase-grown cells were used as templates in each RT-PCR.

deficient strains contributes to cell filamentation, we compared the intracellular localization of AcrA in normal AG100/pUC18 or filamentous AG100AX/pUC-AcrA cells. AcrA was immunolabeled with anti-AcrA antibody followed by labeling with fluorescein (FITC)-conjugated goat anti-rabbit antibody. AcrA was found in the cell membrane to be clustered at the poles and intermediate positions of growing cells (Fig. 1.6). This result suggested that the lateral diffusion of AcrA in the inner membrane is restricted. However, the clustering of AcrA is similar in both normal and filamentous cells.

To examine the localization of AcrA in live cells, as an alternative approach we examined the fluorescence pattern of green fluorescent protein (GFP) in normal and filamentous cells expressing GFP-AcrA fusion protein. GFP was fused to the N-terminal of a recombinant AcrA containing the transmembrane domain of CvaA protein, a close homolog of AcrA (Gilson *et al.*, 1990). The N-terminal signal peptide of AcrA, which contains the consensus (Leu_{21}-Thr_{22}-Gly_{23}-Cys_{24}) lipid modification sequence (Ma *et al.*, 1993), was replaced with the transmembrane domain of CvaA protein. The recombinant CvaA-AcrA was constructed on pUC151A plasmid carrying *acrAB* genes. This plasmid, when transformed into the drug-susceptible strain AG100AX, restored drug resistance to the same level as native proteins with all the drugs tested (Table 1.1) despite a lower protein expression (Fig. 1.7A). This construct was used for the fusion of GFP. GFP was fused to the N-terminal of the CvaA-AcrA recombinant protein. The amounts of the 70kDa GFP-CvaA-AcrA expressed from pUC-GFP-AcrA were roughly equal to levels of the chromosomally produced wild-type AcrA and about 20- to 30-fold lower than those of wild-type AcrA produced from pUC151A (Fig. 1.7A). The GFP-CvaA-AcrA (70kDa)

AG100/pUC18 **AG100AX/pUC-AcrA**

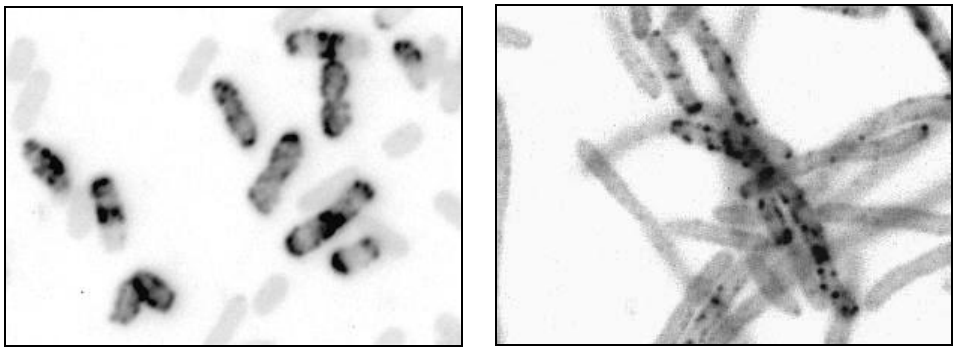

Figure 1.6 Fluorescence microscopy of normal and filamentous cells immunolabeled with anti-AcrA antibody. AG100(WT) carrying pUC18 (left panel) and AG100AX strain (ΔacrAB ΔacrEF) carrying pUC-AcrA (right panel) were immunolabeled with anti-AcrA antibody. Images are inverted. Labeled areas appear black.

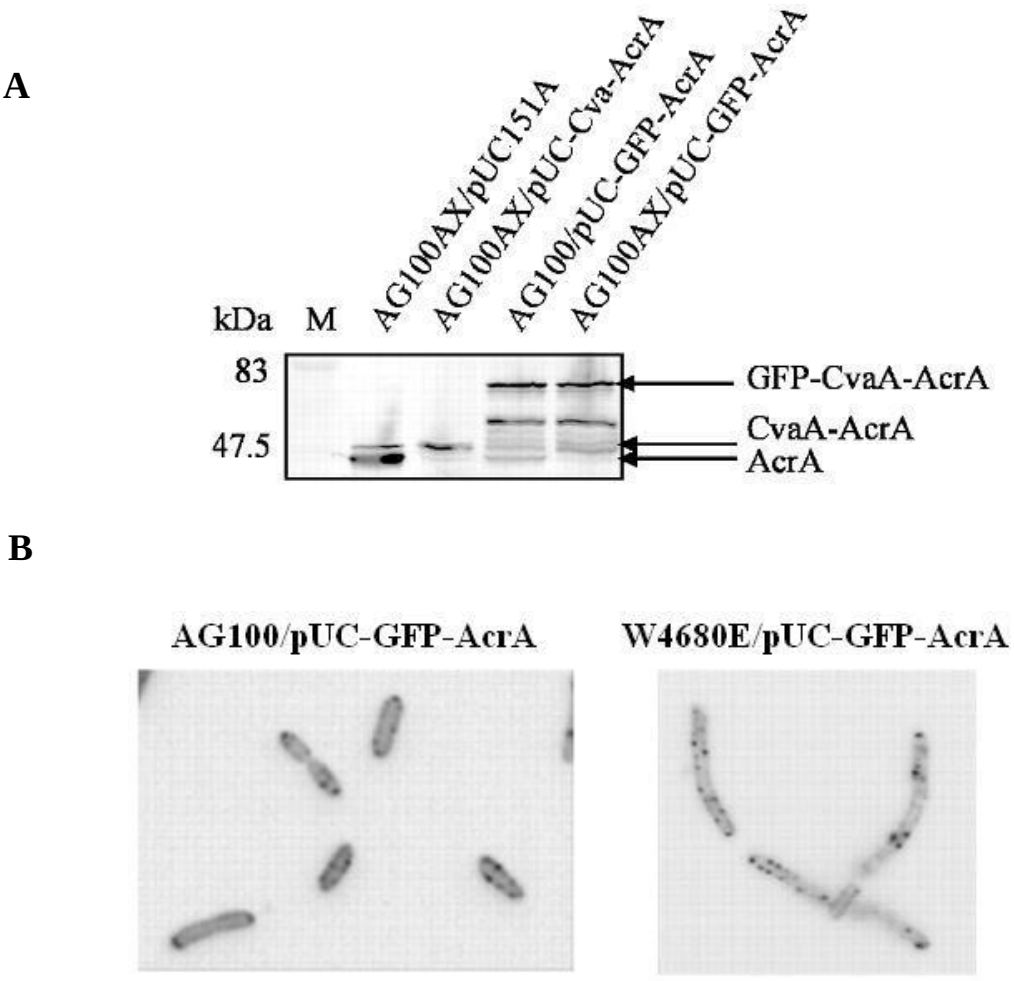

Figure 1.7 Localization of GFP-CvaA-AcrA fusion protein. (A) Immunobloting analysis of total membranes isolated (Appendix F) from cells expressing AcrA, CvaA-AcrA and GFP-CvaA-AcrA fusion proteins using anti-AcrA antibody. Ten times less of total membranes from AG100AX/pUC151A (2 μg) were loaded onto the gel to avoid overloading. (B) Inverted images of the GFP-CvaA-AcrA fusion protein expressed from pUC-GFP-AcrA in the wild-type AG100 strain and the AcrEF null mutant W4680E.

construct appears to be unstable as degradation products can be seen on western blot analysis with anti-AcrA antibody (Fig. 1.7A). However, when expressed in AG100AX strain, it is able to restore drug resistance to the level comparable to that of the native protein (Table 1.1), indicating that the construct is functional.

Because the amount of GFP-CvaA-AcrA is substantially lower than the amount of wild-type AcrA produced from pUC151A, ECM2112 (ΔtolC) or W4680E (ΔacrEF), which contains a chromosomal copy of AcrA was only mildly filamentous when transformed with pUC-GFP-AcrA (Fig. 1.7B). The morphology of AG100AX/pUC-GFP-AcrA, which does not contain a chromosomal copy of AcrA, was normal. We observed that the distribution of GFP fluorescence signal follows a similar clustering pattern in both normal and filamentous cells. Therefore, we conclude that the cell division defects of acrEF mutants are not caused by mislocalization of overproduced AcrA.

1.3.5 Increased expression of AcrA does not cause membrane aberrations. Since the overproduction of membrane proteins could lead to morphological and compositional changes of the cytoplasmic and/or outer membrane (Lefman *et al.*, 2004), we investigated whether high levels of AcrA causes aberrations in the cell membrane that could not be tolerated in these filamentous strains. We examined both normal AG100AX/pUC18 and filamentous strain AG100AX/pUC-AcrA using transmission electron microscopy (TEM). An evenly distributed cytoplasm packed with ribosomes and nucleoid can be seen in both cell preparations (Fig. 1.8). Distinct layers corresponding to the inner membrane, peptidoglycan and outer membrane can be seen in the surrounding cell envelope. Even though constriction of the cell envelope thickness can be seen in some of the cross-

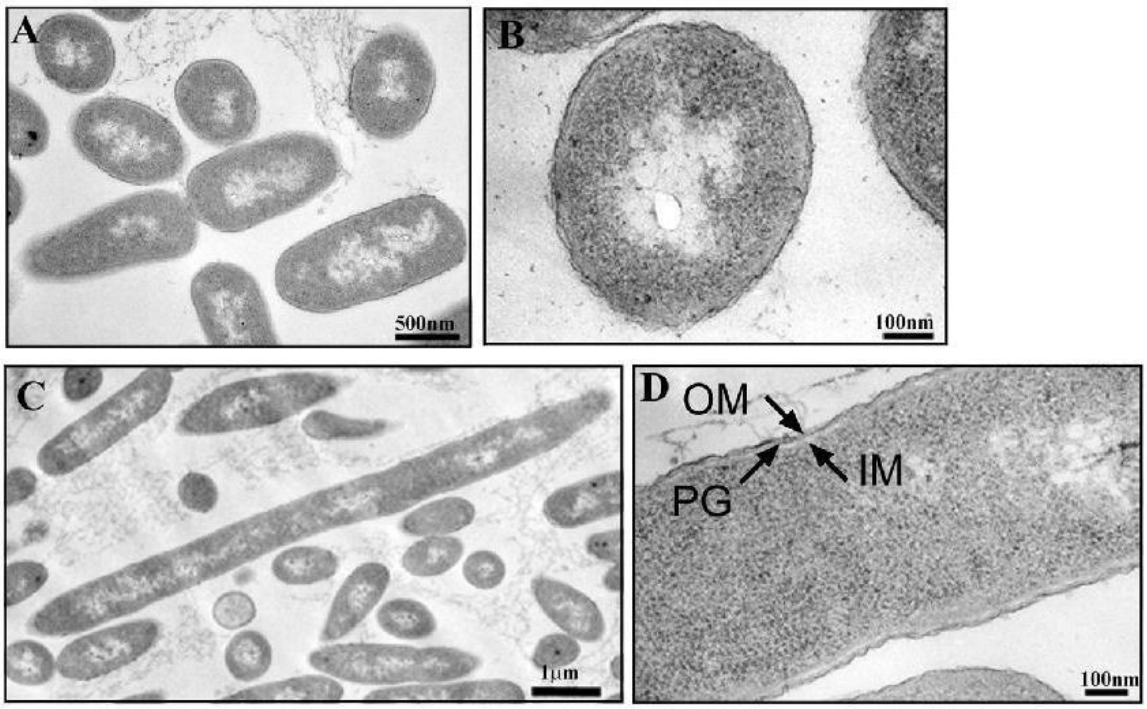

Figure 1.8 Transmission electron microscopy of negatively stained normal AG100AX/ pUC18 (A and B) and filamentous AG100AX/pUC151A cells (C and D). The inner membrane (IM), peptidoglycan (PG) layer, and outer membrane (OM) are indicated by arrows.

sections of filamentous cells, other regions showed no difference in structure to that of normal cells. Since conventional specimen preparation, involving chemical fixation, dehydration, embedding and heavy-metal staining often produces artifacts (Dubochet *et al.*, 1983) the constriction we observed could be a result of sample preparation and processing. Overall, the membrane morphology was very similar in both normal and filamentous cells. Therefore, we conclude that the overproduction of AcrA does not significantly perturb the structure of the *E. coli* cell envelope.

However, we found that complete or partial septum is absent filamentous cells (Fig. 1.8C). In contrast, septum formation, even in the very early stages of cell division was clearly detected in normal cells (Fig. 1.8A). The lack of septa in the filamentous AcrEF mutant with increased expression of AcrA suggested that filamentation could be due to defects in septum assembly.

1.3.6 AcrEF deficient mutants exhibit normal levels of penicillin binding proteins (PBPs). Since the filamentous cells are defective in septum formation, it is possible that components involved in septum formation are compromised, and the problem is aggravated under conditions of overproduction of AcrA. Penicillin binding proteins (PBPs), specifically PBP3, also known as FtsI, is important for the formation of peptidoglycan at the cell division site (Spratt, 1977). Thermosensitive PBP3 mutants were shown to produce filaments at nonpermissive temperature (Pogliano *et al.*, 1997). To test whether the defect in septum formation is the result of the absence of PBPs, we examined the PBP composition in all *E. coli* strains studied. Since PBPs are membrane-bound and targets of β-lactams, we used Bocillin FL (Zhao *et al.*, 1999), a fluorescent

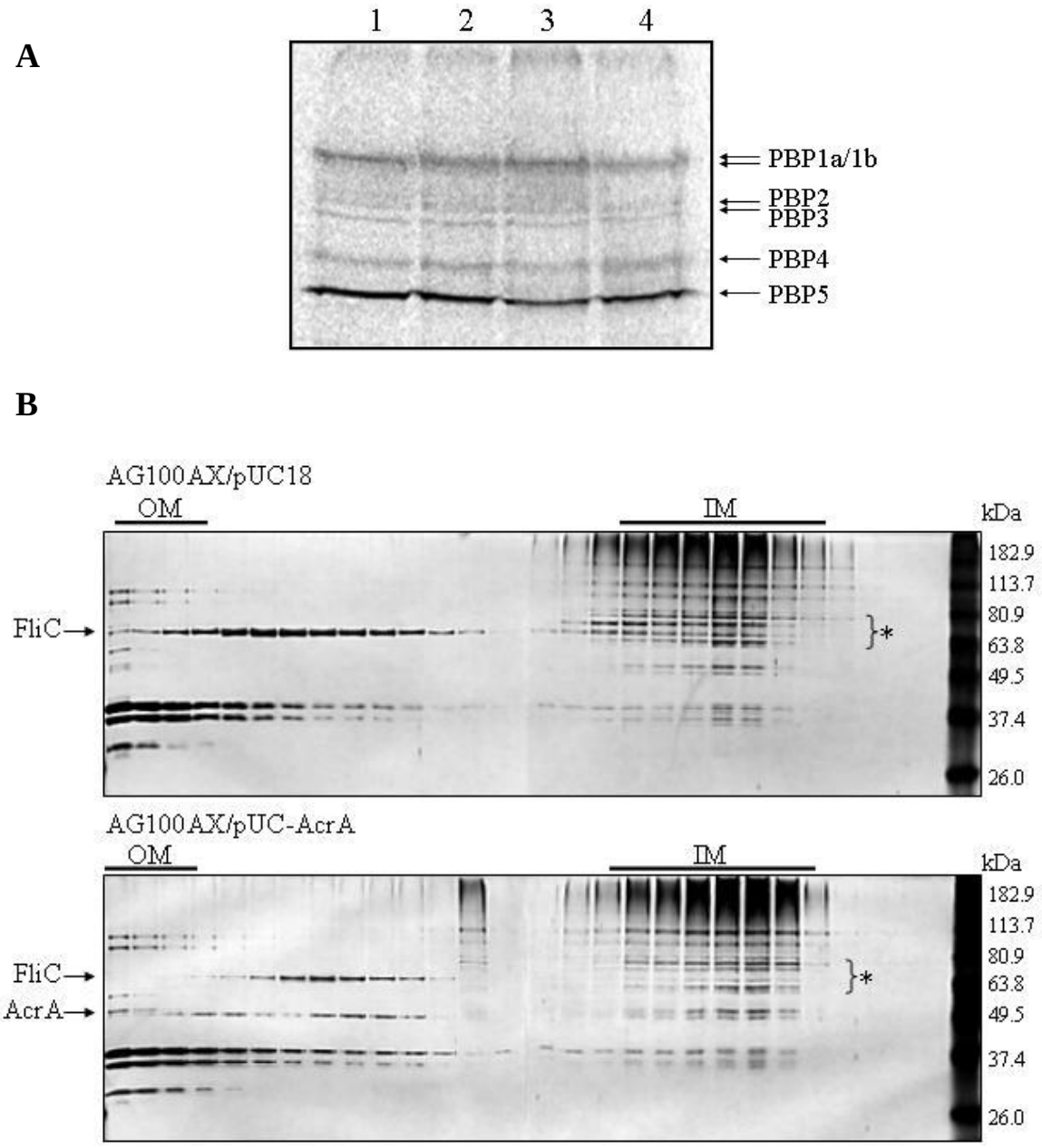

Figure 1.9 Membrane protein compositions of normal and filamentous cells. (A) Bocillin FL labeling of total membranes isolated from various *E. coli* strains (1 – AG100; 2 – AG100A; 3 – AG100AX; 4 – W4680E). (B) Sucrose density fractionation of total membranes isolated from normal and filamentous cells. Areas of the inner membrane fractions with differential levels of proteins are marked with a star.

penicillin to label PBPs in membrane fractions prepared from four different strains: AG100 (WT), AG100A (ΔacrAB), AG100AX (ΔacrAΔacrEF) and W4680E (ΔacrEF). The Bocillin Binding Assay showed that there is no difference in the PBP composition in all four strains studied (Fig. 1.9A). Our result shows that the loss of AcrEF does not affect PBPs of *E. coli*.

1.3.7 Increased expression of AcrA does not cause aberrations in membrane protein composition. To determine whether the overexpression of AcrA affects membrane protein composition, we compared total membranes isolated from normal AG100AX/ pUC18 and filamentous AG100AX/pUC-AcrA strains by sucrose density gradient. Consistent with previous studies (Ishidate *et al.*, 1986), the inner membrane and outer membranes from both cell types migrated to expected positions on the sucrose gradient, 1.16 to 1.18g/mL and 1.22 to 1.26 g/mL for the inner and outer membrane respectively (data not shown). The overall protein compositions in the inner and outer membranes look similar for both the normal and filamentous cells (Fig. 1.9B). The only differences that we observed are two major bands in the intermediate density fractions and a few minor bands in the inner membrane fractions. The major band migrated in the intermediate density fractions of the cell envelopes isolated from normal cells is identified by the N-terminal sequencing as flagellin encoded by *fliC* genes. The amount of flagellin is lower in the filamentous cells than normal cells. Correspondingly, the minor bands in the inner membrane fractions are lower in filamentous strains. Therefore, we concluded that the differences could be due to the differential expression of flagellum genes or posttranslational effects on flagellum in normal and filamentous cells and not

AG100AX/pUC18

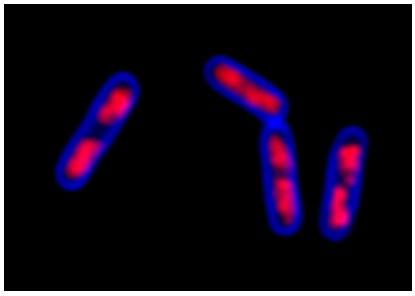

AG100AX/pUC-AcrA

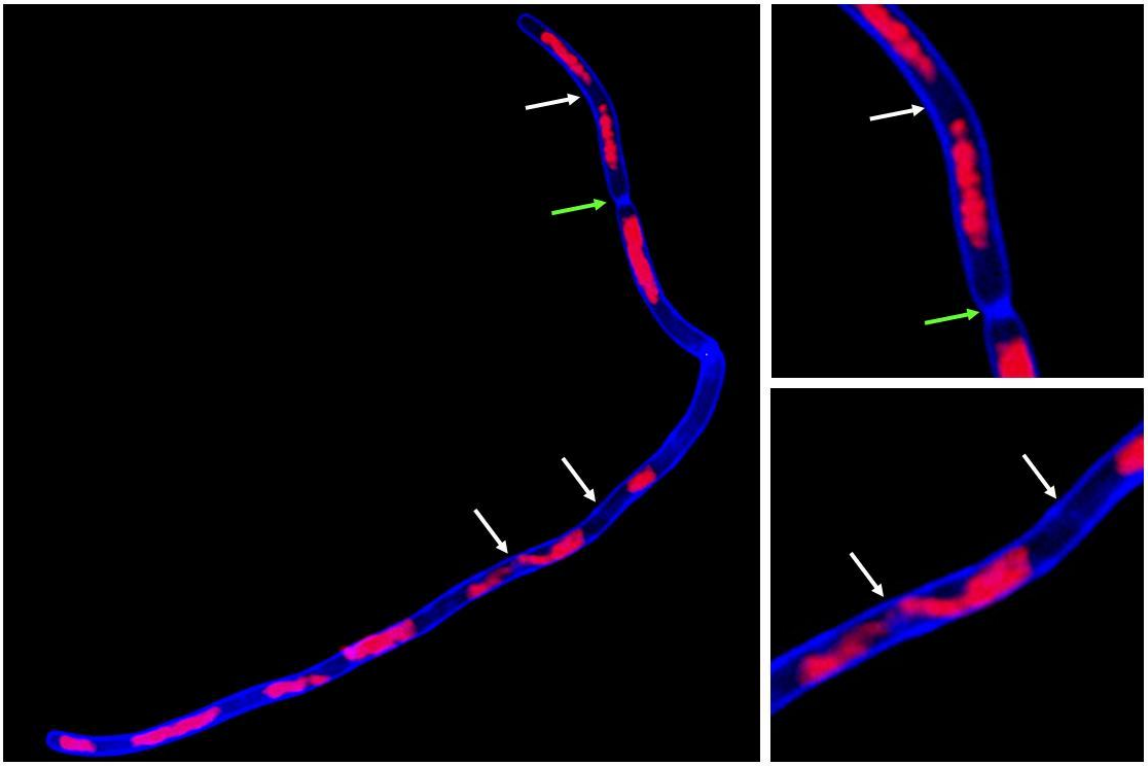

Figure 1.10 Fluorescence microscopy of DAPI and Sypro Orange-stained normal and filamentous cells. (A) AG100AX/pUC18 (B) AG100AX/pUC-AcrA. The Sypro Orange-stained membranes are shown in blue and the DAPI-stained nucleoids are shown in red. The artificial colors are generated by Adobe Photoshop Software. White and green arrows marked areas of filaments lacking or containing a septum respectively.

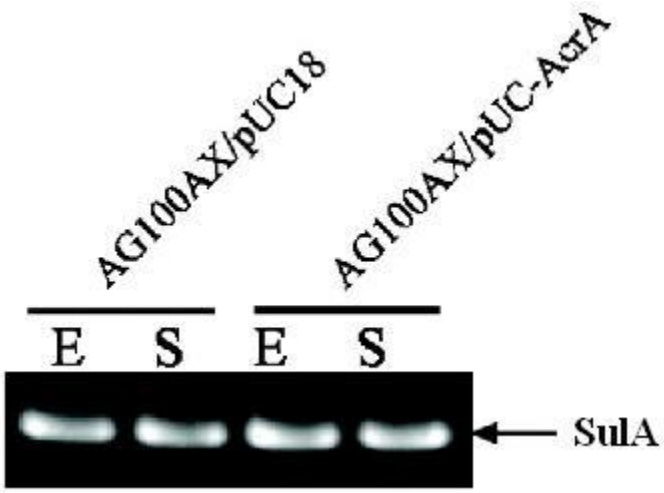

Figure 1.11 RT-PCR analysis of *sulA* mRNA in normal and filamentous cells. Total RNA (2 µg) purified from exponential (E) – and stationary (S) – phase cells were used as templates in each RT-PCR as described in materials and methods.

the effect of overexpression of AcrA in AcrEF null strain.

1.3.8 Increased levels of AcrA in acrEF null cells interfere with chromosome segregation. Septum formation is defective in filamentous cells. Cell division arrest and cell filamentation are often induced by DNA damage or defects in chromosome segregation (Errington *et al.,* 2003). To examine whether chromosomes are properly segregated in normal and filamentous cells, exponentially growing cells were fixed, stained with DAPI and Sypro orange, and observed by fluorescence microscope. DAPI and Sypro orange stained the chromosome and cell membrane respectively. The nucleoid staining pattern revealed that nucleoids are asymmetrically positioned in the filament and large aggregates of nucleoids or decondensed nucleoids are found to occupy an extensive part of the filament (Fig. 1.10). Septum formation, while irregular throughout the filamentous cells is not defective. Our results suggest that the acrEF mutants with increased expression of AcrA are defective in chromosome segregation and condensation.

Inhibition of cell division can occur as a result of DNA damage. SulA, a component of the SOS response is induced in response to DNA damage and is thought to inhibit division through direct interaction with FtsZ (Bi and Lutkenhaus, 1993; Huang *et al.*, 1996). To test whether SulA is induced in our filamentous strain we analyzed the amounts of SulA transcript from normal and filamentous cells by RT-PCR. We found that the amount of SulA transcript is similar in both normal and filamentous cells (Fig. 1.11). We conclude that the AcrA induced cell filamentation is not related to the activation of SOS response.

1.4 Discussion

In this study, we found that the overexpression of the membrane fusion protein AcrA produces filamentous phenotype in strains deficient of AcrEF. Previous studies with AcrEF were focused on its role as a multidrug resistance pump. Overproduction of AcrEF was shown to confer drug resistance in AcrAB deficient strain (Nishino and Yamaguchi, 2001). However, chromosomal deletion of AcrEF did not affect the intrinsic drug resistance. It remains unclear whether AcrEF is expressed in *E. coli* under normal growth condition or whether it plays any physiological role. The fact that AcrEF deficient *E. coli* and not wild type *E. coli* that exhibit morphological defect when AcrA is overexpressed, is an indication of the importance of this "MDR pump" to the normal physiological function of the cell. We showed that the aberrant phenotype under condition of overproduction of AcrA is due to the loss of AcrEF function as the same phenotype can be induced in a ΔtolC deficient strain and TolC is a required component of a functional AcrEF pump. Consistent with this, a functional AcrF was able to restore cell morphology of filamentous AG100AX/pUC151A. Using RT-PCR, we detected acrEF transcript in both exponential and stationary phase of cells, carrying the *acrEF* operon (Fig. 1.5). The filamentous cells exhibit defects in chromosome segregation and condensation (Fig. 1.10). Our results revealed that AcrEF is expressed under normal growth condition and its transport activity plays an important role in normal maintenance of cell division. How does AcrA contribute to the defect in cell division and how does AcrEF alleviate this toxic effect?

Previous studies supported the role of AcrEF in cell division. The overexpression of AcrEF suppressed cell division defect in an envC mutant (Klein *et al.*, 1991). EnvC

was identified as a murein hydrolase responsible for septal murein cleavage to allow outer membrane constriction and daughter cell separation (Bernhardt and de Boer, 2004). *E. coli* encodes a wide array of periplasmic and OM-bound murein hydrolases with potential access to the murein sacculus (Bernhardt and de Boer, 2004). Perhaps these hydrolases are not as effective as EnvC, which would explain why envC mutants are defective in cell division despite the various hydrolases available to do the job. The cell division defect of envC mutants is alleviated by the overproduction of AcrEF, an efflux component. AcrEF may play an important role in cleaning the periplasm from products of membrane and murein cycling, which would otherwise interfere with the functions of other proteins involved in cell division.

The detrimental effect of the overproduction of AcrA in AcrEF deficient mutants is due to the loss of AcrEF function. AcrA overproduced from plasmids pUC151A and pUC-AcrA did not lead to filamentation in wild type or AcrAB deficient cell (Fig. 1.2), indicating that the overproduction of AcrA alone does not interfere with membrane functions (Fig. 1.8 and 1.9). In addition, the overall membrane morphology and composition is similar in both normal and filamentous cells. The localization of AcrA verified by both immunolabeling and fluorescent GFP-CvaA-AcrA fusion (Fig. 1.6 and 1.7B) revealed that the localization of overproduced AcrA is similar. The overproduction of AcrA homologues, such as AcrE and MacA, also leads to filamentation of AcrEF deficient cells (data not shown). Our data suggested that the effect of AcrA overproduction is nonspecific and secondary to the loss of AcrEF function. It is likely that the overproduction of AcrA adds to an already overcrowded periplasmic space due the accumulation of toxic recycling products.

The *E. coli* genome encodes a vast number of drug efflux pumps (Nishino and Yamaguchi, 2001). Interestingly, it was found that nonpathogenic bacteria also contain comparable numbers of chromosomally encoded multidrug efflux systems, suggesting that these systems are inherent properties of bacteria and may play important physiological roles in the extrusion of naturally occurring toxic substances (Saier *et al.*, 1998). The natural substrates for these pumps remain a subject of interest and warrant further investigation.

1.5 Materials and Methods

Media and growth conditions, standard protein assays and total membrane fractionation are described in appendices D, E and F respectively.

1.5.1 Plasmid construction. The pUC-AcrA plasmid was obtained by treatment of pUC151A with DraIII and NsiI restriction enzymes followed by incubations with T4 DNA polymerase and T4 DNA ligase. In pUC-AcrA, the C-terminal 716 amino acid residues of AcrB are deleted. Judging from complementation studies of the drug susceptible phenotype of AG100AX the truncated AcrB is nonfunctional (data not shown). To construct pUC-Cva-AcrA, a 163-bp PCR fragment encoding the transmembrane domain of CvaA was amplified from plasmid pHK11 (Gilson *et al.*, 1990) using the forward primer fNCvaAXhoI and the reverse primer rNCvaAMscI. The PCR fragment was digested with XhoI and MscI restriction enzymes and inserted into plasmid pUC151A treated with the same restriction enzymes. This fragment replaced the coding sequence for the first 28 amino acids of AcrA. To construct pUC-GFP-AcrA, the

gfp gene was amplified from the pQB1T7 plasmid using primers fGFPXhoI and rGFPXhoI, with flanking XhoI restriction sites. The 747-bp PCR fragment was digested with XhoI and inserted into pUC-Cva-AcrA, treated with XhoI and calf intestinal alkaline phosphatase. To construct pACYC-AcrEF, the *acrEF* operon was amplified by PCR from *E. coli* K-12 chromosomal DNA template using the primers fAcrEFAvaI and rAcrEFHindIII. The PCR fragment was treated with the AvaI and HindIII restriction enzymes and ligated into pACYC184 treated with the same enzymes. The 781-bp fragment of *acrE* was deleted from pACYC-AcrEF by digestion with AleI and ApaLI restriction enzymes followed by treatment with T4 DNA polymerase and T4 DNA ligase. The resulting plasmid, pACYC-AcrF, expressed AcrF, presumably under the native *acrEF* promoter.

1.5.2 Phase contrast microscopy. We mixed 300 µl of cell culture, collected when cell culture reached an optical density at 600 nm (OD_{600}) of 0.6 to 0.8, with 15 µl of 25 µg/ml poly-L-lysine. The mixture was spread on coverslips and incubated for 5 min. Excess liquid was removed and the coverslips were rinsed six times in phosphate-buffered saline (PBS) solution (pH 7.3); 5 µl of PBS were spotted onto a slide and the coverslips were placed on the top. Slides were photographed with a Black and White Spot camera (Insight) mounted on an Olympus BX50 microscope through an UPlanFI x100/1.3 oil-immersion objective.

1.5.3 Fluorescence microscopy. To visualize chromosomes and membranes, cells were fixed by mixing 400 µl of cell culture with 6.6 ml of ice-chilled PBS/ethanol (75%). Cells were collected by centrifugation, washed once with PBS, and resuspended in 300 µl of

PBS. Slides were prepared as described for the phase contrast microscopy. For the last step 5 µl of PBS supplemented with 1x Sypro Orange stain (a nonspecific hydrophilic fluorescent protein dye that does not stain nucleic acids) and 100 nM 4',6'-diamidino-2-phenylindole (DAPI) (Molecular Probes) were used.

To determine the intracellular localization of green fluorescent protein (GFP)-CvaA-AcrA fusion protein, live exponential-phase bacteria expressing GFP-CvaA-AcrA fusion protein were spotted onto glass slides and photographed as described above.

1.5.4 Immunolabeling of intracellular AcrA. Cells were fixed and immunolabeled as described in (den Blaauwen *et al.*, 2001). Formaldehyde and glutaraldehyde were added to cell culture (10mL) to a final concentration of 2.8% and 0.04% respectively and incubated at room temperature (RT) for 15min. Cells were then harvested and washed three times in phosphate buffered saline (PBS). After the PBS washes, cells were resuspended in PBS supplemented with 100mg/mL lysozyme and 5mM EDTA and incubated at RT for 45min. Lysozyme in the presence of EDTA partially permeabilized cells to allow antibodies to reach its binding site. After the lysozyme-EDTA treatment, cells were washed three times with PBS followed by incubation in PBS supplemented with 0.5g dry milk (blocking buffer) for 30min at 37^0C. After blocking of nonspecific binding sties, cells were then incubated with anti-AcrA antibody prepared in blocking solution for 1hr at 37^0C. Cells were washed three times with 0.02% Tween-20 prepared in PBS followed by incubation with fluorescein (FITC)-conjugated goat anti-rabbit antibody for 1hr at 37^0C. Cells were washed three times with Tween-20 buffer and visualized with fluorescence microscopy.

1.5.5 Transmission electron microscopy. Cells were collected directly from LB plates supplemented with 100 µg/ml of ampicillin. Fixation was done as described in (Burdett and Murray, 1974). Briefly, cells were fixed with mixture of glutaraldehyde and acrolein and enrobed in agar. Fixed cells enrobed in agar were sliced into small cubes and postfixed with 1% OsO_4 in 0.05 M sodium cacodylate buffer for 1 h at room temperature. After OsO_4 fixation, cells were washed three times with Milli-Q H_2O. Dehydration was done at room temperature in 15-min sequential steps of 30%, 50%, 70%, 80%, and 95% ethanol followed by three 15-min wash in 100% ethanol. The dehydrated cells were embedded in Embed-812 resin and sectioned to a thickness of 50 to 70 nm. The sectioned blocks were stained 10 min with saturated uranyl acetate and 5 min with Sato's lead (Hanaichi *et al.,* 1986) and observed using JEOL 2000-FX electron microscope in the Samuel Roberts Noble Electron Microscopy Laboratory at the University of Oklahoma.

1.5.6 Sucrose density gradient fractionation All sucrose solutions used in this procedure were preapared in 5mM EDTA. Membrane pellet was isolated as described in Appendix F and resuspended in solution of 20% sucrose. All subsequent steps for membrane preparation were done as described before (Ishidate *et al.,* 1986; Tikhonova and Zgurskaya, 2004). Briefly, 1.6 mL of membrane vesicles in 20% sucrose was layered on a two-step sucrose gradient containing 3.2 mL of 60% Sucrose and 7.5 mL of 25% sucrose. After centrifugation in Beckman SW40 rotor at 40,000 rpm for 3.5 h, two bands collected at the 25%-60% sucrose interface was removed by puncturing the side of the tube with a needle attached to a syringe. Approximately 0.8 mL of the resulting suspension was mixed with equal volumes of [10mM Tris, 5mM EDTA] and layered on top of a 30-60% sucrose gradient. Membranes separated in the sucrose gradient were

collected in 0.1 to 0.2 ml fractions from the bottom of the centrifuge tube. Fractions were mixed with sodium dodecyl sulfate (SDS) sample buffer, boiled for 10 min, analyzed by 10% sodium dodecyl sulfate-polyacrylamide gel electrophoresis (PAGE) and visualized by silver nitrate staining.

1.5.7 Bocillin FL binding assay. The bocillin binding assay was performed as described (Zhao *et al.*, 1999) with the following modifications. Cells were first grown in 5 ml LB medium supplemented with appropriate antibiotics overnight. Overnight cultures were inoculated into 200 ml of fresh medium and allowed to grow until an OD_{600} of ~1.0, and harvested at 5,000 x *g* for 20 min. Cell were washed once with 20 mM potassium phosphate buffer (PBS) (pH 7.5) containing 140 mM NaCl and resuspended in 2 ml of the same buffer supplemented with 1 mM EDTA. Lysozyme was added to the mixture to a final concentration 100 µg/ml, cell were incubated on ice for 15 to 30 min and sonicated 3 times for 20 seconds on ice. Unbroken cells and cell debris were removed by centrifugation at 5,000 x *g* for 20 min. The supernatant was collected by centrifugation in Beckman TLA-55 rotor at 40,000 rpm for 40 min. The resulting pellet was washed once and resuspended in 0.5 ml of the 20 mM PBS (pH 7.5) containing 140 mM NaCl. 15µL of membrane preparations (~300µg of protein) was mixed with 5µL of 200µM Bocillin FL (Invitrogen) and incubated at 35^0C for 30 min. Equal volume of SDS-sample buffer was added and mixture was boiled for 3 min. 10µL of samples were resolved on 10% SDS-PAGE. The gel was rinsed with water after electrophoresis and directly scanned with Storm PhosphoImager.

1.5.8 Reverse transcription-PCR. Reverse transcription (RT)-PCR was performed by using QIAGEN OneStep RT-PCR, which allows reverse transcription and PCR to be carried out sequentially in the same reaction tube. Total RNA was isolated from exponentially growing cells at OD_{600} of 0.8 to 1.0 and stationary phase cells using QIAGEN RNeasy kit. Purified total RNA (2 µg) was used as a template in RT-PCR. For AcrEF, forward primer fAcrEF and reverse primer rAcrEF were used to yield a product of 4,280 bp. For SulA, forward primer fSulA and reverse primer rSulA were used to yield a product of 482 bp.

Chapter 2

The C-terminal domain of MacA is Important for Its Interaction with the *Escherichia coli* Macrolide Transporter MacB

2.1 Abstract

Many transport systems in Gram-negative bacteria function with a periplasmic membrane fusion protein (MFP) and an outer membrane (OM) channel. Membrane fusion proteins are thought to facilitate the efflux of diverse substrates, such as proteins and small molecules across two membranes by providing the physical link between the inner and outer membrane components. This study is focused on the function of MacA, the periplasmic component of the macrolide transporter MacAB-TolC in *Escherichia coli*. MacB is an ABC-type transporter and functions with the periplasmic MFP MacA and the OM channel TolC in the efflux of macrolides. Upon reconstitution of MacB into proteoliposomes, MacB exhibit a MacA-dependent ATPase activity. MacA is the first member of the MFP family of proteins that was found to stimulate the ATPase activity of its cognate ABC transporter. In this study, we investigated the role of the C-terminal domain of MacA in its function with MacB. We found that the deletion of the C-terminal domain of MacA abolishes the activity of MacB in vivo and in vitro. The C-terminal deletion mutant failed to co-purify with 6His-tagged MacB, suggesting that the C-terminal domain is important for its functional interaction with MacB. MacA devoid of its N-terminal membrane anchor co-purified with MacB. Our results revealed that the periplasmic domain is sufficient for the interaction of MacA with MacB, most likely

through its C-terminal domain. We also found in our studies that LPS is consistently co-purified with MacA, suggesting that LPS could be a natural substrate of MacAB-TolC.

2.2 Introduction

Gram-negative bacteria contain two membrane layers: a cytoplasmic membrane and an outer membrane. The transport of molecules across the cell envelope of Gram-negative bacteria requires specialize transport systems that delivers molecules across this two-membrane barrier (Zgurskaya and Nikaido, 2000b). Tripartite transport systems consisting of an inner membrane (IM) transporter, an outer membrane (OM) channel and a periplasmic membrane fusion proteins (MFPs) associate to form a continuous conduit that spans the two-membrane envelope of Gram-negative bacteria, thus allowing the direct efflux of substrates into the external medium bypassing the periplasmic space. In *Escherichia coli*, the proton antiporter AcrB, belonging to the resistance-nodulation-cell division (RND) superfamily functions with the MFP AcrA and the OM channel TolC in providing intrinsic resistance to wide range of antimicrobials, detergents and bile salts (Nikaido, 1994; Sulavik *et al.*, 2001). Similarly, the ATPase HlyD, functions with the MFP HlyB and OM channel TolC in the type I secretion of α-haemolysin (Thanabalu *et al.*, 1998). The MFPs are proposed to interact with both IM transporter and OM channel components of the transport systems. MFPs are found to form cross-linked complexes to the IM and OM components in vivo (Husain *et al.*, 2004; Hwang *et al.*, 1997; Thanabalu *et al.*, 1998; Touze *et al.*, 2004; Zgurskaya and Nikaido, 2000a). The interaction between MFPs and the transport components are also supported by co-purification and ITC studies

(Tikhonova and Zgurskaya, 2004; Touze *et al.*, 2004). However, it is unclear how MFPs coordinate the efflux of substrates across two membranes.

In this study we examine the role of the MFP MacA in a reconstituted system. MacA is an essential component of the macrolide pump MacB in *E. coli*. MacB is the first ABC-type drug efflux transporter to be characterized in a Gram-negative bacterium (Kobayashi *et al.*, 2001b). It was shown that the overexpression of MacAB led to an increase of resistance to 14- and 15- membered macrolides in AcrAB deficient cells, which are otherwise susceptible to these drugs. The OM channel TolC is required for the function of MacAB. Deletion of TolC abolished the MacAB-mediated macrolide resistance. A typical ABC transporter consists of four domains: two hydrophobic transmembrane domains (TMDs) and two nucleotide binding domains (NBD) (Higgins, 1992). MacB represents a half type ABC transporter where an NBD and TMD are fused in a single polypeptide and thus predicted to function as a dimer. While a typical TMD of ABC transporter contains six transmembrane segments, MacB contains only four transmembrane segments. Another atypical feature of MacB is that the NBD is located at the N-terminus (Kobayashi *et al.*, 2003). We took advantage of the capability of MacAB-TolC in hydrolyzing ATP to study how the three components assemble into a functional complex and how each of the components contributes to the efflux of substrates across two membranes. In this study, we successfully purified and reconstituted MacA and MacB into proteoliposomes and characterized the ATPase activity of MacB in the presence or absence of its cognate MFP. We found that MacA stimulates the ATPase activity of MacB and demonstrated the importance of the C-terminal domain of MacA in forming a functional interaction with MacB.

2.3 Results

2.3.1 Purification of MacA and MacB. Plasmids pBA^{His} and pBB^{His} were constructed by Elena Tikhonova expressing MacA-6His and MacB-6His respectively. For purification of MacA and MacB, these plasmids were transformed into ET103 (BW25113ΔOmpT) *E. coli* strain. Both MacA and MacB are inserted into the inner membrane of *E. coli*. Therefore, membrane fractions were collected and solubilized with Triton X-100 (TX). Proteins were recovered from the TX-soluble fraction using Cu^{2+}-chelate chromatography. Purified proteins were resolved on standard SDS-PAGE. A major band corresponding to MacA (48kDa) was detected on the gel (Fig. 2.1A). Two major bands were observed with purified MacB with MWs of 70kDa and 140kDa (Fig. 2.1B). Both bands reacted with INDIA anti-His probe (Pierce), suggesting that the two bands correspond to monomeric and dimeric forms of MacB. MacB dimers were stable and remained even after boiling in the presence of reducing agents suggesting that the MacB dimers were stabilized by non-disulphide covalent bonds. N-terminal sequencing confirmed that the 140kDa band contains MacB (Tikhonova *et al.*, 2007).

2.3.2 MacA exhibit strong binding to LPS. Lipopolysaccharide (LPS)-like molecules were found in purified MacA preparation and can be clearly detected on tricine-sodium dodecyl sulfate-polyacrylamide gel electrophoresis (TSDS-PAGE) (Fig. 2.2A). The presence of this "LPS" is specific for MacA as no LPS-like molecules were found in our MacB or TolC preparation (Fig. 2.2A). The MacA preparation was tested for presence of 2-keto-3-deoxyoctonate (KDO), which is a normal constituent of LPS. Purified MacA was precipitated with TCA and resuspended in 1% SDS, which is compatible with KDO

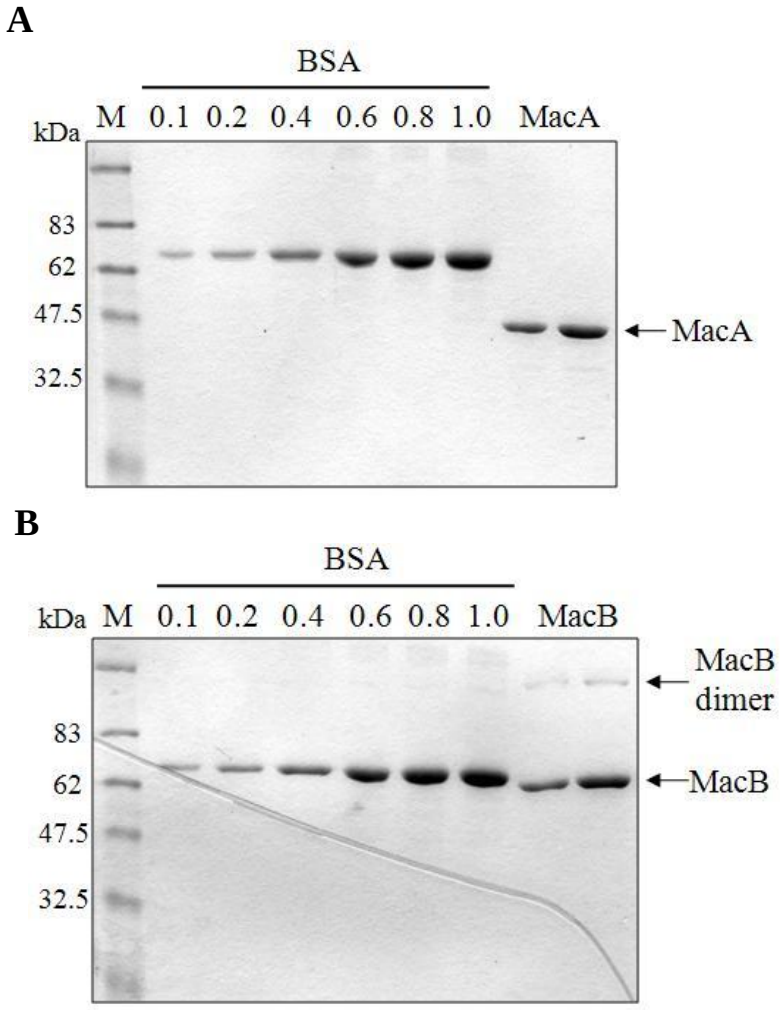

Figure 2.1 Quantitative SDS-PAGE of purified MacA and MacB. BSA in the amounts of 0.1, 0.2, 0.4, 0.6, 0.8 and 1.0 μg and purified MacA (A) or MacB (B) were boiled for 10 min in sample buffer, resolved on SDS-PAGE and stained with CBB.

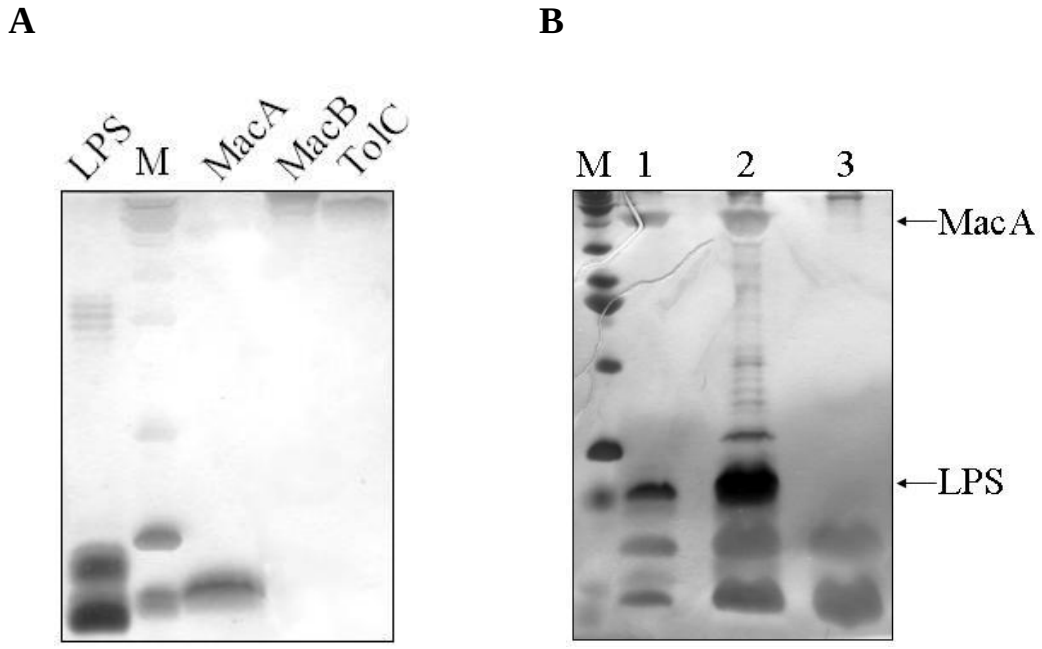

Figure 2.2 TSDS-PAGE of purified MacA, MacB and TolC. (A) 1μg of *E. coli* LPS or purified proteins MacA, MacB and TolC were resolved on TSDS-PAGE and visualized with Bio Rad silver stain. (B) MacA precipitated with TCA and resolubilized in 1% SDS was analyzed for presence of LPS on TSDS-PAGE. (lane 1 – untreated MacA, lane 2-TCA treated MacA, lane 3 – TCA treated MacB)

assay. LPS remained bound to MacA after TCA precipitation (Fig. 2.2B). KDO was detected in MacA samples at 4 moles of KDO per mole of MacA (Fig. 2.3, Table 2.1). In contrast, MacB tested negative for KDO. KDO is a normal constituent of LPS. Therefore, we conclude that the LPS-like band detected in purified MacA preparation is likely to be LPS.

In order to remove LPS from MacA we passed the purified MacA through HiTrap Octyl-Sepharose column. MacA was eluted from the column in both high and low salt concentrations (Fig. 2.4A). Fractions from both high and low salt concentrations were pooled, concentrated with dialysis against 20% PEG (2.5.2 Materials and methods) and tested for presence of LPS using TSDS-PAGE. LPS was detected in both fractions (Fig. 2.4B). However, the mobility of the LPS on the gel appeared diffused unlike the sharp band we see in purified MacA preparation before running the hydrophobic column (Fig. 2.4B, lane 1). The LPS appear to form strong association with MacA. However, we cannot exclude the possibility that the binding condition used was not optimal for separation of LPS from MacA.

An alternative method was used to remove LPS from MacA using Detoxi-Gel™ Endotoxin Removing Gel (Pierce), which utilizes immobilized polymyxin B to bind LPS (see Materials and methods). *E. coli* LPS (Sigma) or MacA were passed through column containing the endotoxin removing gel (Pierce). LPS remained bound to the column and were eluted only in 1% sodium deoxycholate (SDO) (Fig. 2.5A). The LPS found in purified MacA eluted with MacA in column washes (Fig. 2.5B and 2.5C), indicating that LPS bound tightly to MacA.

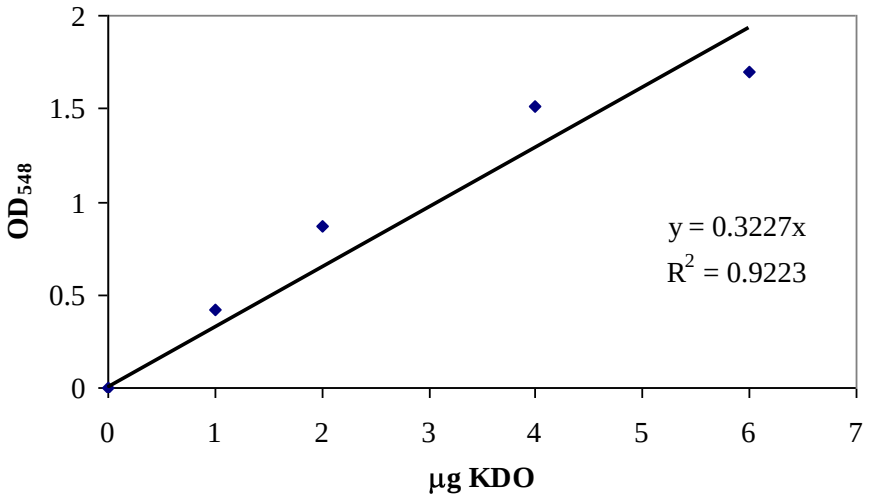

Figure 2.3 KDO standard curve. KDO – 2-keto-3-deoxyoctonate.

MacA (μg)	OD_{548}	μg of KDO	KDO: MacA
12.5μg	0.1082	0.335	4.25: 1
25.0μg	0.2285	0.708	4.50: 1

Table 2.1 KDO content of MacA proteins. Molar ratio of KDO to MacA was calculated with molecular weight (MW) of KDO at 255.22 g/mol and theoretical MW of MacA at 40.6 kDa.

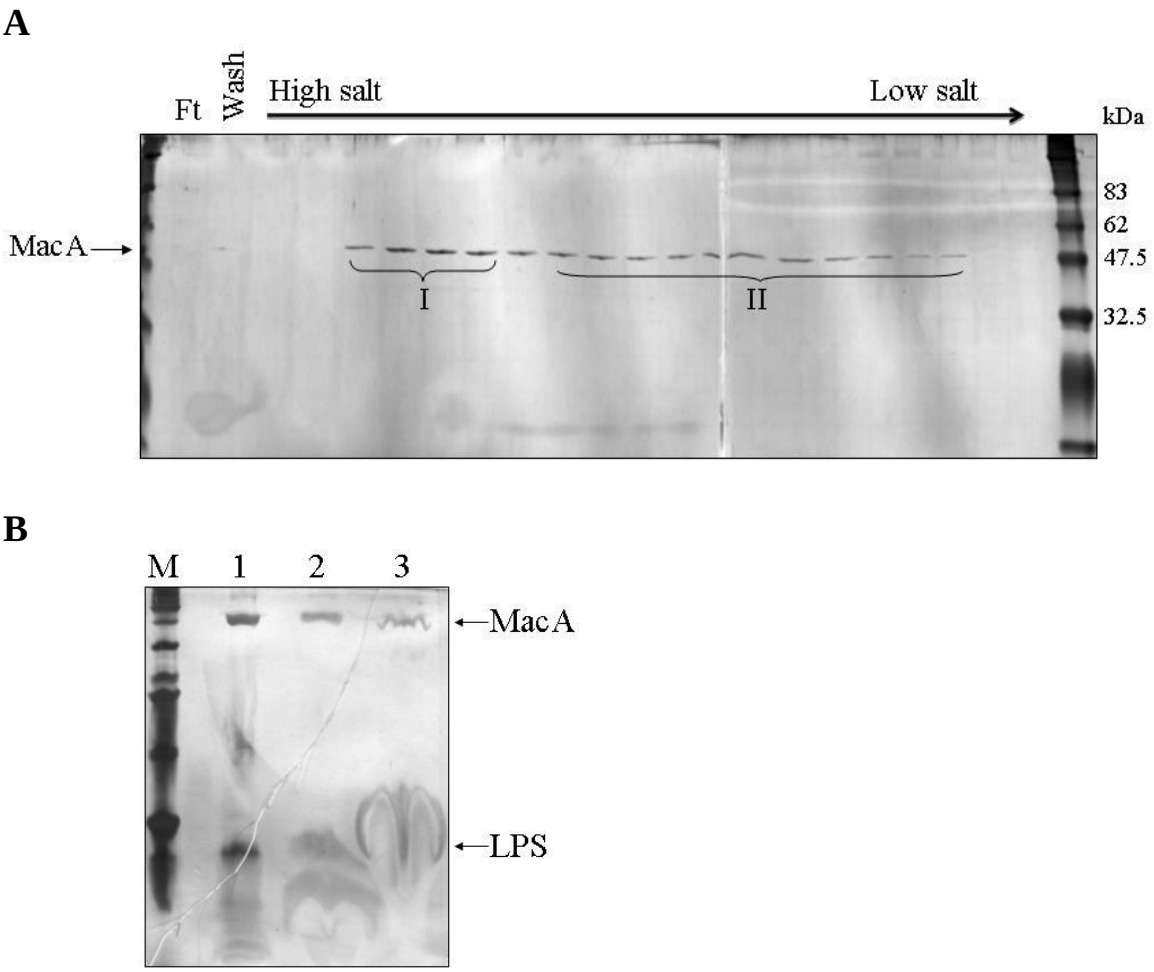

Figure 2.4 SDS-PAGE and TSDS-PAGE of purified MacA. (A) Purification profile of MacA from octyl sepharose column. Samples were resolved on SDS-PAGE and stained with silver stain. (B) TSDS-PAGE of 1 - purified MacA; 2 - MacA pooled from high salt fractions I; 3 - MacA pooled from low salt fractions II.

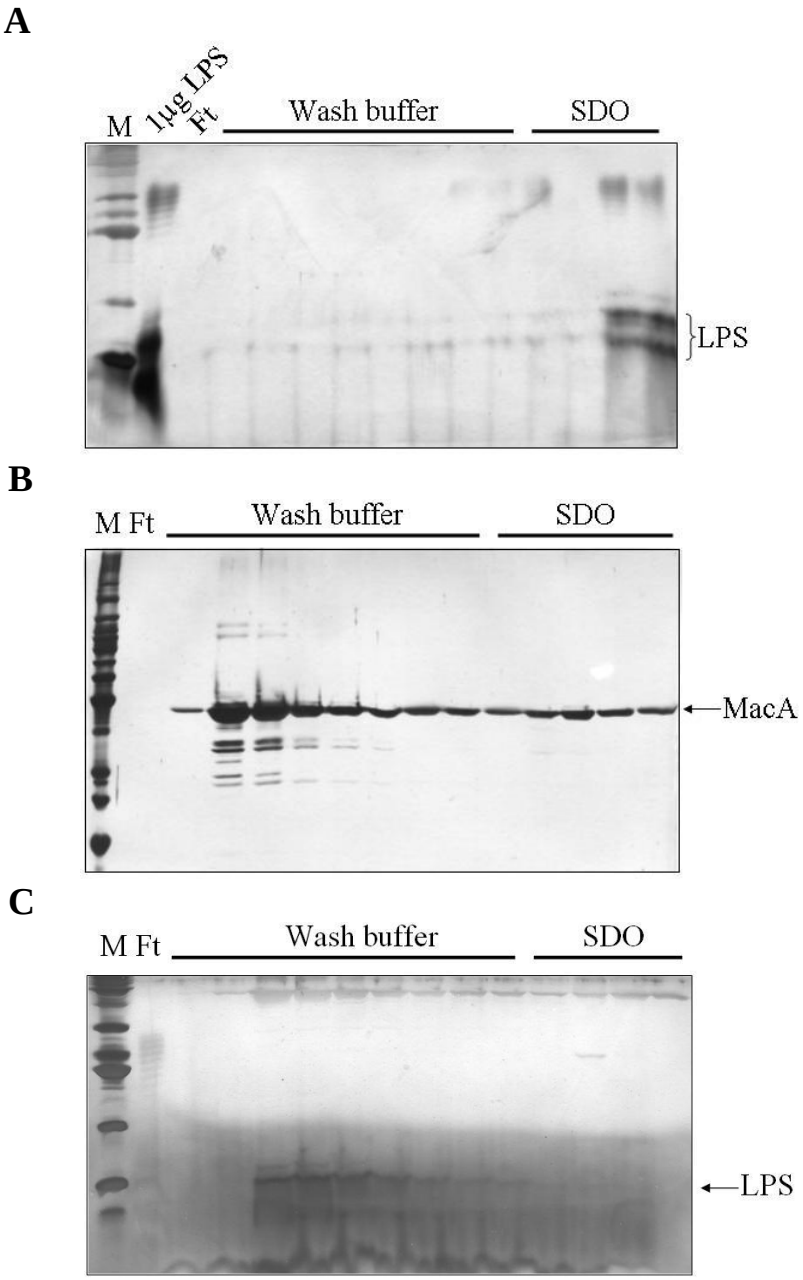

Figure 2.5 Removal of LPS by affinity chromatography. (A) Fractions of *E. coli* LPS eluted from column containing Detoxi-Gel™ Endotoxin Removing Gel were analyzed on TSDS-PAGE. (B) and (C) Silver stained SDS-PAGE and TSDS-PAGE of fractions of MacA eluted from endotoxin removing column respectively.

2.3.3 MacA stimulates the ATPase activity MacB. To investigate whether a functional relationship exist between MacA and MacB, we reconstituted MacA and MacB separately or together into proteoliposomes and tested the ATPase activity of MacB. When present alone in proteoliposome, MacB exhibit a specific activity of 11 ± 2 nmol ATP min^{-1} mg^{-1} (Fig. 2.6). When both MacA and MacB were reconstituted together into proteoliposomes, the ATPase activity of MacB was much more efficient with specific activity of 291 ± 9 nmol ATP min^{-1} mg^{-1}, 25-fold higher than when MacB was reconstituted alone. Elena Tikhonova showed that the LPS-like molecules purified from MacA preparation did not stimulate ATPAse activity of MacB (data not shown). The macrolide oleandomycin and the OM channel TolC also did not stimulate the ATPase activity of MacB (Tikhonova *et al.*, 2007), suggesting that MacA is solely responsible for the stimulation of the ATP hydrolysis by MacB.

2.3.4 The C-terminal domain of MacA is required for its function in vitro an in vivo. Chimeric analysis of AcrA, the MFP component of the multidrug efflux pump AcrAB-TolC of *E. coli*, revealed that the C-terminal domain is important for its interaction with the AcrB multidrug efflux pump (Elkins and Nikaido, 2003). Studies with isothermal titration calorimetry (ITC) showed that the C-terminal of AcrA formed energetically favorable interaction with AcrB (Touze *et al.*, 2004). To test whether the C-terminal of MacA is also important for forming a functional interaction with MacB in vitro, C-terminal mutants of MacA lacking 12, 19, 47, 67, 80 and 90 C-terminal amino acid residues expressed from pET21d(+) plasmid were constructed by Elena Tikhonova. All constructed deletion mutants were readily expressed in *E. coli*. Expression studies were

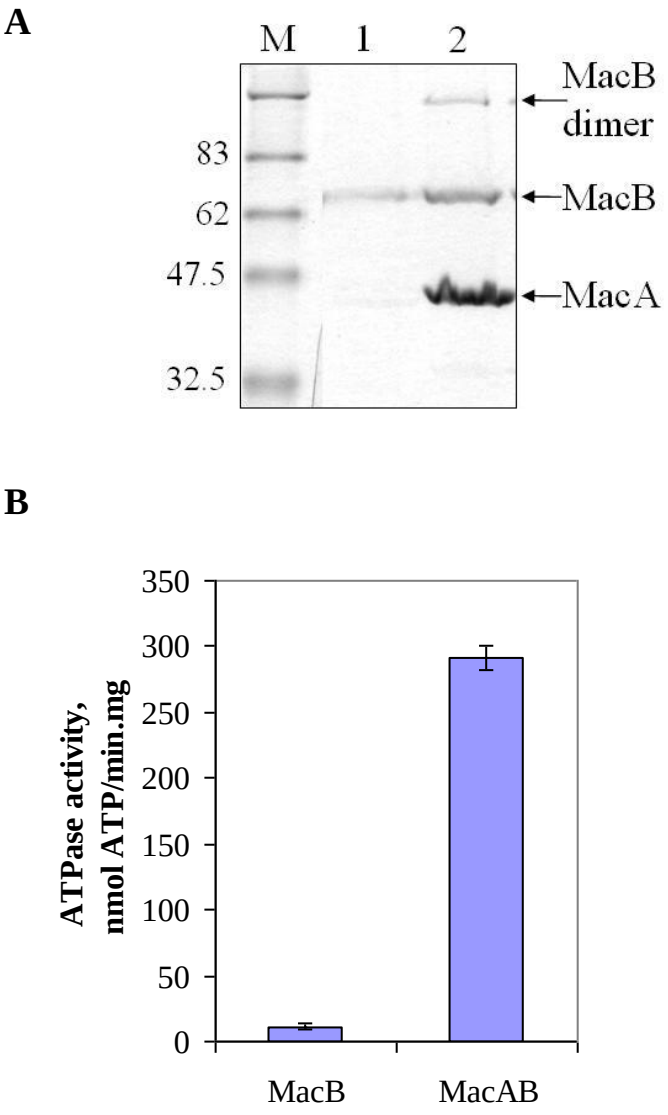

Figure 2.6 MacA stimulation of MacB ATPase activity. (A) Proteoliposomes containing 1—MacB; 2 – MacA and MacB were resolved on SDS-PAGE and stained with CBB. (B) ATPase activity of MacB in the presence or absence of MacA in proteoliposomes.

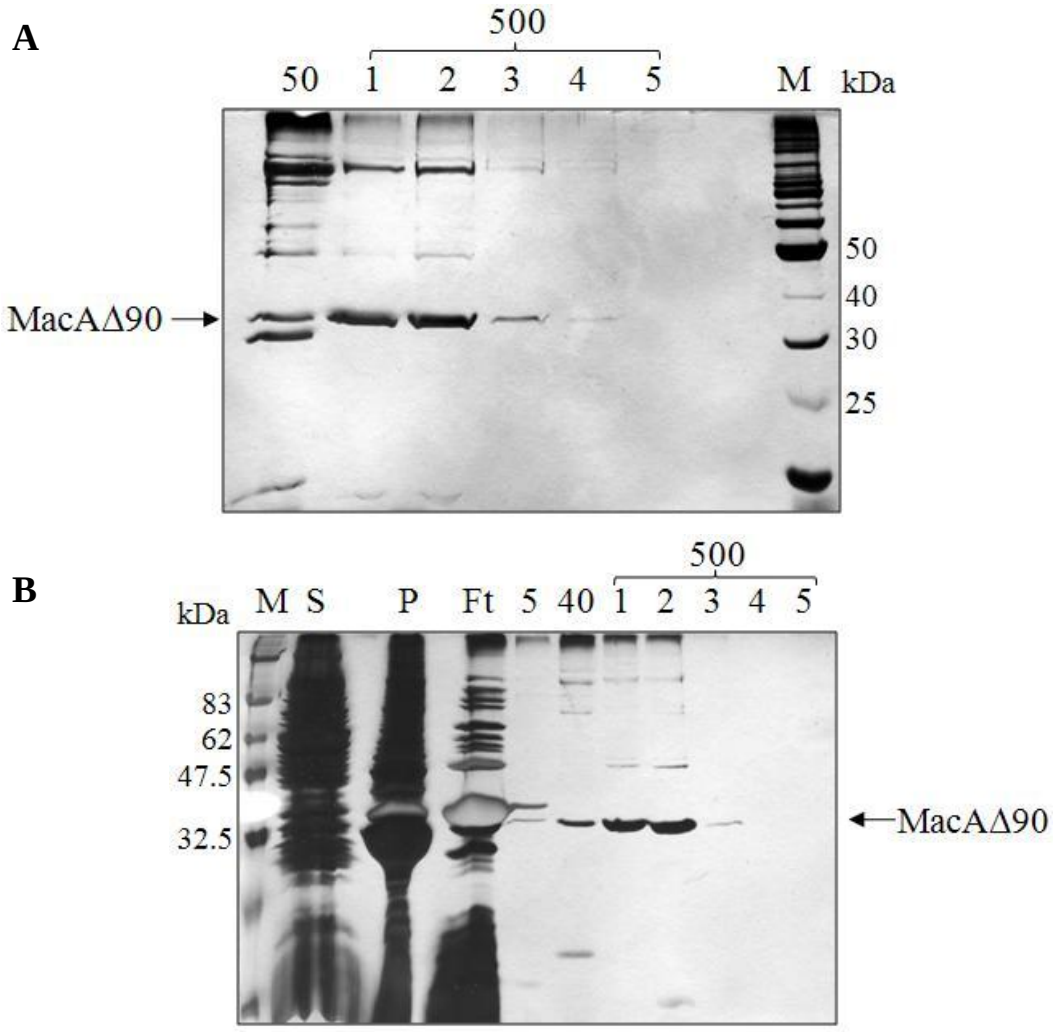

Figure 2.7 Purification of MacAΔ90. (A) Total membranes of ET103/pETAΔ90 were solubilized in 5% TX. The TX soluble fraction was loaded onto Cu^{2+}charged-NTA column and bound protein were eluted with imidazole gradient of 50mM and 500mM. (B) S – TX soluble fraction and P – TX insoluble fraction of ET103/pETAΔ90; TX insoluble fraction was solubilized in 0.6% DDM and soluble fraction was loaded onto Cu^{2+}charged-NTA column and bound protein were eluted with imidazole gradient of 5mM, 40mM and 500mM.

done by Vishakha Dastidar (data not shown). We found that with the exception of MacAΔ90 mutant, all other deletion mutants were insoluble in non-ionic detergents and presumably formed inclusion bodies (data not shown). MacAΔ90 was only partially soluble in Triton X-100 (TX) as the deletion mutant was detected in the TX insoluble fraction (Fig. 2.7B). MacAΔ90 was purified from the TX soluble fraction (Fig. 2.7A) albeit at low concentration. We were able to recover and purify MacAΔ90 from the insoluble fraction using alkyl-β-D-maltoside (DDM) (Fig. 2.7B). However, DDM was shown to irreversibly inactivate the ATPase activity of MacB (Tikhonova *et al.*, 2007). MacAΔ90 was also purified using CTAB, which gives a higher yield of protein. MacA was also purified with the same detergent for the ATPase hydrolysis assay. The purifications were done by Elena Tikhonova. MacAΔ90 purified with CTAB did not stimulate the ATPase activity of MacB (Fig. 2.8). MacA purified using CTAB stimulates the activity of MacB but exhibit a specific activity of 35.5 nmol ATP min^{-1} $mg^{-}1$, 8-fold lower than the stimulation effect of MacA purified using TX (Fig. 2.6 and 2.8), indicating the inhibitory effect of CTAB on ATPase assay. Nevertheless, the stimulation was still 6-fold higher than MacAΔ90, indicating that the C-terminus is required for the stimulation of MacB ATP hydrolysis. Similarly, MacAΔ90 purified from TX soluble fraction did not stimulate the activity of MacB (Tikhonova *et al.*, 2007).

The C-terminus of MacA was also shown to be important for its macrolide transport function. MacAΔ90 deletion mutant when expressed together with MacB from the plasmid $pUA_{\Delta 90}B$ failed to confer resistance to macrolides (Tikhonova *et al.*, 2007). Our results showed that the C-terminal of MacA is important for both the stimulation of MacB ATPase activity in vitro as well as for the function of this protein in vivo.

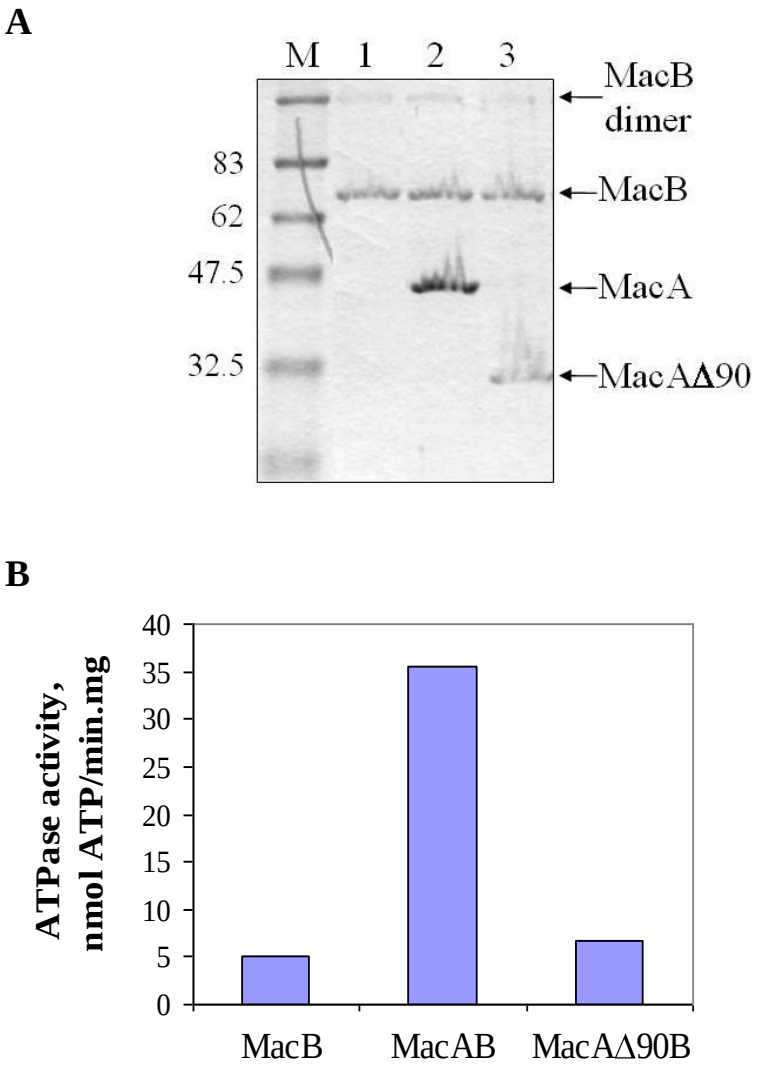

Figure 2.8 MacAΔ90 stimulation of MacB ATPase activity. MacB was reconstituted in proteoliposomes alone or together with MacA or MacAΔ90B purified using CTAB. (A) Proteoliposomes containing 1—MacB; 2 – MacA and MacB; or 3 – MacAΔ90 and MacB were resolved on SDS-PAGE and stained with CBB. (B) ATPase activity of MacB in the presence of MacA or MacAΔ90.

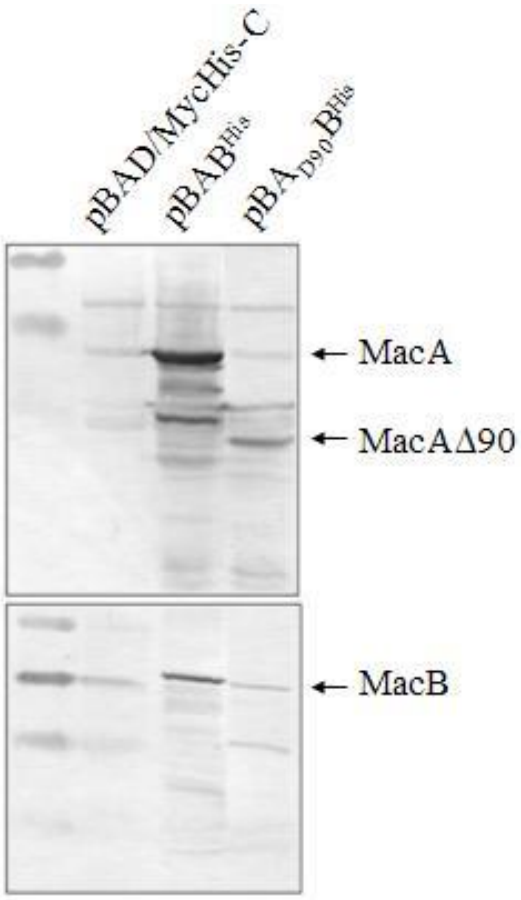

Figure 2.9 Expression of MacAΔ90. Equal amounts of whole cell extracts of ET103 carrying corresponding plasmids were resolved on 12% SDS-PAGE and proteins are identified by immunoblotting. MacA antibody (top); MacB antibody (bottom).

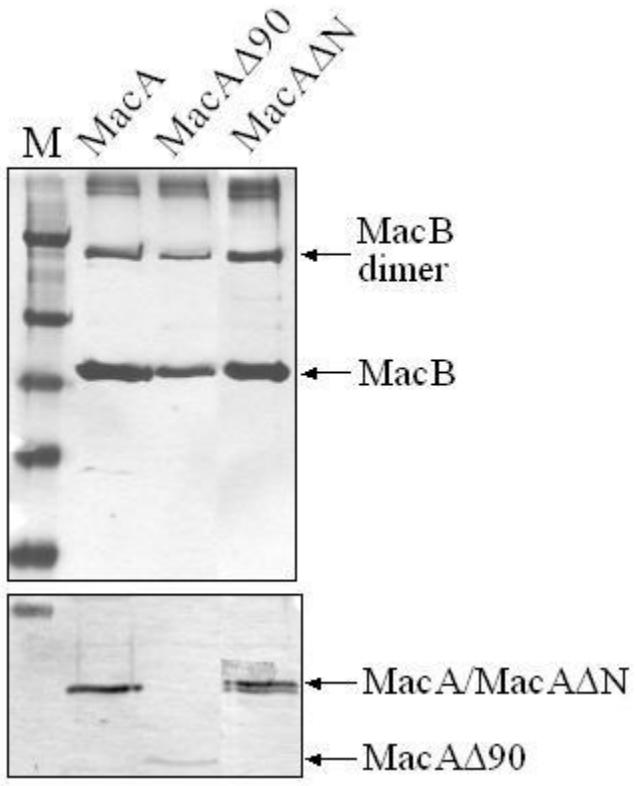

Figure 2.10 C-terminial of MacA is required for interaction with MacB. Proteins (0.5μg) purified from ET103 strain carrying either pBAB^{His}, pBA$_{\Delta 90}$B^{His} or pUA$_{\Delta N}$B^{His} were separated on 12% SDS-PAGE and stained with silver stain (top panel). The same samples were also analyzed by immunoblotting with anti-MacA antibodies.

2.3.5 The C-terminal domain of MacA interacts with MacB. To examine whether the loss of function is due to the loss of interaction with MacB, we examined the copurification of MacA and MacA deletion mutants with MacB-6His. MacAΔ90 deletion mutant was introduced into $pBAB^{His}$ plasmid, obtained from Elena Tikhonova, which contains MacA and six-histidine tagged MacB in a single operon. Both pAB^{His} and $pBA_{\Delta 90}B^{His}$ were introduced into ET103 strain. Immunoblotting analysis with anti-MacA and anti-MacB antibodies revealed that both MacAΔ90 and MacB are produced from the $pBA_{\Delta 90}B^{His}$ construct albeit at levels several folds lower than MacA and MacB produced from pAB^{His} (Fig. 2.9). Nevertheless, MacB-6His was successfully purified from this construct (Fig. 2.10, top panel). Immunoblotting analysis of MacB preparation with anti-MacA antibodies reveal that MacA was reproducibly co-purified with MacB whereas only traces of MacAΔ90 were detected (Fig. 2.10, bottom panel), suggesting that this mutant is defective in its interaction with MacB. MacA devoid of its membrane anchor, MacAΔN was also consistently purified with MacB-6His (Fig. 2.10). Purification studies were done with Vishakha Dastidar. Our results suggested that the periplasmic domain is sufficient for the interaction of MacA with MacB, most likely through its C-terminal domain.

2.4 Discussion

Membrane fusion proteins constitute a novel family of bacterial transport accessory proteins (Dinh *et al.*, 1994). MFP functions with an inner membrane transporter and an outer membrane channel in the efflux of substrates across the two-membrane cell envelope of Gram-negative bacteria. MFPs are proposed to serve a structural role by

acting as a bridge between the IM transporter and OM channel. In this study, we show for the first time that in addition to serving as linkers, MFPs can play an active functional role. Upon reconstitution into proteoliposomes, MacA stimulates the ATP hydrolysis of MacB. The stimulation by MacA is independent of substrates or the outer membrane TolC. MacA is the first member of the MFP family of proteins that was found to stimulate the ATPase activity of its cognate ABC transporter.

Previous studies have implicated the C-terminus domain of MFPs in forming a functional interaction with the IM transporter (Elkins and Nikaido, 2003; Touze *et al.*, 2004). Solved crystal structures of two MFPs, MexA and AcrA (Akama *et al.*, 2004; Higgins *et al.*, 2004; Mikolosko *et al.*, 2006) also supported the role of the C-terminal in interaction with the IM transporter. Structures of both proteins exhibit a central α-helical hairpin, formed when the two central α-helices of the MFPs fold back to form the coiled-coil as predicted (Johnson and Church, 1999) (Fig. I. 1). The hairpin is held together by the interlocking of two lipoyl motifs that flanked the α-helices. The formation of this α-helical hairpin brings the N- and C-terminal into close proximity. Because MFPs are anchored to the IM through the N-terminal via either a transmembrane segment or lipid moiety, this must place the C-terminal near the IM, allowing it to interact with the IM transporter. Consistent with this, the MacA mutant lacking the C-terminal domain MacAΔ90 lost its ability to confer resistance to macrolides in vivo and to stimulate the ATPase activity of MacB in vitro. We showed that MacAΔ90 fails to bind MacB (Fig. 2.10), suggesting that the C-terminal of MFP is essential for forming a functional interaction with its cognate transporter. The crystal structure of AcrB revealed that three AcrB protomers assembled to form a jellyfish-like structure comprising a 50Å

thick transmembrane domain and a 70Å thick periplasmic headpiece (Murakami *et al.*, 2002). The periplasmic headpiece is formed by six large periplasmic loops, two from each AcrB protomer. Regions within the headpiece are thought to form the binding sites for the MFP AcrA. Reminiscent to AcrB, MacB also contains a large periplasmic loop that connects its TM1 and TM2 (Kobayashi *et al.*, 2003), which could interact with the MFP MacA.

The interaction between MFP with components of the efflux complex underlies the mechanism of transport across both membranes. Questions remain as to how these components co-ordinate the efflux process. While the N- and C-terminal of MFPs are situated near the IM, the α-helical hairpin extends half the distance into the periplasmic space. The interaction between the α-helical hairpin and the aperture helices of TolC is proposed to be involved in the opening of TolC (Andersen *et al.*, 2002; Koronakis *et al.*, 2000). Indeed, interacting surface of the MFP AcrA, involved in interaction with TolC, were mapped within the α-helical coiled-coil (Lobedanz *et al.*, 2007). Perhaps the opening of TolC requires energy afforded by the IM transporter, in the case of MacB, through the hydrolysis of ATP. MFP may serve to transduce the energy from the IM component to the opening of the OM channel.

We found in our studies that LPS-like molecules form strong association with MacA. The "LPS" was tested positive for presence of KDO, a normal constituent of LPS. The use of Detoxi-Gel™ Endotoxin Removing Gel (Pierce), which utilizes immobilized polymyxin B to bind LPS/ endotoxins fail to separate MacA from "LPS". Polymyxin B exhibit strong binding to Lipid A moiety of LPS (Issekutz, 1983; Morrison and Jacobs, 1976). Several reasons could explain why LPS fail to bind to the endotoxin gel. First,

MacA could have a stronger affinity for LPS than polymyxin B. Second, MacA bound to the LPS protected it from binding to polymyxin B. It is interesting that LPS, an outer membrane component was found in tight association with and inner membrane protein. Perhaps, MacAB-TolC is involved in cell wall biosynthesis by transporting LPS to the outer membrane. LPS could be the natural substrate of the pump. The physiological functions of drug efflux pumps remain a subject of interest. It is thought that these pumps extrude drugs that happen to resemble the natural substrates of the pump. Therefore, drug efflux is only secondary to the physiological roles of these pumps. However, the detrimental impact of drug efflux in the treatment of bacterial infections is evident and continues to pose serious threat to human health. Understanding the functions of these pumps will help us gain more insight to how these pumps work and therefore find better ways treat these bacterial infections.

2.5 Materials and Methods

Media and growth conditions, standard protein assays and total membrane fractionation are described in appendices D, E and F respectively.

2.5.1 Plasmid construction. Plasmid $pBA_{\Delta 90}B^{His}$ was constructed by PCR using $pBAB^{His}$ as a template. $pBAB^{His}$ was amplified using the forward primer fMacBXbaI and the reverse primer rMacAdel90XbaI, both containing the XbaI restriction site. The amplified PCR product was restricted with Xba I restriction enzyme and religated using T4 DNA ligase.

2.5.2 Purification of His-tagged proteins using Cu^{2+} chelate chromatography. For purification of MacB-His, total membranes of ET103/pBB^{His} cells (Tikhonova *et al.*, 2007) were collected and resuspended in 5% Triton X-100: Membranes were first resuspended with binding buffer [20mM Tris-HCl (pH 7.0), 200mM NaCl, 1mM PMSF, 2mM $MgCl_2$, 0.05mM β-mercaptoethanol and 5mM imidazole]. An equal volume of 10% Triton X-100 (TX) in binding buffer was added to the membrane suspension and allowed to mix overnight by stirring at 4^0C. Triton insoluble fraction was removed by ultracentrifugation at 70,000 x g for 30min. Solubilized membrane proteins were loaded onto Cu^{2+}charged NTA column equilibrated with binding buffer containing 0.2% TX (equilibration buffer). The column was washed with an imidazole gradient of 5mM, 20mM, 40mM, 100mM and 250mM in equilibration buffer. Majority of MacB elutes in the 100mM imidazole fraction. This fraction was dialyzed with storage buffer containing 20mM HEPES-KOH (pH 7.7), 2mM DTT, 200mM NaCl, 1mM PMSF, and 0.2% TX to remove imidazole. MacB was concentrated by dialysis against 20% polyethylene glycol (PEG) in 20mM HEPES-KOH (pH 7.7), 2mM DTT, 200mM NaCl, and 1mM PMSF and kept in storage buffer containing 50% glycerol.

MacA and MacAΔ90 expressed from ET103/pBA^{His} and ET103/pETAΔ90 respectively were purified in the same way with the following modifications. MacA was purified from membranes solubilized in 5% TX. Binding buffer contains 20mM HEPES-KOH (pH7.7), 500mM NaCl, 1mM PMSF and 5mM imidazole. Cu^{2+}-NTA column was equilibrated with the same buffer supplemented with 0.2% TX. The column was washed with imidazole gradient of 5mM, 20mM, 50mM, 100mM and 500mM. MacAΔ90 was purified from membranes solubilized either in 5% TX or 0.6% alkyl-β-D-maltoside (DDM).

Binding buffer contains 20mM Tris-HCl (pH8.0), 500mM NaCl, 1mM PMSF and 5mM imidazole. Cu^{2+}-NTA column was equilibrated with the binding buffer supplemented with 0.2% TX. The column was washed with an imidazole gradient of 5mM, 40mM, 50mM and 500mM. Majority of MacA and MacAΔ90 elute in the 500mM imidazole fraction. The fraction was dialyzed in with storage buffer containing 20mM HEPES-KOH (pH 7.7), 200mM NaCl, 1mM PMSF, and 0.2% TX to remove imidazole. Purified MacA and MacAΔ90 was concentrated by dialysis against 20% PEG in 20mM HEPES-KOH (pH 7.7), 200mM NaCl, and 1mM PMSF and kept in storage buffer containing 50% glycerol.

2.5.3 ATP hydrolysis assay. The rate of ATP hydrolysis by MacAB in proteoliposomes was assayed in 10μL of reaction mixture. Proteoliposomes containing 0.2μg of ATPase were mixed in buffer containing 20mM HEPES-KOH (pH7.0), 5mM DTT, 50mM KCl, 2mM $MgCl_2$, and 1mM Mg-ATP. The ^{32}P γ-phosphate labeled ATP (3000 Ci $mmol^{-1}$, Amersham) was mixed with unlabelled Mg-ATP prior to addition into the reaction mix. The molar ratio of MFP: ATPase was adjusted to 3: 1. The reaction was initiated by incubating the reaction mixture in 37 ^{0}C waterbath. Aliquots of 1 μL were removed at different time points and added to 10 μL of stop buffer containing 50 mM Tris-HCl (pH 8.0), 20 mM EDTA, 0.5 % SDS, 200 mM NaCl and 0.5 mg mL^{-1} proteinase K. The hydrolysis of ^{32}γ-ATP was analyzed using thin-layer chromatography. 1μL of samples were loaded onto PEI-F cellulose (10cm x 20cm). The mobile phase contained 10% formic acid and 0.5mM LiCl. Hydrolyzed Pi was quantified using Storm PhosphoImager and ImageQuant software (Molecular Dynamics).

2.5.4 Octyl-Sepharose column. Purified MacA was prepared in buffer A containing 20mM HEPES (pH 7.7), 2M $(NH_4)_2SO_4$, 1mM PMSF, 0.1% DDM and 5% glycerol and passed through HiTrap Octyl-Sepharose column (Amersham Biosciences). The column was washed with buffer A followed by a decreasing $(NH_4)SO_4$ gradient. Fractions eluted from the column were resolved on 12% SDS-PAGE and TSDS-PAGE.

2.5.5 Removal of LPS by affinity chromatography. Purified MacA (400 μg) or 750(μg) lipopolysaccharide (LPS) (Sigma) was prepared in buffer containing 20mM HEPES-KOH (pH 7.7), 200mM NaCl, 1mM PMSF and 0.2% TX (equilibration buffer) and loaded onto column containing Detoxi-Gel™ Endotoxin Removing Gel (Pierce), equilibrated with the equilibration buffer, and allowed to incubate for 2hrs. Unbound protein was washed from the column with the same buffer. Bound LPS was eluted from the column with 1% sodium deoxycholate (SDO).

2.5.6 Tricine-sodium dodecyl sulfate-polyacrylamide gel electrophoresis (TSDS-PAGE). TSDS-polyacrylamide gel was prepared as described in (Lesse *et al.*, 1990). Separating gels were prepared by adding 16.6mL of stock solution A (49.5% acrylamide and bisacrylamide, 6% bis), 16.6mL gel buffer (3.0M Tris-HCl (pH 8.45), 0.3% SDS), 10.4mL 50% glycerol, 11.5mL water, 100μL 10% ammonium persulfate solution (APS) and 10μL TEMED. Stacking gels were prepared by adding 1mL stock solution B (49.5% acrylamide and bisacrylamide, 3% bis), 3.1mL gel buffer, 150μL 10% APS and 15μL TEMED. Anode buffer [0.2M Tris-HCl (pH 8.9)] and cathode buffer [0.1M Tris-HCl (pH8.25), 0.1M tricine, 0.1% SDS] were used for gel electrophoresis. The electrophoresis

was carried out at 100 V for approximately 6-8 h or 1 h after the bromophenol blue dye front had left the gel. Gels were stained with Bio Rad oxidative silver stain (catalog #: 161-0443).

2.5.7 Trichloroacetic acid (TCA) precipitation. Purified MacA, MacB or BSA were incubated in [10% TCA, 20mM HEPES-KOH (pH 7.7)] for 1hr on ice. Precipitated proteins were pelleted at 13,200 rpm for 5-10 min on a Eppendorf microcentrifuge. The pellets were resuspended in 1mL cold acetone (-20^{0}C) and vortexed. After acetone wash, proteins were pelleted at 13,200 rpm for 5-10 min on a Eppendorf microcentrifuge and dried for 10min in vacuum drier. Pellets were resuspended in 1% SDS (compatible with KDO assay) and boiled for 10min. Samples were resolved on TSDS-PAGE and visualized with Bio Rad oxidative silver stain.

2.5.8 KDO assay. 2-keto-3-deoxyoctonate (KDO) was determined by thiobarbituric acid as described in http://www.cmdr.ubc.ca/bobh/methods/KDOASSAY.html based on the method of (Weissbach and Hurwitz, 1959). KDO was first extracted from protein samples as follows: 25μL of protein sample was added to 25μL of 0.5N H_2SO_4 and vortexed. The mixture was heated for 8min at 100^{0}C and cooled to room temperature (RT). (This step is omitted for pure KDO). 25μL of 2.28% H_5IO_6 was added to the mixture, vortexed and permitted to stand for 10min at RT. 100μL of [4% $NaAsO_2$ in 0.5N HCl] was added to the mixture. After vortexing, 400μL of 0.6% thiobarbituric acid (made fresh before use) was added to the mixture and vortexed. The mixture was boiled for 10min at 100^{0}C and allowed to cool to RT. When the mixture had cooled, 750μL of

butanol was added to the mixture. The mixture was mixed by vortexing followed by low speed centrifugation on tabletop centrifuge for 5min at 2000rpm. The upper butanol layer was collected and optical density was measured at 548nm. To generate a standard curve, different amounts of pure KDO (Sigma) at 1μg, 2μg, 4μg and 6 μg were subjected to the same treatment. Heating after addition of 0.5N H_2SO_4 is omitted for KDO.

Chapter 3

Reconstitution of YknWXYZ, an MFP-dependent ABC Transporter System in *Bacillus subtilis*

3.1 Abstract

MFP homologues functioning as essential accessory proteins of ABC type transporters were also identified in Gram-positive bacteria, which do not have a two-membrane cell envelope. These findings suggest that MFP may play more than just a structural role in the efflux process. Recent studies with the macrolide extrusion pump MacAB-TolC from *Escherichia coli* showed that the MFP MacA stimulates the ATPase activity of MacB (Tikhonova *et al.*, 2007), an ABC type transporter, thus pointing to the role of MFP as an active efflux component. To examine whether MFPs from Gram-positive bacteria also play an active role in the efflux process, we examined the functional properties of reconstituted MacAB homologue, YknXYZ from the Gram-positive bacteria *Bacillus subtilis*. The *yknWXYZ* operon encoding YknX, YknY, YknZ and an unknown protein YknW is implicated in providing self-resistance to endogenously produced peptide toxin, SdpC (Butcher and Helmann, 2006). YknX, YknY and YknZ are the putative MFP, ATPase and permease respectively. We cloned and expressed the *Bacillus* proteins: YknW, YknX and the fusion protein YknY-YknZ (YknYLZ) in *E. coli*. We showed that YknX stimulates the ATPase activity of YknYLZ in lipid vesicles. YknX cannot substitute MacA in stimulating the ATPase activity of MacB, suggesting that the YknX stimulation of YknYLZ is specific. Our results suggest that the MFPs of both Gram-

negative and Gram-positive bacteria play an active functional role by stimulating the activity of a corresponding transporter.

3.2 Introduction

Membrane Fusion Proteins (MFP), constitute a homologous family of extracytoplasmic proteins that allow the transport of molecules across both the inner membrane (IM) and outer membrane (OM) of Gram-negative bacteria (Dinh *et al.*, 1994). MFPs are essential components of various transport systems including those from the Major Facilitator Superfamily (MFS), ATP-binding Cassette Superfamily (ABC) and the Resistant-Nodulation-Cell Division (RND) family. These transporters form a tripartite complex that spans the two-membrane cell envelope of Gram-negative bacteria, thus facilitating the extrusion of substrates directly into the medium, bypassing the periplasm. MFPs are thought to act as the physical link between the IM and OM components of the transport system. MFPs are anchored to the cytoplasmic membrane through an N-terminal transmembrane segment or a lipid moiety, while the rest of the protein extends into the periplasm. AcrA, the MFP component of the multidrug resistant pump AcrAB-TolC of *E. coli*, was shown to be an elongated protein capable of spanning the periplasm (Avila-Sakar *et al.*, 2001; Zgurskaya and Nikaido, 1999a). The crystal structure of MexA of the multidrug resistance pump MexAB-OprM of *Pseudomonas aeruginosa* revealed an elongated structure with a length of 89Å (Higgins *et al.*, 2004). Biochemical evidences showed that MFPs can interact with both the IM and OM components. AcrA was found to form cross-linked complexes with its cognate transporter AcrB and the OM channel TolC (Husain *et al.*, 2004; Touze *et al.*, 2004; Zgurskaya and Nikaido, 2000a).

MFPs were thought to be unique to Gram-negative bacteria, but structural homologues of MFPs have also been identified in Gram-positive bacteria that lack an OM membrane, suggesting that MFPs may play more than just a structural role (Harley *et al.*, 2000). The Gram-positive MFPs function as essential components of ABC transporters such as SapT which is involved in the production of the bacteriocin sakacin A in lactobacillus sake (Axelsson and Holck, 1995). It is unclear whether the functions of MFPs from Gram-positive bacteria are similar to that of Gram-negative bacteria. In order to investigate whether the functional role of MFPs are conserved in both Gram-negative and Gram-positive bacteria, we purified and reconstituted in vitro a MacAB homologue from *Bacillus subtilis*, YknXYZ and assessed the ability of the Gram-positive MFP in stimulating the ATP hydrolysis of its cognate transporter.

3.3 Results

3.3.1 Identification of the MacAB homologues in *Bacillus subtilis.* Using Blast search we identified four proteins that showed sequence homology to MacB: YvrO, YvrN, YknY and YknZ. YvrO and YknY are putative ATP-binding proteins, whereas YvrN and YknZ are putative permeases. The ATP-binding protein YvrO, showed a 53% identity and 74% similarity to the nucleotide binding domain (NBD) of MacB, whereas YknY showed 48% identity and 73% similarity. Both YvrO and YknY contains the highly conserved Walker A and B consensus nucleotide binding motif and the LSGGQ signature motif of ABC transporters (Jones and George, 2004) (Fig. 3.1, data shown for YknY only). The permease YvrN exhibit a 30% identity and 50% similarity to the transmembrane domain (TMD) of MacB, whereas YknZ exhibits a 33% identity and 55%

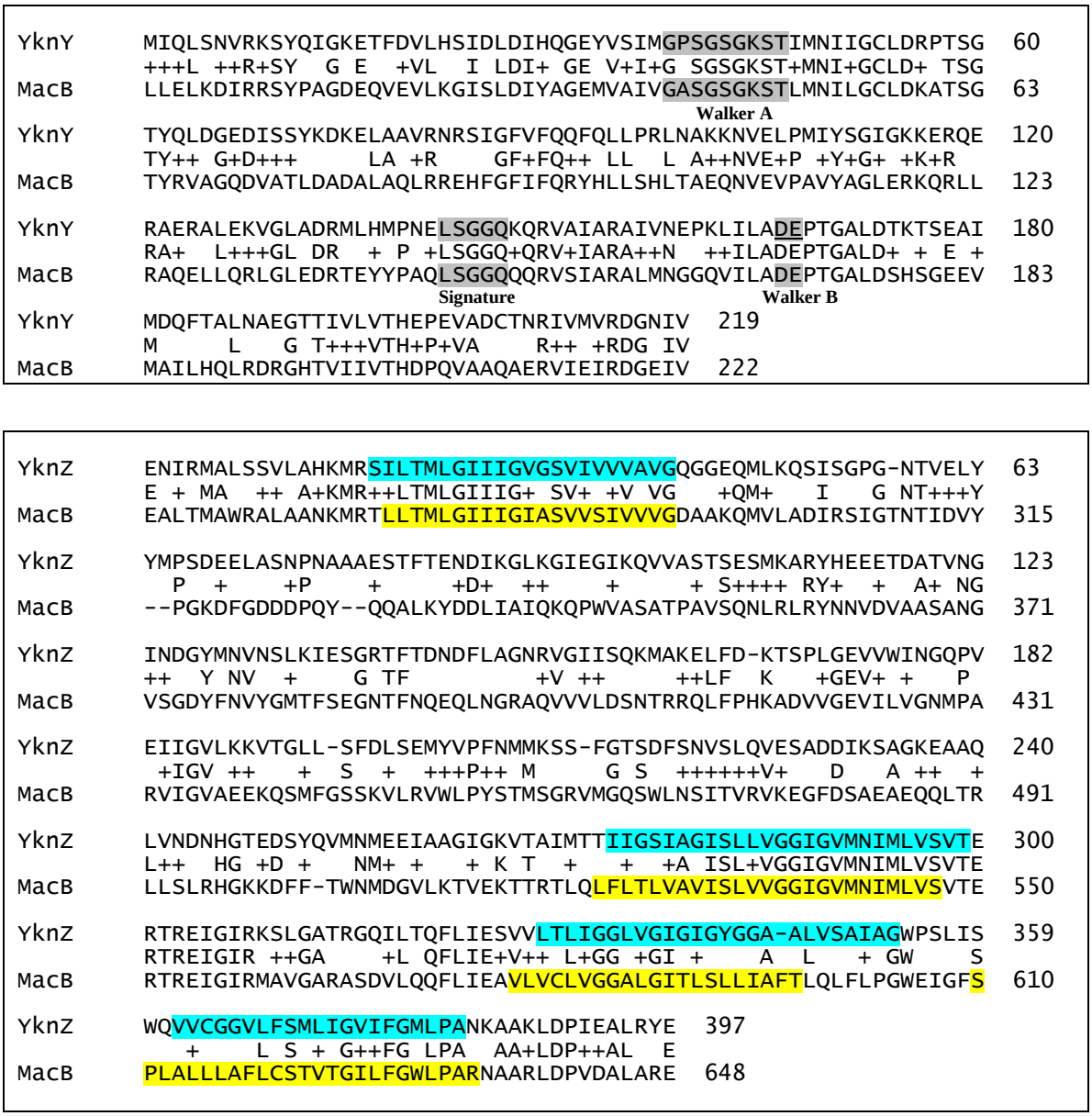

Figure 3.1 Alignment of YknY and YknZ protein sequences to MacB (*Top*) Sequence alignment of YknY to Nucleotide Binding Domain (NBD) of MacB. Grey highlights consensus sequences of ABC transporters. (*Bottom*) Sequence alignment of YknZ to transmembrane domain (TMD) of MacB. Transmembrane segments in YknZ and MacB are highlighted in cyan and yellow respectively

similarity. The sequence similarity between MacB and putative ABC transporters in Gram-positive organisms such as MsrA was shown to be restricted to the ATP binding domain (Kobayashi *et al.*, 2001b). However, the sequence similarity between MacB with YvrN and YknZ extends into the TMD (Fig. 3.1, data shown for YknZ only). Hydropathy analysis revealed that similar to the TMD of MacB, YvrN and YknZ contain four predicted transmembrane segments (TMS) (Fig. 3.2B). Global TMS alignment of YvrN and YknZ with MacB revealed that the TMS1 and TMS2 have high sequence conservation (Fig. 3.1, data shown for YknZ only), suggesting that a common function exist.

MFP-dependent transporters are usually encoded in the same operon with its cognate MFP. The same is true for YvrON and YknYZ. *yvrON* genes are encoded within an operon that encodes a putative MFP YvrP, which exhibits 22% identity and 41% similarity to MacA. Similarly, *yknYZ* genes are encoded within an operon that also encodes a putative MFP YknX, which exhibit 21% identity and 42% similarity to MacA. Hydropathy analysis of YvrP and YknX revealed that both proteins contain a putative N-terminal transmembrane helix (Fig. 3.2B data shown for YknX only). YknX is also predicted to have a signal peptide (Tjalsma *et al.*, 2000). Encoded within the same operon as YknXYZ, is a fourth component YknW (Fig. 3.2A), the function of which is not known. YknW is predicted to be a membrane protein with five transmembrane helices (Fig. 3.2B) and homologues are often encoded either upstream or downstream of *yknXYZ*-like genes in other *Bacillus* strains (Butcher and Helmann, 2006). The *yknWXYZ* operon is implicated in providing self-resistance to endogenously produced SdpC toxin in the absence of the immunity protein SdpI. The *yvrPON* operon is found to be regulated

A


YknW
YknX
YknY
YknZ

B

YknW

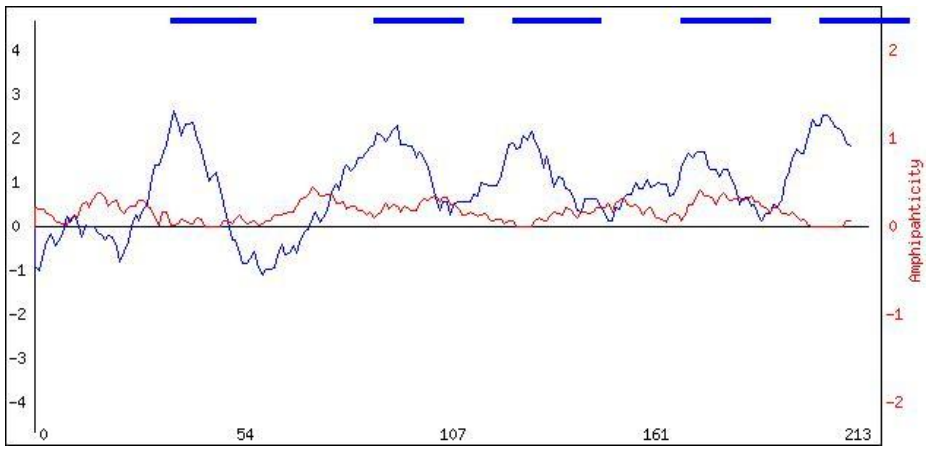
4
3
2
1
0
-1
-2
-3
-4
0
54
107
161
213
2
1
0
-1
-2
Amphipahticity

YknX

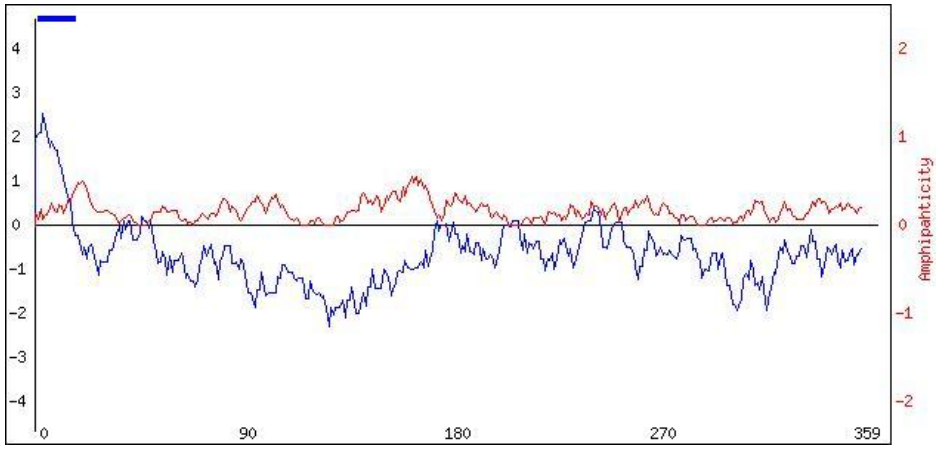
4
3
2
1
0
-1
-2
-3
-4
0
90
180
270
359
2
1
0
-1
-2
Amphipahticity

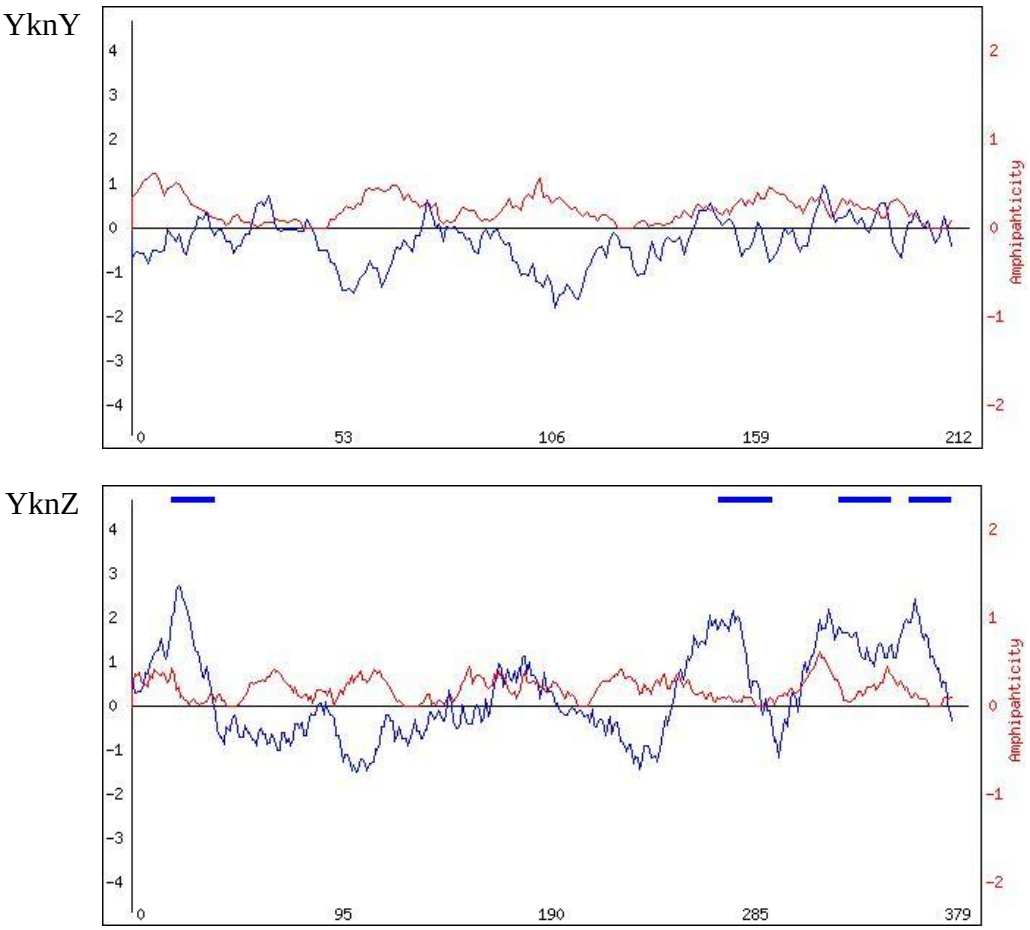

C

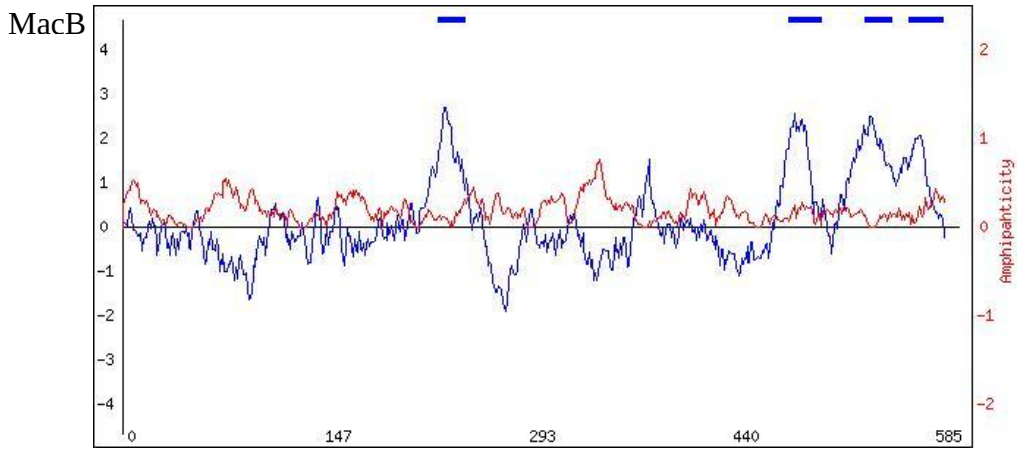

Figure 3.2 *yknWXYZ* operon and hydropathy analysis. (A) *yknWXYZ* operon. (B) Hydropathy anaylysis of YknW, YknX, YknY and YknZ. (C) Hydropathy analysis of MacB. (Blue curve – hydropathy; Red curve – amphipathicity; Blue bars – putative TMS)

by ComK competence transcription factor but its function is unknown (Berka *et al.*, 2002). It is unclear what role does MFP play in the transport systems of Gram-positive bacteria or whether the MFPs from Gram-positive and Gram- negative bacteria share similar mechanisms. It was demonstrated that the MFP MacA stimulates the ATPase activity of MacB in vitro (Tikhonova *et al.*, 2007). To examine whether the role of MFP is conserved in both Gram-negative and Gram-positive bacteria we cloned y*vrPON* and y*knWXYZ* genes for reconstitution studies. We wanted to test whether the Gram-positive MFP also stimulates the ATPase activity of its cognate ATPase in vitro.

3.3.2 Expression of *yvrPON* in *E. coli.* To test the functionality of YvrPON in marcrolide transport in *E. coli*, *yvrPON* operon was cloned into pUC18 as described in Materials and Methods. The resulting plasmid, pUC-YvrPON was transformed into DH5α. Membrane fractionation (Appendix F) was carried out with DH5α/pUC-YvrPON, grown to exponential phase. No bands corresponding to YvrP or YvrN was detected, suggesting that these proteins were not expressed. A 30kDa band corresponding to YvrO was found in the membrane fraction albeit at very low level (data not shown). We next cloned the *yvrPON* operon into an arabinose inducible expression vector pBAD/MycHis-C. The expression of YvrPON from the resulting plasmid, pBPON^{His}, in DH5α *E. coli* strain was induced at different concentrations of L-arabinose. Membrane fractionation revealed that a 30kDa band corresponding to YvrO was detected in the membrane fraction after 2 hours of induction with 0.1% arabinose (Fig. 3.3A). YvrO is a hydrophilic ATP-binding protein and was expected to be found in the soluble fraction. Its localization to the membrane fraction could be due to association with a membrane component.

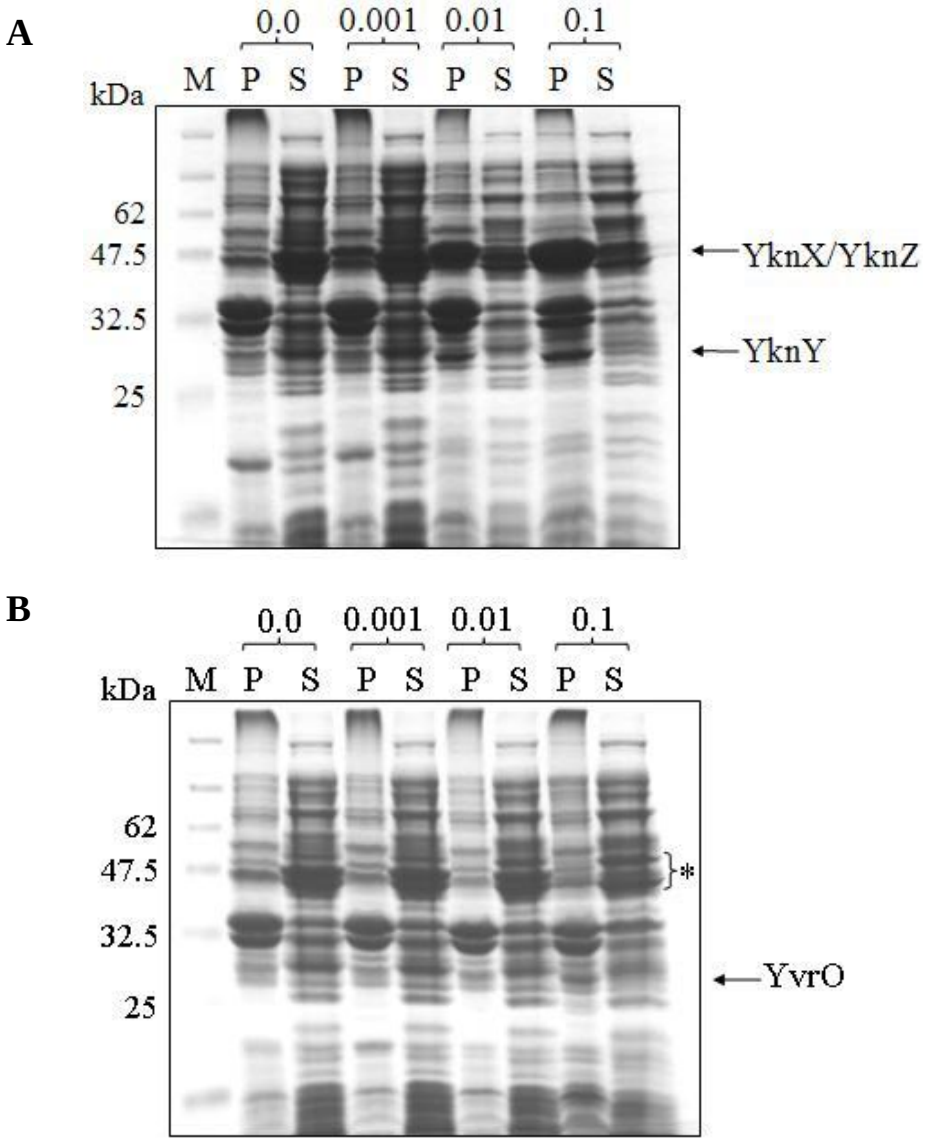

Figure 3.3 Expression of YknXYZ and YvrPON. Membrane fractionation of DH5α strain carrying (A) pBXYZ^{His} or (B) pBPON^{His} after 2hrs of induction at different concentration of arabinose. P – membrane fraction; S – soluble fraction. (*) represents differential protein expression.

However, no bands corresponding to YvrP or YvrN was detected in the membrane fraction. Unexpectedly, differential protein expression was observed in the soluble fraction. A 50kDa band was induced whereas a 47.5kDa band was missing. The identity of these proteins remained to be clarified. Our results suggest that the expression of *yvrPON* could be toxic to *E. coli*.

3.3.3 Expression of and localization of YknWXYZ in *E. coli.* Similar to YvrPON, we wanted to test the function of YknXYZ in macrolide transport in *E. coli*. *yknXYZ* operon was cloned into pUC18 and the resulting plasmid, pUC-YknXYZ was transformed into DH5α. However, yknXYZ was not expressed from this construct. We next cloned *yknXYZ* into an arabinose inducible expression vector, pBAD/MycHis-C. The expression of YknXYZ from the resulting plasmid pBXYZ^{His} in DH5α *E. coli* strain was induced at different concentrations of L-arabinose. Membrane fractionation revealed that a 30kDa band corresponding to YknY was detected in the membrane fractions when induced with 0.01% arabinose (Fig. 3.3A). Similar to YvrO, YknY is a hydrophilic ATP-binding protein (Fig. 3.2). Its localization to the membrane fraction could also be due to association with a membrane component. Another band running close to the 47.5 kDa marker corresponding to either YknX or YknZ was overexpressed at the same arabinose concentration. Since the proteins share sequence homology to MacA and MacB, we tried to detect the proteins using MacA and MacB antibodies. Neither antibody reacted with the 47.5kDa band. Since YknZ is tagged with six histidines, we used INDIA anti-His probe (Pierce) to detect YknZ-His. The INDIA anti-His probe did not react with the band (data not shown), suggesting that the 47.5kDa band is YknX. Our results suggested that

YknZ was either not expressed from the construct or that expression was too low for detection. We were unable to express all three proteins for functional assay.

To test the function of these proteins in vitro, genes encoding YknW, YknX, YknY and YknZ were cloned separately into pET21d(+) vector, under the control of T7 promoter. To facilitate purification, six-histidine tags were added to the C termini of each protein. Plasmids $pETW^{His}$, $pETX^{His}$, $pETY^{His}$ and $pETZ^{His}$ were transformed into BL21(DE3) expression strain and expression of each was induced with 1mM of isopropyl-β-D-thiogalactopyranoside (IPTG). To examine the expression of the *Bacillus* proteins, whole cell extracts before and after induction were analyzed by sodium dodecyl sulfate-polyacrylamide gel electrophoresis (SDS-PAGE). To determine the intracellular localization of expressed *Bacillus* proteins in *E. coli*, strains carrying the corresponding plasmids were harvested and disrupted by sonication. The total membrane fraction and soluble fraction were separated by ultracentrifugation. Both the fractions were resolved by SDS-PAGE and visualized by staining with Coomassie brilliant blue (CBB). YknX showed high levels of expression in BL21(DE3) (Fig. 3.4A) with apparent molecular weight (MW) of 50kDa. As expected, YknX, which contains a putative N-terminal transmembrane domain localized in the membrane (Fig. 3.4B). YknY also showed high levels of expression in BL21(DE3) (Fig. 3.4C) with an apparent MW of 31kDa. The ATPase YknY, homologous to the cytoplasmic NBD of MacB, is hydrophilic (Fig. 3.2B) and localized in the soluble fraction (Fig. 3.4D).YknW and YknZ on the other hand, were not detected (data not shown).

It is possible that the overexpression of these membrane proteins is toxic for *E. coli*. A mutant host C43(DE3), a derivative of BL21(DE3) which allows the over-

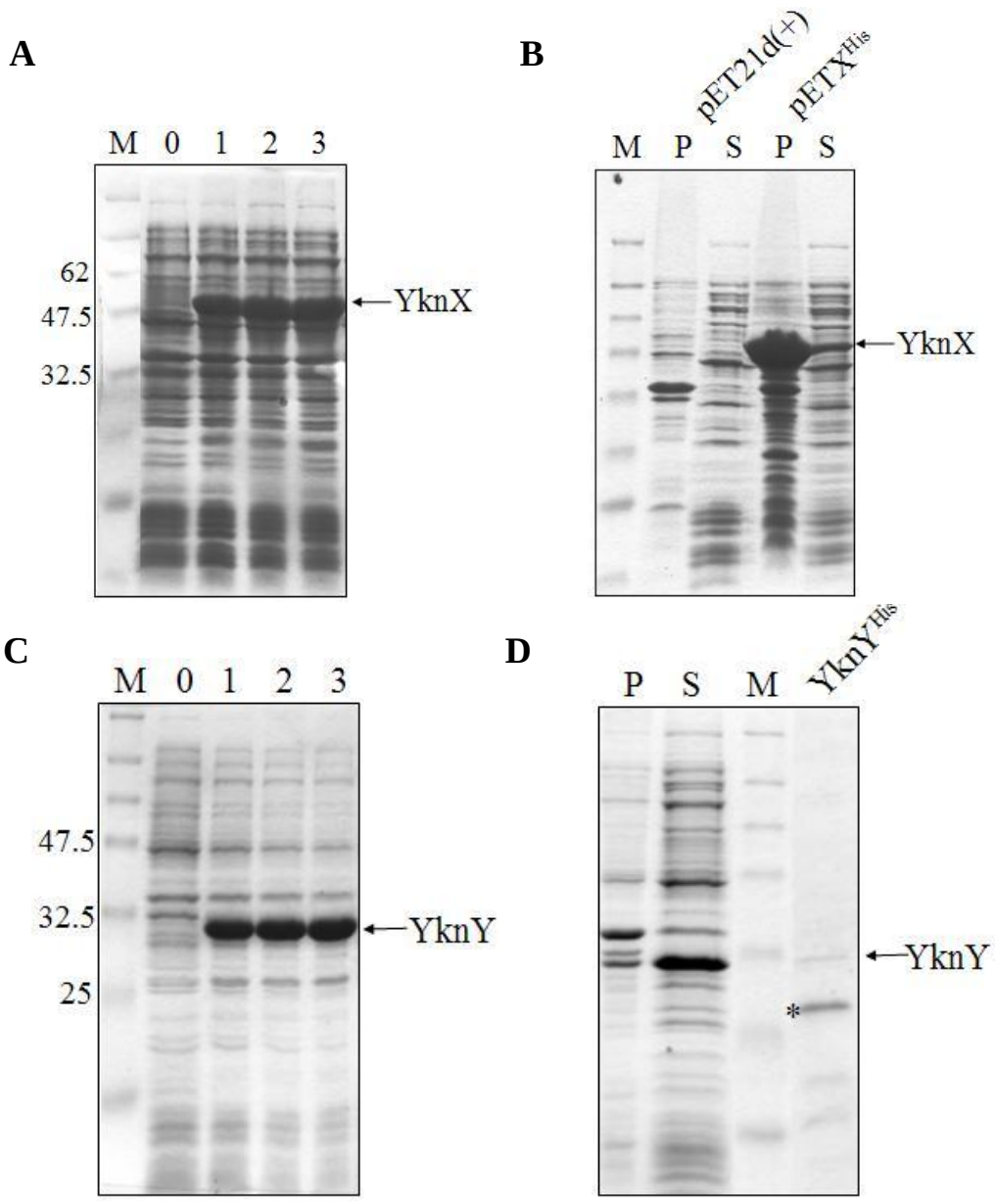

Figure 3.4 Expression and localization of YknX and YknY. (A) and (C) Whole cell extracts of BL21(DE3) carrying pETX^{His} or pETY^{His} were collected at different time points after induction with 1mM IPTG and resolved on 12% SDS-PAGE and stained with CBB. (B) and (D) Membrane fractionation of BL21(DE3)/ pETX^{His} or pETY^{His}; P – Membrane fraction, S – Soluble fraction. YknY^{His} – YknY purified from C43(DE3)/pETY^{His}. Samples were separated on 12% SDS-PAGE and stained with CBB. (*) represents YknY degradation product.

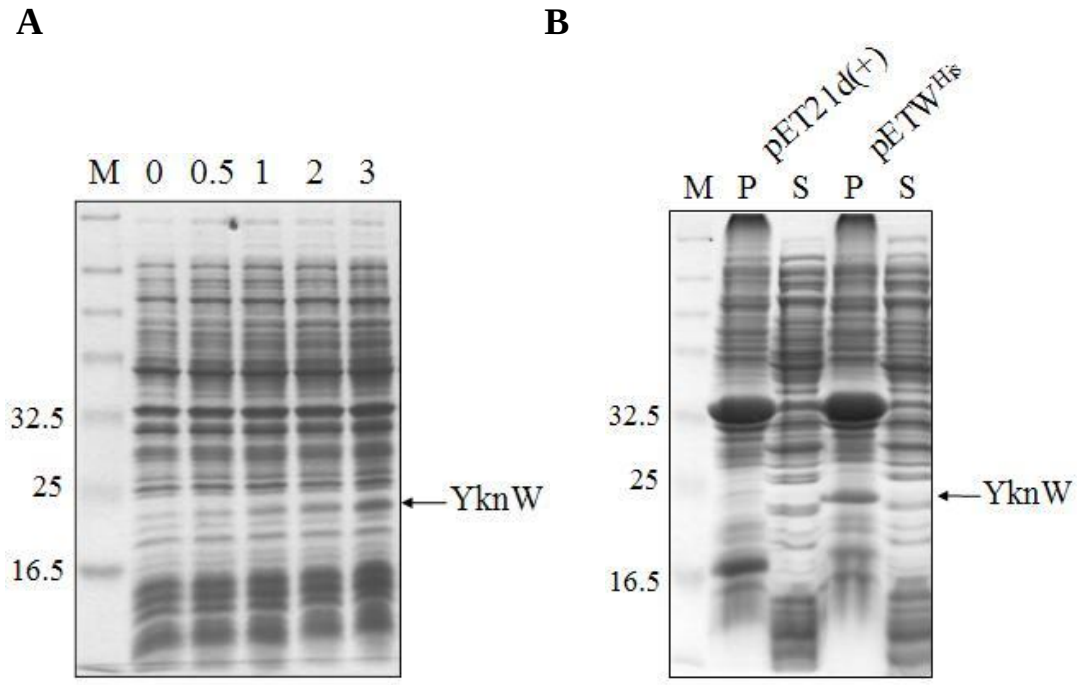

Figure 3.5 Expression and localization of YknW. (A) Whole cell extracts of BL21(DE3) carrying pETW^{His} were collected at different time points after induction with 1mM IPTG and resolved on 12% SDS-PAGE and stained with CBB. (B) Membrane fractionation of BL21(DE3)/pET21d(+) or pETW^{His}; P – Membrane fraction, S – Soluble fraction. Samples were separated by 12% SDS-PAGE and stained with CBB.

production of membrane proteins in *E. coli* (Miroux and Walker, 1996) was used for expression of YknW and YknZ. Only YknW can be expressed in this strain albeit at very low levels (Fig. 3.5A). YknW has an apparent MW of 23kDa. Expression can be seen only after 3 hours of induction. YknW, a predicted membrane protein comprising five putative transmembrane segments is also localized in the membrane (Fig. 3.5B). Prolonged induction up to 24 hrs did not improve the level of expression (data not shown). YknZ was not expressed under similar conditions. In order to test whether the expression of YknZ is dependent on YknY, yknYZ genes are cloned into pET21d(+) vector and checked for expression. YknY was expressed but no YknZ was detected (data not shown).

3.3.4 Purification of histidine-tagged YknW, YknX and YknY. Both YknW-6His and YknX-6His were purified from Triton X-100 (TX) soluble membrane fraction. Total membrane fractions collected from cells expressing YknW-6His or YknX-6His were solubilized in 5% TX. Insoluble fractions were removed by ultracentrifugation and His-tagged proteins were purified from the soluble fractions using Cu^{2+} affinity chromatography. The cytoplasmicYknY-6His was purified from soluble fraction following initial removal of total membrane fraction. Purified proteins were analyzed on SDS-PAGE and visualized with silver stain (Fig. 3.6A) or immunoblotting with INDIA anti-His probe (Fig. 3.6B). Two major bands can be observed for purified YknW corresponding to the previously observed 23kDa band and a second band, which ran lower that the 16.5kDa marker. The smaller band may correspond to the degraded product of YknW. However, both the bands failed detection with the anti-His probe (Fig.

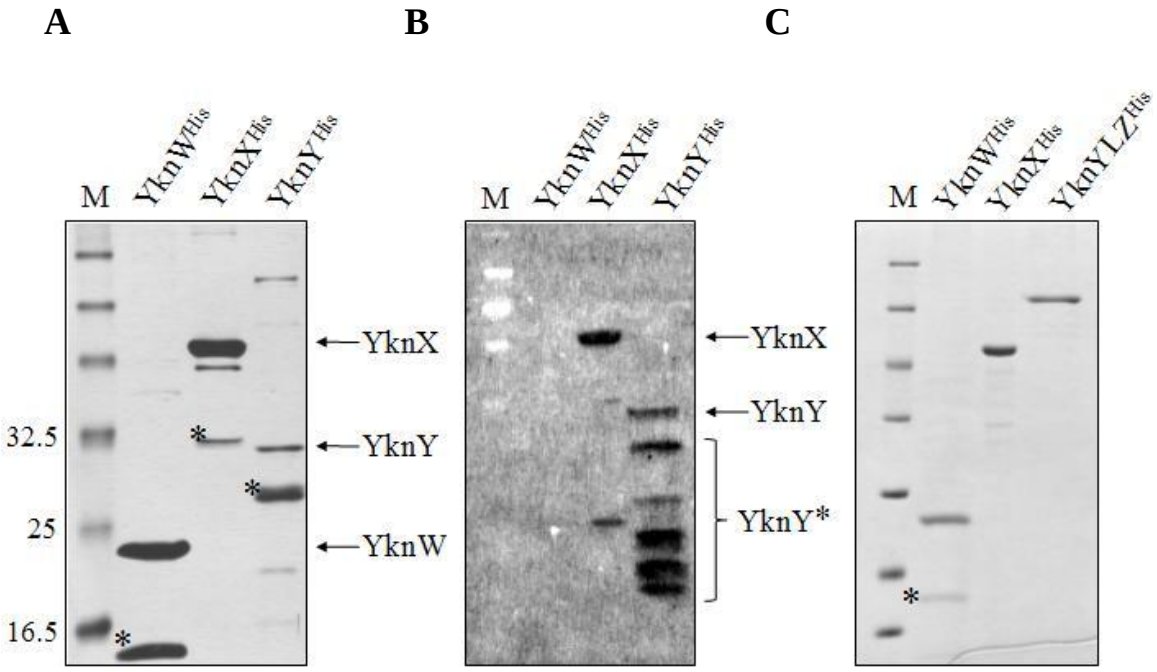

Figure 3.6 Purification of YknW, YknX and YknY. (A) Purified YknW, YknX and YknY were resolved on 12% SDS-PAGE and visualized by silver stain. (B) Immunoblotting analysis of purified proteins using INDIA anti-His probe (Pierce). C. Purified YknW, YknX and YknYLZ were resolved on 12% SDS-PAGE and stained with CBB.

3.6B). It is possible that the C-terminal His-tagged is cleaved and thus could not be detected. A 50kDa band corresponding to purified YknX was detected on silver stained SDS-PAGE along with several smaller bands (Fig. 3.6A). All observed bands were detected by the anti-His probe (Fig. 3.6B), and thus could correspond to degraded products of YknX-6His. The overproduced 31kDa YknY was detected on SDS-PAGE, not as a major band but a minor band (Fig. 3.4D and 3.6A). Instead, a 28kDa major band was detected as well as several other smaller bands. Both the 31kDa and 28kDa bands were detected by the anti-His probes. Smaller bands corresponding to degradation products of YknY can also be detected (Fig. 3.6B). Both the 31kDa and 28kDa bands remain stable under storage in 50% glycerol containing buffer.

3.3.5 YknX cannot stimulate the ATPase activity of MacB. The ATP hydrolysis activity of MacB was shown to be stimulated by MacA (Tikhonova *et al.*, 2007). To determine whether the MacA homologue YknX can stimulate the ATPase activity of MacB, we measured the rate of ATP hydrolysis by MacB when reconstituted into proteoliposomes together with YknX. YknX did not stimulate the ATPase activity of MacB (Fig. 3.7). The stimulation of MacB by MacA was shown to be concentration dependent, achieving a half-maximum stimulation when the molar ratio of MacB: MacA was about 2:3 (Tikhonova *et al.*, 2007). To verify that the lack of stimulation is not due to the condition tested, we measured the ATPase activity of MacB at different molar ratio of MacB: YknX. Under all tested conditions, YknX showed no stimulation of MacB (Fig. 3.8), revealing that the functional relationship between the MFP and its cognate transporter is specific and is not interchangeable.

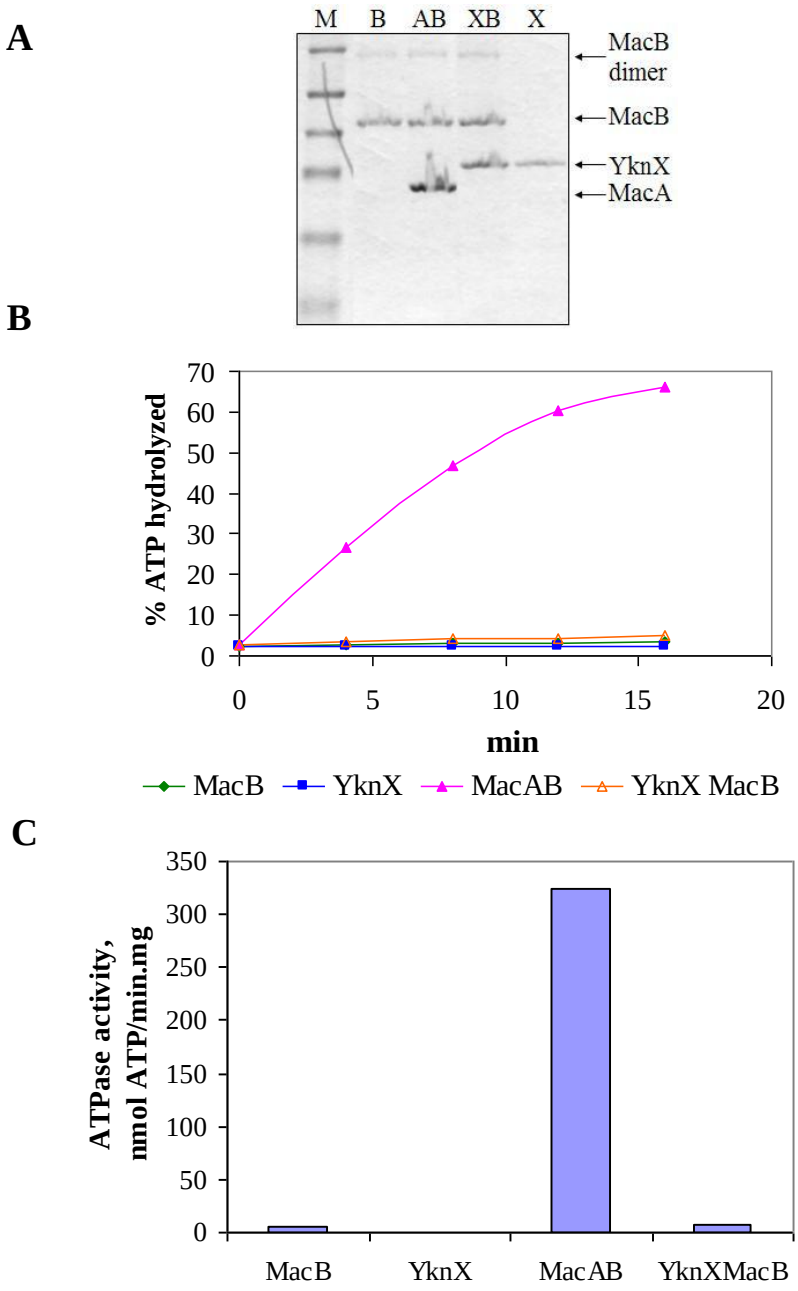

Figure 3.7 ATPase activity of MacB reconstituted into proteoliposomes. (A) Proteoliposomes containing MacB, MacAB, YknXMacB, or YknX were resolved on 12% SDS-PAGE and stained with CBB. (B) Relative rate of ATP hydrolysis. (C) Specific activity of reconstituted MacB

A

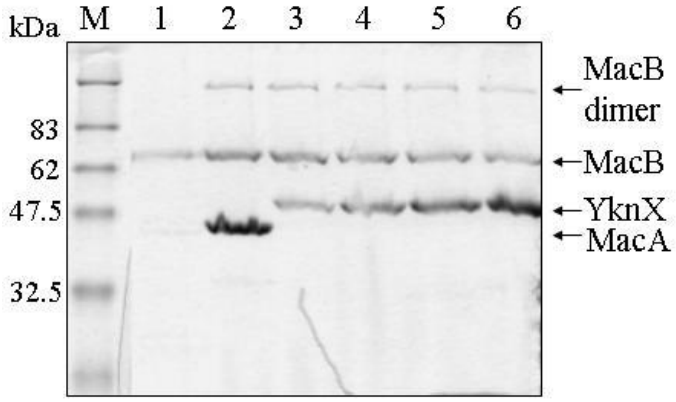

B

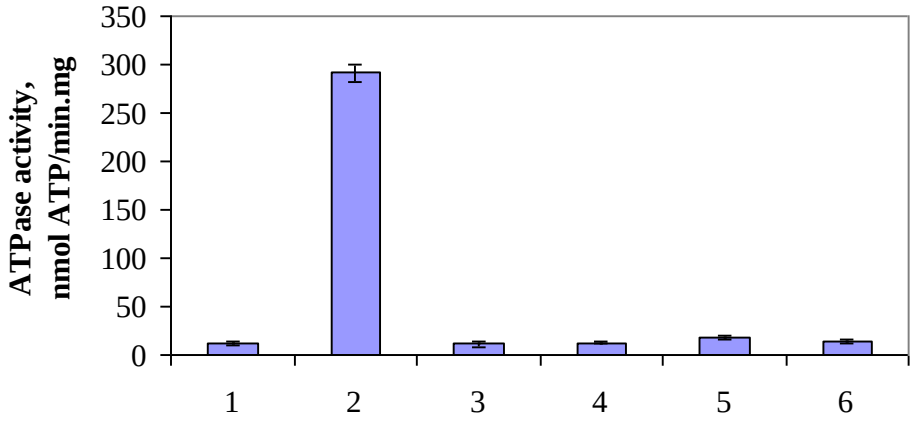

Figure 3.8 ATPase activity of MacB reconstituted into proteoliposomes. (A) MacB was reconstituted into proteoliposomes at different molar ratio of MacB: YknX. (lane 3 – 1:1, lane 4 – 1:2, lane 5 – 1:3, lane 6 – 1:6). Proteoliposomes were resolved by 12% SDS-PAGE and stained with CBB. (B) Specific activity of reconstituted MacB.

3.3.6 YknY purified from *E. coli* is an active ATPase. To ascertain whether an active ATPase was purified, we tested the ATP hydrolysis of the purified YknY in detergent solution. The rate of ATP hydrolysis in the reaction mixture containing 0, 0.25, 0.5, 1.0 or 1.5 μg of total protein was measured and we found that the rate of ATP hydrolysis increased with increasing amount of purified YknY (Fig. 3.9). The purified YknY exhibited the specific ATPase activity of 38 nmol ATP min^{-1} mg^{-1} of protein.

3.3.7 Construction of YknY-YknZ fusion protein. Attempts to express YknZ protein in *E. coli* were unsuccessful. *E. coli* could suppress the expression of YknZ due to its toxic effects. YknZ may lack the targeting sequence that can be recognized by *E. coli*. Even though membrane proteins in *Bacillus* are also secreted through a similar sec pathway, the secretory signals may vary between the two species. In order to cope with this problem, we constructed a fusion protein between YknY and YknZ. The stretch of amino acid linking the NBD and TMD of MacB was used to link YknY and YknZ (Fig. 3.10A). The YknY-YknZ fusion protein mimics the *E. coli* MacB protein (compare Fig. 3.10B and 3.2C). The linker region was PCR amplified with flanking XhoI sites. The linker was restricted and inserted into pETY plasmid to yield $pETYL^{His}$. The yknZ gene was subsequently introduced in the $pETYL^{His}$ plasmid. The resulting plasmid, $pETYLZ^{His}$ was transformed into BL21(DE3) strain. The fusion protein YknYLZ was expressed in *E. coli* at low level after two hours of induction (Fig. 3.11). YknYLZ has an apparent MW of 70kDa. Increasing the induction time did not increase the level of expression (data not shown). YknYLZ was found in the membrane fraction (P), suggesting that the fusion protein is properly targeted to the cell membrane of *E. coli*.

A

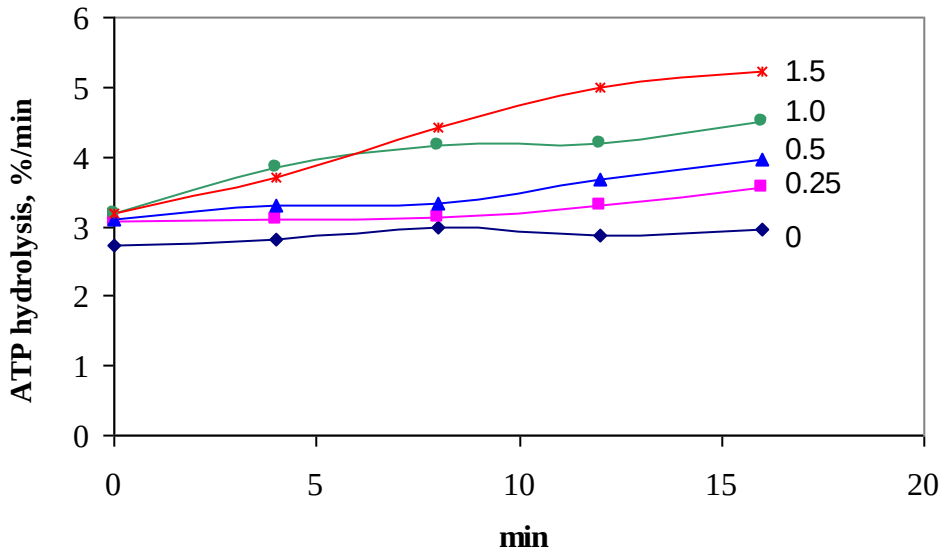

B

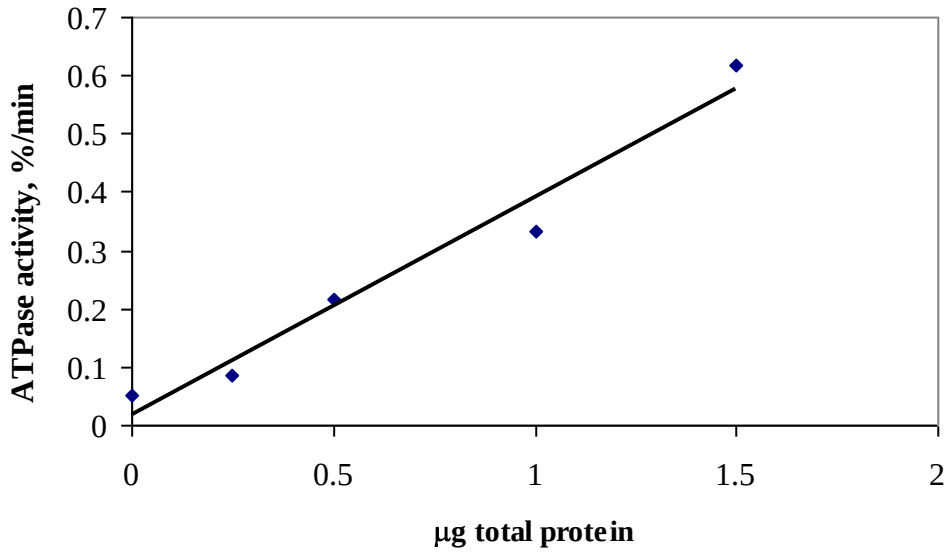

Figure 3.9 ATPase of YknY. (A) and (B) ATP hydrolysis of YknY in detergent solution. The rate of ATP hydrolysis was determined at varying amounts (0, 0.25, 0.5, 1.0 or 1.5µg) of YknY preparation.

A

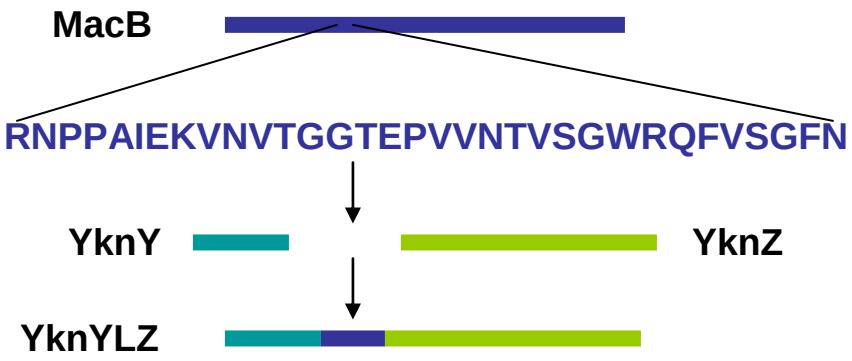

B

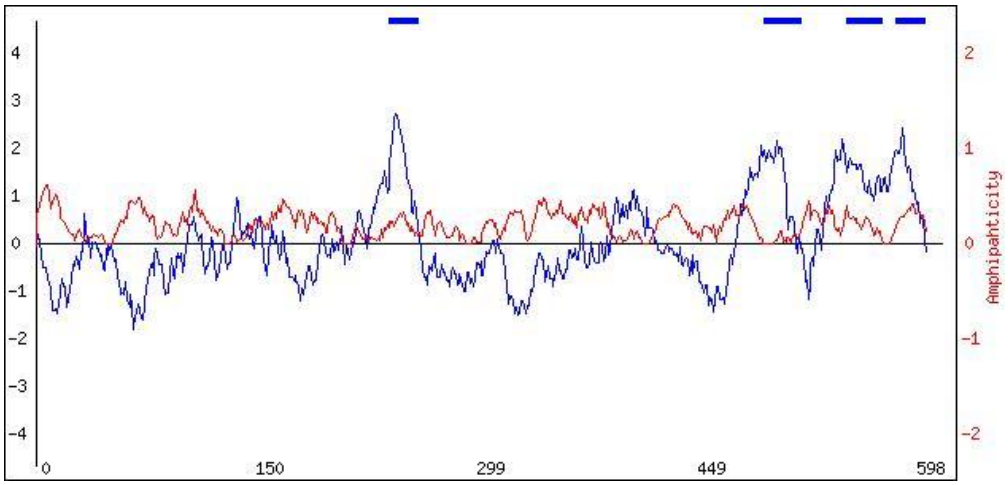

Figure 3.10 Construction of YknY-YknZ fusion protein (YknYLZ). (A) The amino acid stretch that links the NBD and TMD of MacB was used as a linker between YknY and YknZ proteins. (B) Hydropathy analysis of YknYLZ. (Blue curve – hydropathy; Red curve – amphipathicity; Blue bars – putative TMS)

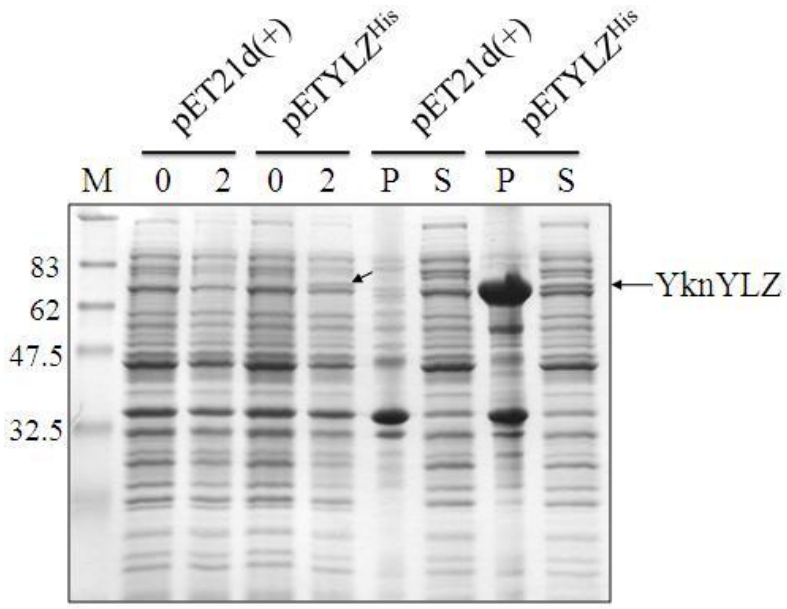

Figure 3.11 Expression and localization of YknYLZ. Whole cell extracts of Bl21(DE3) strain carrying pET21d(+) or pETYLZ^{His} w collected at 0 or 2 hrs after IPTG induction as well as insoluble (P) and soluble (S) fractions collected from membrane fractionation were analyzed on 12% SDS-PAGE and stained with CBB.

3.3.8 YknYLZ is insoluble in most common detergents tested. During our initial attempt to purify of YknYLZ, we found that TX failed to solubilize YknYLZ from *E. coli* membranes. We tried several other commonly used detergents including Alkyl-β-D-maltoside (DDM), CHAPS, octyl-polyoxyethylene (octyl-POE), sarkosyl, octyl glucoside (OG) and Igepal (Nonidet-P40). We found that YknYLZ was completely solubilized in 1% sarkosyl and only partially solubilized in 0.05% Igepal (IG). None of the other detergents tested could solubilize YknYLZ (Fig. 3.12A). We also tested the solubility of YknYLZ with lysophosphatidylglycerol (LPG), which was shown to be useful for solubilizing membrane proteins with strong tendency to aggregate (Huang *et al.*, 1998). LPG solubilized YknYLZ completely. YknYLZ was detected only in the soluble fraction after LPG treatment (Fig. 3.12B). Because sarkosyl is a strong denaturant, the milder detergents Igepal and LPG were used for purification of YknYLZ.

3.3.9 Purification of YknYLZ. To purify YknYLZ-6His, total membrane of BL21(DE3) /pETYLZ^{His} was solubilized in 0.1% IG. YknYLZ was purified from the soluble fraction using Cu^{2+} affinity chromatography. Proteins were eluted from the column with increasing concentration of imidazole. Surprisingly, YknYLZ was eluted in both 100mM and 250mM imidazole fractions (Fig. 3.13), suggesting that YknYLZ could assumed two different conformation. YknYLZ purified from both fractions were assayed for its ability to hydrolyze ATP in detergent lipid solution. We found that the YknYLZ recovered from the 250mM imidazole fraction was inactive (data not shown) whereas YknYLZ recovered from the 100mM imidazole fraction exhibit a basal ATPase activity of 4.9 nmol ATP $min^{-1}mg^{-1}$. In the presence of the MFP YknX, the ATPase activity of YknYLZ

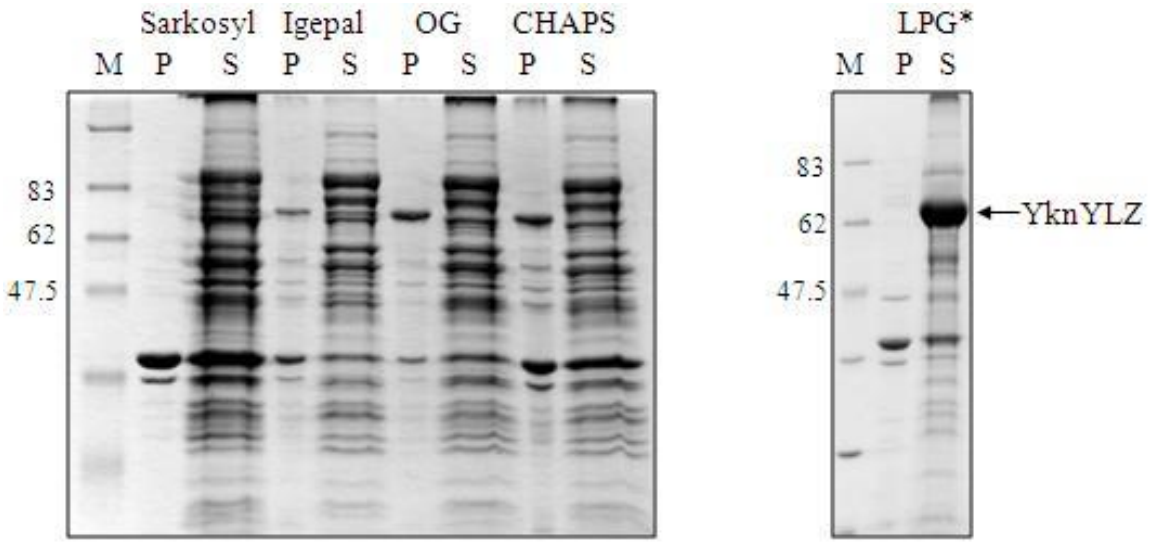

Figure 3.12 Solubilization of BL21(DE3)/pETYLZ^{His} total membrane with different detergents. (A) 1% sarkosyl, 0.05% Igepal, 30mM OG and 10mM CHAPS. (B) 0.6% LPG.

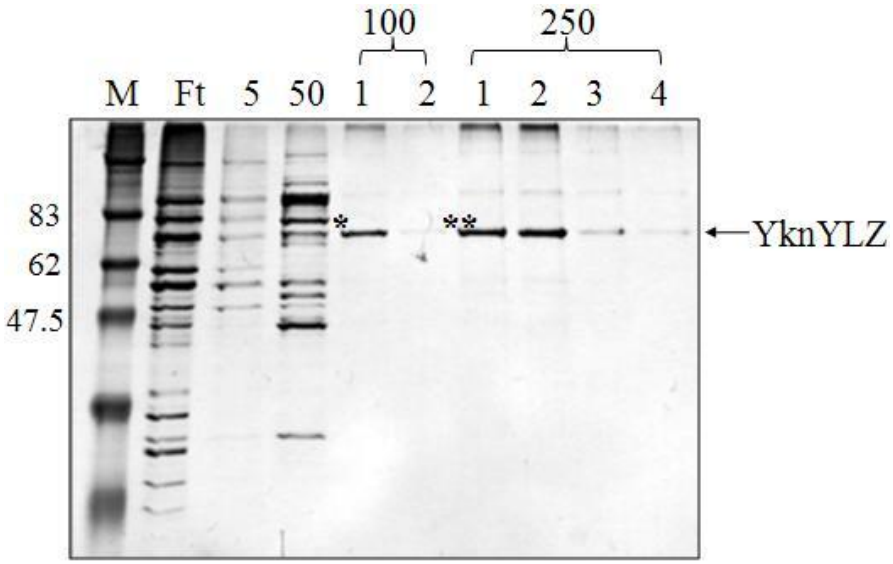

Figure 3.13 Purification profile of YknYLZ-6His. Total membranes of BL21(DE3)/ pETYLZ^{His} were solubilized in 0.1% Igepal (IG). The IG soluble fraction was loaded onto Cu^{2+} charged-NTA column and bound protein were eluted with imidazole gradient of 5mM, 50mM, 100mM and 250mM. Fractions were resolved on 12% SDS-PAGE and visualized with silver stain. (*) and (**) marked the two possible conformation of YknYLZ.

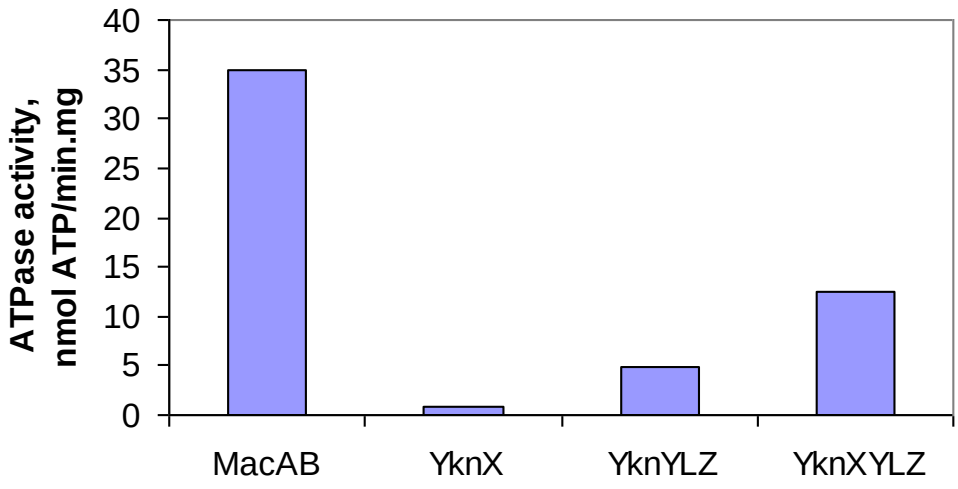

Figure 3.14 ATPase activity of YknYLZ. The rate of ATP hydrolysis was measured in reaction containing 1:1 molar ratio of TX: lipids (7.2mM TX) and 1:3 molar ratio of ATPase: MFP. Reaction contains 0.2μg of YknYLZ.

increased by two fold to 12.4 nmol ATP min^{-1} mg^{-1} (Fig. 3.14). Our results show that the purified YknYLZ is functionally active and exhibit a MFP-dependent ATP hydrolysis.

YknYLZ -6His was also purified from LPG soluble membrane fraction. The elution profile of YknYLZ revealed that similar to the purification of YknYLZ from IG-soluble fraction, the protein peaked at 100mM and 250mM imidazole fractions but the peaks were not as clearly defined (data not shown). So far, the ATPase activity of YknYLZ recovered from these fractions did not show an MFP-dependent ATP hydrolysis in either lipid vesicles or proteoliposomes (data not shown).

Attempts to concentrate purified YknYLZ-6His were unsuccessful as increasing the concentration of YknYLZ protein leads to aggregation. Using quantitative SDS-PAGE to determine the concentration of YknYLZ, we found that monomeric YknYLZ with an apparent MW of 70kDa can be detected at concentration of $\leq$ 0.1mg/mL. Our results showed that YknYLZ has a strong tendency to aggregate when present at high concentration.

3.4 Discussion

The MFP MacA was shown to stimulate the ATPAse activity of the corresponding ABC transporter MacB (Tikhonova *et al.,* 2007) establishing MFPs as an active efflux component. The study of ATP hydrolysis in a reconstituted system proves to be useful in gaining insight to how the efflux components assemble into a functional complex. In this study, we used a similar approach to study the functional relationship between MFP and its cognate transporters from a Gram-positive bacterium. Homologues of MacAB, YvrPON and YknXYZ were identified in *Bacillus subtilis.* Similar to MacB, transporters

from both systems are encoded within the same operon with a MFP. YknXYZ is unique in that a fourth component, YknW is also found encoded in the same operon. The function of YknW is not known but homologues of YknW are often encoded either upstream or downstream of *yknXYZ*-like genes in other *Bacillus* strains (Butcher and Helmann, 2006), suggesting that the YknW may be involved in the function of YknXYZ. Both the MFP and ATP-binding protein from the YknXYZ system were expressed in *E. coli*. The permease on the other hand was not detected. However, the fusion protein YknYLZ, which fuses the ATP-binding protein and the permease to mimic the MacB protein, was expressed in *E. coli*. We found that the MFP YknX stimulates the ATPase activity of YknYLZ fusion protein (purified from TX soluble membrane fraction) in lipid vesicles. The ATPase activity of the fusion protein YknYLZ increased by two fold in the presence of YknX from 4.9 nmol ATP $min^{-1}mg^{-1}$ to 12.4 nmol ATP min^{-1} mg^{-1} (Fig. 3.12). The stimulation was low in comparison to the stimulation of MacB by MacA, which showed a 50-fold increased under the same conditions (Tikhonova *et al.*, 2007). The ATP hydrolysis by YknYLZ at different concentrations of ATP has not been tested. It is likely that YknYLZ has a higher K_M for ATP and therefore exhibit a lower ATPase activity under the condition tested. The data presented here is preliminary but do suggest that the role of MFP is conserved in both Gram-negative and Gram-positive bacteria.

The stimulation of YknYLZ by the MFP YknX is specific as YknX could not substitute the function of MacA in stimulating the ATPase activity MacB. Our result is consistent with previous studies that showed that most MFPs are not interchangeable (Elkins and Nikaido, 2003; Yoneyama et al., 1998). We conclude that the functional interaction between MFPs and the corresponding transporters is specific.

3.5 Materials and Methods

Media and growth conditions, standard protein assays and total membrane fractionation are described in appendices D, E and F respectively.

3.5.1 Cloning and expression of MacAB homologues in *E. coli*. To construct pUC-YvrPON and pUC-YknXYZ, *yvrPON* or *yknXYZ* genes are amplified from *Bacillus subtilis* 168 chromosome using the primer pairs: fyvrPONSacI and ryvrPONkpnI(stop) or fyknXYZSacI and ryknXYZKpnI(stop) respectively. Each PCR product was digested with NcoI and KpnI restriction enzymes and inserted into plasmid pUC18 treated with the same enzymes. To construct pBXYZ^{His} and pBPON^{His}, *yknXYZ* or *yvrPON* genes are amplified from *B. subtilis* 168 chromosome using the primer pairs: fyknXYZNcoI and ryknXYZKpnI or fyvrPONNcoI and ryvrPONkpnI, respectively. Each PCR product was digested with NcoI and KpnI restriction enzymes and inserted into plasmid pBAD/MycHis-C treated with the same enzymes. To facilitate the purification of the *Bacillus* proteins for reconstitution studies in vitro, the *yknW, yknX, yknY, yknZ* or *yknYZ* genes were individually cloned into the His tag expression vector pET21d(+) (Novagen). The primer pairs used for PCR amplification of each gene is as follows (see Table plasmids): *yknW*, fyknWNcoI and ryknW XhoI; *yknX*, fyknXYZNcoI and ryknXXhoI; *yknY*, fyknYZ NcoI and ryknYXhoI; *yknZ*, fyknZNcoI and ryknYZXhoI; *yknYZ*, fyknYZNcoI and ryknYZXhoI. Respective PCR product was digested with NcoI and XhoI restriction enzymes and inserted into plasmid pET-21d (+) treated with the same enzymes. The resulting plasmids pETW^{His}, pETX^{His}, pETY^{His}, pETZ^{His} or pETYZ^{His} were

transformed into BL21(DE3) or C43(DE3) strains and expression were induced with 1mM IPTG. Whole cell extracts were analyzed for protein expression. Samples were resolved on SDS-PAGE and stained with Coomassie brilliant blue (CBB).

To construct fusion protein between YknY and YknZ, the DNA sequence encoding region between the nucleotide binding domain (NBD) and transmembrane (TM) segment of MacB was PCR amplified from pUMacAB (Tikhonova *et al.*, 2007) using the primers fLinkerSalI and rLinkerXhoI. The PCR amplified fragment was digested with SalI and XhoI endonuleases and cloned into XhoI site of $pETY^{His}$ to produce $pETYL^{His}$. yknZ gene was PCR amplified using the primers fyknZSalI and ryknYZXhoI, treated with SalI and XhoI and cloned into the XhoI site of $pETYL^{His}$ to produce $pETYLZ^{His}$. Protein expression was analyzed as described above.

3.5.2 Purification of His-tagged proteins. Total membranes of *E. coli* strains expressing respective His-tagged proteins: $YknW^{His}$, $YknX^{His}$, $YknY^{His}$ and $YknYLZ^{His}$ were collected as described in Appendix F. For purification of $YknW^{His}$, total membranes were solubilized in 5% Triton X-100 (TX) prepared in binding buffer containing 20mM Tris-HCl pH 7.0, 200mM NaCl, 1mM PMSF, and 5mM imidazole as follows: First, membrane pellet was resuspended in binding buffer. Sonication was carried out to help dissolve the membrane pellet. An equal volume of 10% Triton X-100 (TX) prepared in binding buffer was then added to the membrane suspension and allowed to mix overnight by stirring at 4^0C. After removal of TX insoluble fraction by ultracentrifugation at 70,000 x g for 30min, the supernatant was loaded onto Cu^{2+} charged-NTA column equilibrated

with binding buffer containing 0.2% TX (wash buffer). The column was washed with an imidazole step-gradient containing 5mM, 25mM, 50mM, 100mM and 250mM.

YknX^{His} and YknYLZ^{His} were purified as described for YknW^{His} with the following modifications. For purification of YknX^{His}, binding buffer contains 20mM HEPES-KOH pH 7.7, 500mM NaCl, 1mM PMSF and 5mM Imidazole. An imidazole gradient of 5mM, 20mM, 50mM and 100mM was used. For purification of YknYLZ^{His} using the detergent IGEPAL (IG), binding buffer contains 20mM Tris-HCl pH 7.0, 200mM NaCl, 1mM PMSF, 0.05 mM β-mercaptoethanol and 5mM imidazole. Total membrane was solubilized with 0.1% IG-containing binding buffer (also the wash buffer). For purification of YknYLZ-6His using the detergent lysophosphatidylglycerol (LPG), binding buffer contains 20mM Tris-HCl pH 7.0, 100mM NaCl, 1mM PMSF, and 0.05 mM β-mercaptoethanol. Total membrane was solubilized in 0.6% LPG-containing binding buffer. LPG solubilized fraction was adjusted with binding buffer to 0.1% LPG and supplemented with 5mM imidazole before loading onto Cu^{2+} charged-NTA column. The wash buffer comprised of binding buffer supplemented with 0.01%LPG, 0.1% IG and varying concentration of imidazole. YknYLZ was eluted with imidazole gradient of 5mM, 50mM, 100mM and 250mM.

For purification of YknY^{His}, harvested cells were resuspended in buffer containing 20mM Tris-HCl, 200mM NaCl, 1mM PMSF, 0.05mM β-mercaptoethanol and 5mM imidazole. Lysozyme were added to the cell suspension to a final concentration of 100μg/mL and incubated on ice for 30min. Cells were then sonicated and unbroken cells were removed by low speed centrifugation. Membrane fraction was separated by ultracentrifugation at 250,000 x g for 1 hr. The soluble fraction was loaded onto Cu^{2+}

charged-NTA column. The column was washed with an imidazole gradient of 5mM, 50mM, 100mM, 250mM and 500mM.

3.5.3 Reconstitution of proteins into proteoliposomes. *E. coli* polar lipids (Avanti) were dissolved in reconstitution buffer [20mM HEPES-KOH (pH7.0), 5mM DTT] to a final concentration of 20mg/mL. The mixture was sonicated until mixture looked transparent. 5mg of E. coli lipids were mixed in 0.5mL reconstitution buffer containing 0.45% TX. Equal volumes of protein sample (25-50μg) prepared in the same buffer was added to the lipid mix and incubated for 30 min at room temperature (RT). TX was then removed using SM-2 Adsorbent Bio-Beads (Bio-Rad). Before use, the beads were washed 3 times in methanol, 5 min each. This step is repeated with water and reconstitution buffer. The protein-lipid mixture was incubated with 40mg of beads for 1 hr at RT. This step was repeated with fresh beads for 1 hr at RT and again for 1 hr at 4^0C. Proteoliposomes were diluted with two volumes of ice cold reconstitution buffer and collected by centrifugation at 250,000 g for 1 hr at 4^0C. The pellet was resuspended in 50μL of buffer containing 20mM HEPES-KOH (pH7.0), 5mM DTT and 50mM KCl and briefly sonicated. The proteoliposomes were stored at 4^0C and used for assays within 2-3 days.

The concentration of proteins reconstituted into proteoliposomes was determined by quantitative SDS-PAGE. Proteoliposomes samples and bovine serum albumin (BSA) in increasing concentration were resolved on 12% SDS-PAGE and stained with CBB. Gels were scanned and the peak area of each protein band was quantified using ImageQuant proGram (Molecular Dynamics).

3.5.4 ATP hydrolysis assay. The ATP hydrolysis by YknYLZ assayed in detergent solution was carried out in 20μL of reaction mixture containing 0.2 to 0.4 μg of ATPase, 20mM HEPES-KOH (pH7.0), 5mM DTT, 50mM KCl , 2mM $MgCl_2$, 0.45% TX and 1mM Mg-ATP. The ^{32}P γ-phosphate labeled ATP (3000 Ci $mmol^{-1}$, Amersham) was mixed with unlabelled Mg-ATP prior to addition into the reaction mix. The molar ratio of MFP: ATPase was adjusted to 3: 1. A final concentration of 7.2mM *E. coli* lipids was also included in the reaction mix where needed. The reaction was incubated at 37^0C and 1μL aliquots were collected at different time points and added to 10 μL of stop buffer containing 50mM Tris-HCl (pH 8.0), 20mM EDTA (pH8.0), 0.5% SDS, 200mM NaCl and 0.5mg/mL proteinase K. The mixture was incubated at 50^0C for 20min to inactivate ATPase activity.

The ATPase activity of YknY was determined with the following modifications. The rate of ATP hydrolysis of YknY (0, 0.25, 0.5, 1.0 or 1.5μg) was assayed in solution containing 20mM HEPES-KOH (pH7.0), 5mM DTT, 50mM KCl, 2mM $MgCl_2$ and 50% glycerol and 1mM Mg-ATP.

The rate of ATP hydrolysis by YknYLZ in proteoliposomes was assayed in 10μL of reaction mixture in the same manner as described for YknYLZ ATP hydrolysis in detergent solution with the following modification. Proteoliposomes containing 0.2μg of ATPase was added to reaction mixture [20mM HEPES-KOH (pH7.0), 5mM DTT, 50mM KCl , 2mM $MgCl_2$, and 1mM Mg-ATP].

The hydrolysis of ^{32}γ-ATP was analyzed using thin-layer chromatography. 1μL of samples collected at different time points were loaded onto PEI-F cellulose (10cm x 20cm). The mobile phase contained 10% formic acid and 0.5mM LiCl. Hydrolyzed Pi

was quantified using Storm PhosphoImager and ImageQuant software (Molecular Dynamics). The peak area corresponding to hydrolyzed Pi represents the percent of ATP hydrolyzed. The percent of ATP hydrolyzed is quantified for each time point and the rate of ATP hydrolysis can be calculated as percent ATP hydrolyzed per min.

References

Aires, J.R., Kohler, T., Nikaido, H., and Plesiat, P. (1999) Involvement of an active efflux system in the natural resistance of Pseudomonas aeruginosa to aminoglycosides. *Antimicrob Agents Chemother* **43**: 2624-2628.

Aires, J.R., and Nikaido, H. (2005) Aminoglycosides are captured from both periplasm and cytoplasm by the AcrD multidrug efflux transporter of Escherichia coli. *J Bacteriol* **187**: 1923-1929.

Akama, H., Matsuura, T., Kashiwagi, S., Yoneyama, H., Narita, S., Tsukihara, T., Nakagawa, A., and Nakae, T. (2004) Crystal structure of the membrane fusion protein, MexA, of the multidrug transporter in Pseudomonas aeruginosa. *J Biol Chem* **279**: 25939-25942.

Andersen, C., Koronakis, E., Bokma, E., Eswaran, J., Humphreys, D., Hughes, C., and Koronakis, V. (2002) Transition to the open state of the TolC periplasmic tunnel entrance. *Proc Natl Acad Sci U S A* **99**: 11103-11108.

Avila-Sakar, A.J., Misaghi, S., Wilson-Kubalek, E.M., Downing, K.H., Zgurskaya, H., Nikaido, H., and Nogales, E. (2001) Lipid-layer crystallization and preliminary three-dimensional structural analysis of AcrA, the periplasmic component of a bacterial multidrug efflux pump. *J Struct Biol* **136**: 81-88.

Axelsson, L., and Holck, A. (1995) The genes involved in production of and immunity to sakacin A, a bacteriocin from Lactobacillus sake Lb706. *J Bacteriol* **177**: 2125-2137.

Berka, R.M., Hahn, J., Albano, M., Draskovic, I., Persuh, M., Cui, X., Sloma, A., Widner, W., and Dubnau, D. (2002) Microarray analysis of the Bacillus subtilis K-state: genome-wide expression changes dependent on ComK. *Mol Microbiol* **43**: 1331-1345.

Bernhardt, T.G., and de Boer, P.A. (2004) Screening for synthetic lethal mutants in Escherichia coli and identification of EnvC (YibP) as a periplasmic septal ring factor with murein hydrolase activity. *Mol Microbiol* **52**: 1255-1269.

Bi, E., and Lutkenhaus, J. (1993) Cell division inhibitors SulA and MinCD prevent formation of the FtsZ ring. *J Bacteriol* **175**: 1118-1125.

Burdett, I.D., and Murray, R.G. (1974) Septum formation in Escherichia coli: characterization of septal structure and the effects of antibiotics on cell division. *J Bacteriol* **119**: 303-324.

Butcher, B.G., and Helmann, J.D. (2006) Identification of Bacillus subtilis sigma-dependent genes that provide intrinsic resistance to antimicrobial compounds produced by Bacilli. *Mol Microbiol* **60**: 765-782.

Carmeli, Y., Troillet, N., Karchmer, A.W., and Samore, M.H. (1999) Health and economic outcomes of antibiotic resistance in Pseudomonas aeruginosa. *Arch Intern Med* **159**: 1127-1132.

den Blaauwen, T., Lindqvist, A., Lowe, J., and Nanninga, N. (2001) Distribution of the Escherichia coli structural maintenance of chromosomes (SMC)-like protein MukB in the cell. *Mol Microbiol* **42**: 1179-1188.

Dinh, T., Paulsen, I.T., and Saier, M.H., Jr. (1994) A family of extracytoplasmic proteins that allow transport of large molecules across the outer membranes of gram-negative bacteria. *J Bacteriol* **176**: 3825-3831.

Dubochet, J., McDowall, A.W., Menge, B., Schmid, E.N., and Lickfeld, K.G. (1983) Electron microscopy of frozen-hydrated bacteria. *J Bacteriol* **155**: 381-390.

Elkins, C.A., and Nikaido, H. (2003) Chimeric analysis of AcrA function reveals the importance of its C-terminal domain in its interaction with the AcrB multidrug efflux pump. *J Bacteriol* **185**: 5349-5356.

Errington, J., Daniel, R.A., and Scheffers, D.J. (2003) Cytokinesis in bacteria. *Microbiol Mol Biol Rev* **67**: 52-65, table of contents.

Fernandez-Recio, J., Walas, F., Federici, L., Venkatesh Pratap, J., Bavro, V.N., Miguel, R.N., Mizuguchi, K., and Luisi, B. (2004) A model of a transmembrane drug-efflux pump from Gram-negative bacteria. *FEBS Lett* **578**: 5-9.

Gerken, H., and Misra, R. (2004) Genetic evidence for functional interactions between TolC and AcrA proteins of a major antibiotic efflux pump of Escherichia coli. *Mol Microbiol* **54**: 620-631.

Gilson, L., Mahanty, H.K., and Kolter, R. (1987) Four plasmid genes are required for colicin V synthesis, export, and immunity. *J Bacteriol* **169**: 2466-2470.

Gilson, L., Mahanty, H.K., and Kolter, R. (1990) Genetic analysis of an MDR-like export system: the secretion of colicin V. *Embo J* **9**: 3875-3884.

Grkovic, S., Brown, M.H., and Skurray, R.A. (2002) Regulation of bacterial drug export systems. *Microbiol Mol Biol Rev* **66**: 671-701, table of contents.

Hagman, K.E., Pan, W., Spratt, B.G., Balthazar, J.T., Judd, R.C., and Shafer, W.M. (1995) Resistance of Neisseria gonorrhoeae to antimicrobial hydrophobic agents is modulated by the mtrRCDE efflux system. *Microbiology* **141 (Pt 3)**: 611-622.

Hanaichi, T., Sato, T., Iwamoto, T., Malavasi-Yamashiro, J., Hoshino, M., and Mizuno, N. (1986) A stable lead by modification of Sato's method. *J Electron Microsc (Tokyo)* **35**: 304-306.

Hara, H., Narita, S., Karibian, D., Park, J.T., Yamamoto, Y., and Nishimura, Y. (2002) Identification and characterization of the Escherichia coli envC gene encoding a periplasmic coiled-coil protein with putative peptidase activity. *FEMS Microbiol Lett* **212**: 229-236.

Harley, K.T., Djordjevic, G.M., Tseng, T.T., and Saier, M.H. (2000) Membrane-fusion protein homologues in gram-positive bacteria. *Mol Microbiol* **36**: 516-517.

Helling, R.B., Janes, B.K., Kimball, H., Tran, T., Bundesmann, M., Check, P., Phelan, D., and Miller, C. (2002) Toxic waste disposal in Escherichia coli. *J Bacteriol* **184**: 3699-3703.

Higgins, C.F. (1992) ABC transporters: from microorganisms to man. *Annu Rev Cell Biol* **8**: 67-113.

Higgins, M.K., Bokma, E., Koronakis, E., Hughes, C., and Koronakis, V. (2004) Structure of the periplasmic component of a bacterial drug efflux pump. *Proc Natl Acad Sci U S A* **101**: 9994-9999.

Huang, J., Cao, C., and Lutkenhaus, J. (1996) Interaction between FtsZ and inhibitors of cell division. *J Bacteriol* **178**: 5080-5085.

Huang, P., Liu, Q., and Scarborough, G.A. (1998) Lysophosphatidylglycerol: a novel effective detergent for solubilizing and purifying the cystic fibrosis transmembrane conductance regulator. *Anal Biochem* **259**: 89-97.

Husain, F., Humbard, M., and Misra, R. (2004) Interaction between the TolC and AcrA proteins of a multidrug efflux system of Escherichia coli. *J Bacteriol* **186**: 8533-8536.

Hwang, J., Zhong, X., and Tai, P.C. (1997) Interactions of dedicated export membrane proteins of the colicin V secretion system: CvaA, a member of the membrane fusion protein family, interacts with CvaB and TolC. *J Bacteriol* **179**: 6264-6270.

Ishidate, K., Creeger, E.S., Zrike, J., Deb, S., Glauner, B., MacAlister, T.J., and Rothfield, L.I. (1986) Isolation of differentiated membrane domains from Escherichia coli and Salmonella typhimurium, including a fraction containing attachment sites between the inner and outer membranes and the murein skeleton of the cell envelope. *J Biol Chem* **261**: 428-443.

Issekutz, A.C. (1983) Removal of gram-negative endotoxin from solutions by affinity chromatography. *J Immunol Methods* **61**: 275-281.

Johnson, J.M., and Church, G.M. (1999) Alignment and structure prediction of divergent protein families: periplasmic and outer membrane proteins of bacterial efflux pumps. *J Mol Biol* **287**: 695-715.

Jones, P.M., and George, A.M. (2004) The ABC transporter structure and mechanism: perspectives on recent research. *Cell Mol Life Sci* **61**: 682-699.

Klein, J.R., Henrich, B., and Plapp, R. (1991) Molecular analysis and nucleotide sequence of the envCD operon of Escherichia coli. *Mol Gen Genet* **230**: 230-240.

Kobayashi, K., Tsukagoshi, N., and Aono, R. (2001a) Suppression of hypersensitivity of Escherichia coli acrB mutant to organic solvents by integrational activation of the acrEF operon with the IS1 or IS2 element. *J Bacteriol* **183**: 2646-2653.

Kobayashi, N., Nishino, K., and Yamaguchi, A. (2001b) Novel macrolide-specific ABC-type efflux transporter in Escherichia coli. *J Bacteriol* **183**: 5639-5644.

Kobayashi, N., Nishino, K., Hirata, T., and Yamaguchi, A. (2003) Membrane topology of ABC-type macrolide antibiotic exporter MacB in Escherichia coli. *FEBS Lett* **546**: 241-246.

Koronakis, V., Sharff, A., Koronakis, E., Luisi, B., and Hughes, C. (2000) Crystal structure of the bacterial membrane protein TolC central to multidrug efflux and protein export. *Nature* **405**: 914-919.

Lefman, J., Zhang, P., Hirai, T., Weis, R.M., Juliani, J., Bliss, D., Kessel, M., Bos, E., Peters, P.J., and Subramaniam, S. (2004) Three-dimensional electron microscopic imaging of membrane invaginations in Escherichia coli overproducing the chemotaxis receptor Tsr. *J Bacteriol* **186**: 5052-5061.

Lesse, A.J., Campagnari, A.A., Bittner, W.E., and Apicella, M.A. (1990) Increased resolution of lipopolysaccharides and lipooligosaccharides utilizing tricine-sodium dodecyl sulfate-polyacrylamide gel electrophoresis. *J Immunol Methods* **126**: 109-117.

Levy, S.B. (1992) Active efflux mechanisms for antimicrobial resistance. *Antimicrob Agents Chemother* **36**: 695-703.

Li, X.Z., Nikaido, H., and Poole, K. (1995) Role of mexA-mexB-oprM in antibiotic efflux in Pseudomonas aeruginosa. *Antimicrob Agents Chemother* **39**: 1948-1953.

Lobedanz, S., Bokma, E., Symmons, M.F., Koronakis, E., Hughes, C., and Koronakis, V. (2007) A periplasmic coiled-coil interface underlying TolC recruitment and the assembly of bacterial drug efflux pumps. *Proc Natl Acad Sci U S A* **104**: 4612-4617.

Lomovskaya, O., Zgurskaya, H.I., Totrov, M., and Watkins, W.J. (2007) Waltzing transporters and 'the dance macabre' between humans and bacteria. *Nat Rev Drug Discov* **6**: 56-65.

Lory, S. (1998) Secretion of proteins and assembly of bacterial surface organelles: shared pathways of extracellular protein targeting. *Curr Opin Microbiol* **1**: 27-35.

Ma, D., Cook, D.N., Alberti, M., Pon, N.G., Nikaido, H., and Hearst, J.E. (1993) Molecular cloning and characterization of acrA and acrE genes of Escherichia coli. *J Bacteriol* **175**: 6299-6313.

Ma, D., Cook, D.N., Alberti, M., Pon, N.G., Nikaido, H., and Hearst, J.E. (1995) Genes acrA and acrB encode a stress-induced efflux system of Escherichia coli. *Mol Microbiol* **16**: 45-55.

Ma, D., Alberti, M., Lynch, C., Nikaido, H., and Hearst, J.E. (1996) The local repressor AcrR plays a modulating role in the regulation of acrAB genes of Escherichia coli by global stress signals. *Mol Microbiol* **19**: 101-112.

Mikolosko, J., Bobyk, K., Zgurskaya, H.I., and Ghosh, P. (2006) Conformational flexibility in the multidrug efflux system protein AcrA. *Structure* **14**: 577-587.

Mine, T., Morita, Y., Kataoka, A., Mizushima, T., and Tsuchiya, T. (1999) Expression in Escherichia coli of a new multidrug efflux pump, MexXY, from Pseudomonas aeruginosa. *Antimicrob Agents Chemother* **43**: 415-417.

Miroux, B., and Walker, J.E. (1996) Over-production of proteins in Escherichia coli: mutant hosts that allow synthesis of some membrane proteins and globular proteins at high levels. *J Mol Biol* **260**: 289-298.

Morrison, D.C., and Jacobs, D.M. (1976) Binding of polymyxin B to the lipid A portion of bacterial lipopolysaccharides. *Immunochemistry* **13**: 813-818.

Murakami, S., Nakashima, R., Yamashita, E., and Yamaguchi, A. (2002) Crystal structure of bacterial multidrug efflux transporter AcrB. *Nature* **419**: 587-593.

Nikaido, H., and Vaara, M. (1985) Molecular basis of bacterial outer membrane permeability. *Microbiol Rev* **49**: 1-32.

Nikaido, H. (1989) Outer membrane barrier as a mechanism of antimicrobial resistance. *Antimicrob Agents Chemother* **33**: 1831-1836.

Nikaido, H. (1994) Prevention of drug access to bacterial targets: permeability barriers and active efflux. *Science* **264**: 382-388.

Nikaido, H. (1996) Multidrug efflux pumps of gram-negative bacteria. *J Bacteriol* **178**: 5853-5859.

Nikaido, H. (1998a) Antibiotic resistance caused by gram-negative multidrug efflux pumps. *Clin Infect Dis* **27 Suppl 1**: S32-41.

Nikaido, H. (1998b) The role of outer membrane and efflux pumps in the resistance of gram-negative bacteria. Can we improve drug access? *Drug Resist Updat* **1**: 93-98.

Nikaido, H., and Zgurskaya, H.I. (2001) AcrAB and related multidrug efflux pumps of Escherichia coli. *J Mol Microbiol Biotechnol* **3**: 215-218.

Nishino, K., and Yamaguchi, A. (2001) Analysis of a complete library of putative drug transporter genes in Escherichia coli. *J Bacteriol* **183**: 5803-5812.
Osborn, M.J., Gander, J.E., and Parisi, E. (1972) Mechanism of assembly of the outer membrane of Salmonella typhimurium. Site of synthesis of lipopolysaccharide. *J Biol Chem* **247**: 3973-3986.
Piddock, L.J. (2006) Multidrug-resistance efflux pumps - not just for resistance. *Nat Rev Microbiol* **4**: 629-636.
Pimenta, A., Blight, M., Clarke, D., and Holland, I.B. (1996) The gram-negative cell envelope 'springs' to life: coiled-coil trans-envelope proteins. *Mol Microbiol* **19**: 643-645.
Plesiat, P., and Nikaido, H. (1992) Outer membranes of gram-negative bacteria are permeable to steroid probes. *Mol Microbiol* **6**: 1323-1333.
Pogliano, J., Pogliano, K., Weiss, D.S., Losick, R., and Beckwith, J. (1997) Inactivation of FtsI inhibits constriction of the FtsZ cytokinetic ring and delays the assembly of FtsZ rings at potential division sites. *Proc Natl Acad Sci U S A* **94**: 559-564.
Poole, K., Krebes, K., McNally, C., and Neshat, S. (1993) Multiple antibiotic resistance in Pseudomonas aeruginosa: evidence for involvement of an efflux operon. *J Bacteriol* **175**: 7363-7372.
Poole, K. (2001) Multidrug resistance in Gram-negative bacteria. *Curr Opin Microbiol* **4**: 500-508.
Poole, K. (2002) Outer membranes and efflux: the path to multidrug resistance in Gram-negative bacteria. *Curr Pharm Biotechnol* **3**: 77-98.
Putman, M., van Veen, H.W., and Konings, W.N. (2000) Molecular properties of bacterial multidrug transporters. *Microbiol Mol Biol Rev* **64**: 672-693.
Quadri, L.E., Kleerebezem, M., Kuipers, O.P., de Vos, W.M., Roy, K.L., Vederas, J.C., and Stiles, M.E. (1997) Characterization of a locus from Carnobacterium piscicola LV17B involved in bacteriocin production and immunity: evidence for global inducer-mediated transcriptional regulation. *J Bacteriol* **179**: 6163-6171.
Rahmati, S., Yang, S., Davidson, A.L., and Zechiedrich, E.L. (2002) Control of the AcrAB multidrug efflux pump by quorum-sensing regulator SdiA. *Mol Microbiol* **43**: 677-685.
Saier, M.H., Jr., Paulsen, I.T., Sliwinski, M.K., Pao, S.S., Skurray, R.A., and Nikaido, H. (1998) Evolutionary origins of multidrug and drug-specific efflux pumps in bacteria. *Faseb J* **12**: 265-274.
Spratt, B.G. (1977) Temperature-sensitive cell division mutants of Escherichia coli with thermolabile penicillin-binding proteins. *J Bacteriol* **131**: 293-305.
Stegmeier, J.F., Polleichtner, G., Brandes, N., Hotz, C., and Andersen, C. (2006) Importance of the adaptor (membrane fusion) protein hairpin domain for the functionality of multidrug efflux pumps. *Biochemistry* **45**: 10303-10312.
Sulavik, M.C., Houseweart, C., Cramer, C., Jiwani, N., Murgolo, N., Greene, J., DiDomenico, B., Shaw, K.J., Miller, G.H., Hare, R., and Shimer, G. (2001) Antibiotic susceptibility profiles of Escherichia coli strains lacking multidrug efflux pump genes. *Antimicrob Agents Chemother* **45**: 1126-1136.
Tamura, N., Murakami, S., Oyama, Y., Ishiguro, M., and Yamaguchi, A. (2005) Direct interaction of multidrug efflux transporter AcrB and outer membrane channel

TolC detected via site-directed disulfide cross-linking. *Biochemistry* **44**: 11115-11121.

Thanabalu, T., Koronakis, E., Hughes, C., and Koronakis, V. (1998) Substrate-induced assembly of a contiguous channel for protein export from E.coli: reversible bridging of an inner-membrane translocase to an outer membrane exit pore. *Embo J* **17**: 6487-6496.

Tikhonova, E.B., and Zgurskaya, H.I. (2004) AcrA, AcrB, and TolC of Escherichia coli Form a Stable Intermembrane Multidrug Efflux Complex. *J Biol Chem* **279**: 32116-32124.

Tikhonova, E.B., Devroy, V.K., Lau, S.Y., and Zgurskaya, H.I. (2007) Reconstitution of the Escherichia coli macrolide transporter: the periplasmic membrane fusion protein MacA stimulates the ATPase activity of MacB. *Mol Microbiol* **63**: 895-910.

Tjalsma, H., Bolhuis, A., Jongbloed, J.D., Bron, S., and van Dijl, J.M. (2000) Signal peptide-dependent protein transport in Bacillus subtilis: a genome-based survey of the secretome. *Microbiol Mol Biol Rev* **64**: 515-547.

Touze, T., Eswaran, J., Bokma, E., Koronakis, E., Hughes, C., and Koronakis, V. (2004) Interactions underlying assembly of the Escherichia coli AcrAB-TolC multidrug efflux system. *Mol Microbiol* **53**: 697-706.

Wagner, W., Vogel, M., and Goebel, W. (1983) Transport of hemolysin across the outer membrane of Escherichia coli requires two functions. *J Bacteriol* **154**: 200-210.

Wandersman, C., and Delepelaire, P. (1990) TolC, an Escherichia coli outer membrane protein required for hemolysin secretion. *Proc Natl Acad Sci U S A* **87**: 4776-4780.

Weissbach, A., and Hurwitz, J. (1959) The formation of 2-keto-3-deoxyheptonic acid in extracts of Escherichia coli B. I. Identification. *J Biol Chem* **234**: 705-709.

Zgurskaya, H.I., and Nikaido, H. (1999a) AcrA is a highly asymmetric protein capable of spanning the periplasm. *J Mol Biol* **285**: 409-420.

Zgurskaya, H.I., and Nikaido, H. (1999b) Bypassing the periplasm: reconstitution of the AcrAB multidrug efflux pump of Escherichia coli. *Proc Natl Acad Sci U S A* **96**: 7190-7195.

Zgurskaya, H.I., and Nikaido, H. (2000a) Cross-linked complex between oligomeric periplasmic lipoprotein AcrA and the inner-membrane-associated multidrug efflux pump AcrB from Escherichia coli. *J Bacteriol* **182**: 4264-4267.

Zgurskaya, H.I., and Nikaido, H. (2000b) Multidrug resistance mechanisms: drug efflux across two membranes. *Mol Microbiol* **37**: 219-225.

Zgurskaya, H.I. (2002) Molecular analysis of efflux pump-based antibiotic resistance. *Int J Med Microbiol* **292**: 95-105.

Zhao, G., Meier, T.I., Kahl, S.D., Gee, K.R., and Blaszczak, L.C. (1999) BOCILLIN FL, a sensitive and commercially available reagent for detection of penicillin-binding proteins. *Antimicrob Agents Chemother* **43**: 1124-1128.

Appendices

Appendix A: List of Strains

Strains	Description	Source or reference
AG100	*argE3 thi-1 rpsL xyl mtl galK supE441* Δ(gal-uvrB)λ^-	George AM and Levy SB
AG100A	same as AG100 but Δ*acrAB::kan*	Okusu et al.
AG100AX	same as AG100 Δ*acrAB::kan* Δ*acrEF::spe*	Miyamae et al.
W4680E	Δ*acrEF::spe*	Nikaido H
ECM2112	Δ*acrAB::kan* Δ*tolC::tet*	Lomoskaya O
BW25113	*lacI*^{q}*rrnB*$_{T14}$ Δ*lacZ*$_{WJ16}$ *hsdR*514 Δ*araBAD*$_{AH33}$ Δ*rhaBAD*$_{LD78}$	Datsenko and Wanner (2003)
ET103	BW25113 but *ompT*::kan	Tikhonova et.al (2007)
Bacillus subtilis 168	Wild type	Klebba PE
DH5α	*supE*44 Δ*lacU*169 *hsdR*17 *recA*1 *endA*1 *gyrA*96 *thi*-1 *relA*1	
Bl21(DE3)	F$^-$*ompT hsdS*$_B$(r_B^- m_B^-)*gal dcm*	Novagen
C43(DE3)	F$^-$*ompT gal hsdS*^{B} (r^-_B m^-_B) *dcm lon* λDE3 pLys-S and two uncharacterized mutations described in (Miroux and Walker, 1996)	Nakamoto R

Appendix B: List of Plasmids

Plasmids	Description	Source or reference
pUC18	*E. coli* cloning vector, Amp^r	
pACYC184	*E. coli* cloning vector, Cm^r, Tet^r	
pQB1T7	GFP gene under P_{tac} promoter	Quantum
pUC151A	pUC18 vector carrying the *acrAB* genes	Ma et al. (1993)
pBP	pUC18 vector expressing *acrB* under native promoter	Tikhonova et al. (2002)
pHK11	pBR322 with *cvaABC* and *cvi* genes	Gilson et al. (1990)
pUC-AcrA	pUC18 vector carrying the *acrA*	this study
pACYC-AcrEF	pACYC184 with *acrEF*	this study
pACYC-AcrF	pACYC184 with *acrF*	this study
pUC-CvaA-AcrA	pUC151A with translational c*vaA-acrA* fusion	this study
pUC-GFP-AcrA	pUC-CvaA-AcrA with translational *GFP-cva-acrA* fusion	this study
pBAD/MycHis-C	Cloning vector, Amp^r	Invitrogen
pBA^{His}	pBAD/MycHis-C carrying *macA*-6His, Amp^r	Tikhonova et al. (2007)
pBB^{His}	pBAD/MycHis-C carrying *macB*-6His, Amp^r	Tikhonova et al. (2007)
$pBAB^{His}$	pBAD/MycHis-C carrying *macAB*-6His, Amp^r	Tikhonova et al. (2007)
$pBA_{\Delta 90}B^{His}$	$pBAB^{His}$ expressing MacA Δ90	This study

pET-21d(+)	Cloning vector	Novagen
pETA^{His}	pET-21d(+) carrying *macA*-6His, Amp^{r}	Tikhonova et al. (2007)
pETAΔ90	pETA^{His} expressing MacAΔ90, Amp^{r}	Tikhonova et al. (2007)
pUMacAB	pUC18 carrying macAB, Amp^{r}	Tikhonova et al. (2007)
pUA$_{\Delta 90}$B	pUMacAB expressing MacAΔ90, Amp^{r}	Tikhonova et al. (2007)
pUZ11	pUC18 expressing OmpA-AcrA-6His fusion protein	Zgurskaya and Nikaido (1996)
pUA$_{\Delta N}$B^{His}	pUZ11 expressing MacAΔN and MacB-6His	Tikhonova et al. (2007)
pUC-YvrPON	pUC18 expressing *yvrPON*, Amp^{r}	This study
pUC-YknXYZ	pUC18 expressing *yknXYZ*, Amp^{r}	This study
pBXYZ^{His}	pBAD/MycHis-C carrying *yknXYZ*-6His, Amp^{r}	This study
pBPON^{His}	pBAD/MycHis-C carrying *yvrPON*-6His, Amp^{r}	This study
pETW^{His}	pET-21d(+) carrying YknW-6His, Amp^{r}	This study
pETX^{His}	pET-21d(+) carrying YknX-6His, Amp^{r}	This study
pETY^{His}	pET-21d(+) carrying YknY-6His, Amp^{r}	This study
pETZ^{His}	pET-21d(+) carrying YknZ-6His, Amp^{r}	This study
pETYL^{His}	pET-21d(+) carrying YknYL-6His, Amp^{r}	This study
pETYLZ^{His}	pET-21d(+) carrying YknYLZ-6His, Amp^{r}	This study

Appendix C: List of Primers

Primer Name	Sequence 5'→ 3'
fNCvaAXhoI	GGCCGGCTCGAGGTTTACATATGAAGTGGCAGGGACGG
rNCvaAMscI	GGCCGGTGGCCACCTTGTTGGGCCTGGCTATAGGTACCAACAATAATG
fAcrEFAvaI	GACGCTCGGGATAGCGAACTGTATTTTTC
rAcrEFHindIII	GTGAAGGGAGCGGGAACTATAGAAAGC
fAcrEF	GTAATGACGAAACATGCCAGGTTTTTCCTC
rAcrEF	GATTTATCCTTTAAAGCAACGGCGGATCACC
fSulA	GAGTGAATTTTTAGCCCGGAAAGTTGTCTC
rSulA	GTACACTTCAGGCTATGCACATCGTTCTTC
fGFPXhoI	GGGCTCGAGAGGATATAGATATGGCTAGCAAAGGAGAAGAACTCTTCAC
rGFPXhoI	GGGCTCGAGGGTTGTACAGTTCATCCATGCCATGTG
fyvrPONSacI	GCACGAGCTCATGAACCAAGTTGCCGTATC
fyvrPONNcoI	GCATCCCATGGCTAACCAAGTTGCCGTATC
ryvrPONkpnI	GTTCGGTACCTTCATAGCGAAGCGCGTCTAC
ryvrPONkpnI(Stop)	GGTCGGTACCTTATTCATAGCGAAGCGCGTC
fyknXYZSacI	GGCCGGGAGCTCATGAAAAAAGTCTGG
fyknXYZNcoI	GGCCCCATGGCCAAAAAAGTCTGGATC

ryknXYZKpnI	GGAAGGTACCCTCATAACGCAGCGCTTC
ryknXYZKpnI(stop)	GCATCGGTACCCTACTCATAACGCAGCG
fMacBXbaI	GGCGGTCTAGAACATGACGCCTTTGCTCGAATTAAAG
rdelMacA90XbaI	GGCCGTCTAGAGACTTCAAAACGGGCGTAATAG
fyknWNcoI	GACTCCATGGCCGAAACGAATG
ryknWXhoI	GATTAAACTCGAGTGCACCCGC
ryknXXhoI	GCGGCTCGAGGGATTTCACTTCCATTC
fyknYZNcoI	GACTCCATGGCCATTCAGCTTTC
ryknYZXhoI	GCATCTCGAGCTCATAACGCAG
ryknYXhoI	GAATTCTCGAGTTCTCCCACACTCC
fYknZNcoI	GTTACCATGGCCAGCCTGTTG
fYknZSalI	GACGGCGTCGACTTGGAAAACATCAG
fLinkerSalI	GTATTATGTCGACCGCAATCCTCCCGCCATTG
rLinkerXhoI	GGCGGCTCGAGGTTAAAACCGCTGACAAAC
ryknYXhoI	GAATTCTCGAGTTCTCCCACACTCC

Appendix D
Media, growth conditions and drug susceptibility

Media and growth conditions

The bacterial strains and plasmids used in this study are listed in Appendix A. *E. coli* strains were grown at 37°C in Luria-Bertani (LB) medium (10 g of Bactotryptone, 10 g of yeast extract, and 5 g of NaCl per liter). Antibiotics were added when needed to the following final concentration: ampicillin (100 µg/ml), kanamycin (34 µg/ml), spectinomycin (50 µg/ml), tetracycline (25 µg/ml), and chloramphenicol (25 µg/ml).

Drug susceptibility

Luria-Bertani medium supplemented with two-fold increments of drugs tested were prepared on 96-well microtiter plate. Exponentially growing cultures were inoculated at a density of 10^4 per mL. Cells were grown overnight at 37^0C. The lowest concentration of drugs where there is no cell growth represents the minimal inhibitory concentration (MIC).

Appendix E
Protein assays

SDS-PAGE. Protein samples were analyzed with sodium dodecyl sulfate-polyacrylamide gel electrophoresis (SDS-PAGE). Proteins samples were resolved on either 10% or 12% polyacrylamide gels. Protein bands were visualized with Coommassie Brilliant Blue (CBB) or Silver Stain.

Protein concentrations. Proteins concentrations were determined using either the DC Protein Assay (Bio-Rad) or quantitative SDS-PAGE with bovine serum albumin (BSA) as standards. Quantitative SDS-PAGE was mainly used for proteoliposomes and protein samples in detergents incompatible with DC Protein Assay. Samples and bovine serum albumin (BSA) in increasing concentration were resolved on 12% SDS-PAGE and stained with CBB. Gels were scanned and the peak area of each protein band was quantified using ImageQuant proGram (Molecular Dynamics).

Appendix F
Membrane fractionation

Cells were harvested and resuspended in buffer containing 10mM Tris-HCl pH8.0, 5mM EDTA and 1mM PMSF. Lysozyme was added to a final concentration of 100μg/mL and incubated on ice for 30min (Osborn *et al.,* 1972). The spheroplasts formed following the lysozyme-EDTA treatment were sonicated (Branson Sonifier 450) for 45s on ice. After removal of unbroken cells or cell debris, total membranes were collected by ultracentrifugation at 250,000 x g for 30min to 90min in Beckman 70-Ti rotor. For fractionation of the inner and outer membranes, total membranes were solubilized in Triton X-100 (TX) buffer and incubated on ice for at least 2 hrs or overnight at 4^0C. The inner membrane is efficiently solubilized in 5% TX. Insoluble material was removed by ultracentrifugation at 70,000 x g for 30 min in Beckman 70-Ti rotor (Tikhonova and Zgurskaya, 2004).